Dissertation

submitted to the

Combined Faculties of the Natural Sciences and for Mathematics

of the Ruperto-Carola University of Heidelberg, Germany

for the degree of

Doctor of Natural Science

presented by

Diplombiologen Konstantin Gängel

born in Heidelberg

Oral-examination: 25. Mai 2005

Epidermal growth factor receptor signalling regulates ommatidial rotation during *Drosophila* eye development

Referees: Prof. Dr. Bernhard Dobberstein
Prof. Dr. Renato Paro

Meinen Eltern und
Dr. Bernhard Ziegler gewidmet

"Wir spazieren durch einen Garten
Ich wende mich einen Augenblick lang ab
Jetzt tust du's wieder -
Du hast mein Gesicht hier, aber du siehst Dir Blumen an"

Maulana Dschelaluddin Rumi

Table of contents

Acknowledgements

Firstly, I would like to thank Marek Mlodzik for his outstanding supervision, scientific enthusiasm, financial support and for providing the academic freedom that allowed my to choose and complete my own project.

I am grateful to Bernhard Dobberstein and Renato Paro for taking on the correction of this thesis and to Renato Paro for introducing me to the fascinating world of *Drosophila* development in the first place.

I would like to thank Kwang-Wook Choi for generously sharing his supposition that *rlt* might be allelic to *argos* and to Matthew Freeman for sharing data prior to publication.

I am grateful to the *Drosophila* fly community, especially to Paul Adler, Buzz Baum, Sarah Bray, Julius Brennecke, Katja Brückner, Kwang-Wook Choi, Suzanne Eaton, Matthew Freeman, Paul Garrity, Ulrike Gaul, David Gubb, Tapio Heino, Christian Klämbt, Lutz Kockel, Sally Leevers, Stephan Noselli, Hiroki Oda, Hideyuki Okano, Frank Pichaud, Kaoru Saigo, Trudi Schupbach, Jessica Treisman, Tadashi Uemura, Daisuke Yamamoto, Tanya Wolff, Lawrence Zipursky as well as to the Developmental Studies Hybridoma Bank and to the Bloomington Stock Center for providing flies and antibodies.

I would like to thank all past and present lab members for sharing their knowledge and experience with me and for their help and support. A special thanks has to go to Andreas Jenny from whom I learned a lot during these past years. I also would like to thank Micheal Burnett for technical assistance and to Zhongfang Du for embryo injection and preparing fly-food.

I am indebted to Micheal Burnett, Phyllis Shaw and Maria Thuveson for comments on the manuscript that significantly improved the readability of this thesis.

I would like to thank Maria Thuveson for her love, and Julius Brennecke and Lutz Kockel for their friendship.

A special thanks has to go to my high school biology teacher, Bernhard Ziegler, for awakening my interests for biology in the first place.

Finally, I would like to thank my parents for their love, support and patience during the past years.

Summary

Cell motility is essential for many aspects of normal animal development. However, little is known about how cell motility and associated changes in cell shape are regulated in the context of epithelial tissue patterning. This study investigates the cell motility of developing ommatidia, a process known as ommatidial rotation, during *Drosophila* eye development. The *Drosophila* eye consists of approximately 800 ommatidia that have to be precisely aligned with respect to one another for proper eye function. This precise alignment is achieved as ommatidia rotate 90° within the plain of the eye imaginal disc epithelium. Only a few mutations have been identified that disrupt this process and the signalling pathways regulating ommatidial rotation remain yet to be revealed. This study characterizes the *argos*^{roulette} mutation, in which ommatidia rotate to various degrees. Argos is a secreted inhibitor of Spitz, the main activating ligand of the Epidermal growth factor receptor (Egfr). The experiments presented show that modulation of Egfr activity causes defects in ommatidial rotation and implicate the Raf/MAPK/Pointed cascade as well as the Ras binding protein Canoe as downstream effectors of Egfr/Ras in this process. Furthermore, evidence is provided indicating that the regulation of cell adhesion via cadherins is critical for this process. In particular, the atypical cadherin *flamingo*, a gene known to regulate epithelial planar polarity, appears to play a key role in ommatidial rotation, as its sub-cellular localisation is disturbed in *argos*^{roulette} mutants. Genetic interactions further implicate non-muscle Myosin II as well as genes involved in actin polymerisation/depolymerisation in this process.

This study also describes the design of an F_1 screen intended to identify new genes involved in ommatidial rotation. Preliminary results obtained in a pilot screen identified the *Drosophila* PDGF/VEGF receptor orthologue (PVR) as a candidate. The requirement of Egfr and a potential role for PVR in ommatidial rotation are intriguing, as they suggest a remarkable parallel to border cell migration, where partially redundant functions of these signalling pathways have recently been reported. Thus, the regulation of cell motility in *Drosophila* might be controlled through similar pathways and mechanisms in different cellular contexts.

Zusammenfassung

Zellmotilität ist für viele Entwicklungsvorgänge von entscheidender Bedeutung. Es ist jedoch erstaunlich wenig darüber bekannt, wie Zellmotilität und damit einhergehende Änderungen der Zellform im Kontext der Musterbildung epidermaler Gewebe kontrolliert werden. Die hier präsentierte Studie untersucht die Zellmotilität sich entwickelnder Ommatidien, - auch Ommatidienrotation genannt, - während der Entwicklung des Facettenauges von *Drosophila melanogaster*. Das *Drosophila* Facettenauge besteht aus ungefähr 800 Ommatidien, welche in Bezug zueinander präzise orientiert sein müssen, um eine normale Funktion des Auges zu gewährleisten. Die genaue Orientierung der Ommatidien wird durch deren 90° Rotation innerhalb der Ebene des imaginalen Augenepitheliums erreicht. Bisher wurden nur sehr wenige Mutationen identifiziert, die diesen Prozess beinträchtigen und deshalb sind die Signalwege, welche die Ommatidienrotation regulieren, bislang noch unbekannt. Eine jener Mutationen *ist* $argos^{roulette}$*. Argos,* ist ein sekretierter Inhibitor von Spitz, dem wichtigsten Liganden des EGF-Rezeptors (Egfr). Die hier vorliegenden Experimente zeigen, dass die Modulation der Egfr Aktivität Defekte bei der Ommatidienrotation verursacht und implizieren die Raf/MAPK/Pointed Signalkaskade, sowie das an Ras bindende Protein Canoe als Effektoren von Egfr/Ras in diesem Prozess. Darüber hinaus lassen meine Daten vermuten, dass die Regulation der Cadherin-abhängigen Zelladhäsion für die korrekte Ommatidienrotation entscheidend ist. Eine Schlüsselrolle in diesem Prozess scheint das Epithelienpolaritätsgen *flamingo* zu spielen. Flamingo ist ein atypisches Cadherin, dessen subzelluläre Lokalisierung in $argos^{roulette}$ Mutanten deutlich verändert ist. Genetische Interaktionen mit einem haploinsuffizienten *Star* allel weisen auch darauf hin, dass das Motorprotein Nicht-Muskel-Myosin II und Gene, welche die Actin-Polymerisierung/Depolymerisierung regulieren, eine wichtige Rolle während der Ommatidienrotation spielen.

Ferner beschreibt diese Studie die Grundlagen für einen F_1 Screen zur Identifizierung von Genen, welche die Ommatidienrotation kontrollieren. Meine bisherigen Resultate aus einem Vorversuch zeigen, dass das *Drosophila* Ortholog des PDGF/VGEF Rezeptors (PVR) für die Ommatidienrotation wichtig zu sein scheint. Die Beobachtung, dass Egfr und Pvr für die korrekte Ommatidienrotation wichtig sind, weist eine beachtliche Parallele zur Migration von Border-Zellen während der Oogenese von *Drosophila* auf, wo teilweise redundante Funktionen dieser beiden Signalübertragungswege kürzlich publiziert wurden. Diese Ergebnisse weisen darauf hin, dass die Zellmigration in *Drosophila* in unterschiedlichen zellulären Zusammenhängen durch ähnliche Signalwege und Mechanismen kontrolliert wird.

I
Introduction

The *Drosophila* eye as a model system

One of the most fascinating questions in developmental biology is how tissues become patterned and differentiated. The compound eye of *Drosophila melanogaster* has emerged as a particularly important model system for addressing this question. Fundamental biological processes, such as cell cycle regulation, cell proliferation, cell fate induction and cell differentiation, as well as cell death and the establishment of epithelial polarity, can be studied during *Drosophila* eye development due to an unique combination of its features (reviewed in Thomas and Wassarman, 1999). The most striking advantages of the *Drosophila* eye as a model system are the facts that it is dispensable for the viability and fertility of the fly and yet is a very prominent structure, making it an ideal target for genetic screens. Screens can be designed as either gain- or loss-of-function screens and phenotypes can be analysed throughout eye development at the cellular level. In a gain-of-function screen, a gene of interest can be over-expressed using a variety of eye specific promoters (reviewed in Thomas and Wassarman, 1999). Subsequent modifier-screens have proven to be a potent tool to identify enhancers and suppressors of an initial gain-of-function phenotype. This approach often reveals genes that function in the same pathway or biological process as the over-expressed gene, even if the over-expressed gene might not be initially required for eye development (Thomas and Wassarman, 1999; Duffy, 2002). Furthermore, loss-of-function screens can identify viable mutations affecting the shape or the roughness of the eye. Alternatively, the function of otherwise lethal genes can be analysed in clones created in the eye (Xu and Rubin, 1993; Pichaud and Desplan, 2001), which very often reveals the general function of a gene that might be difficult to study in other developmental contexts. Importantly, the majority of all lethal genes can be studied using this technique, which is particularly valuable, since it is estimated that approximately two thirds of all vital *Drosophila* genes are required for eye development (Thaker and Kankel, 1992).

Structure of the adult *Drosophila* eye

The adult *Drosophila* eye is a highly organised structure consisting of about 750 hexagonal shaped unit eyes, called ommatidia (Fig. 1A, B). Each ommatidium is composed of 20 cells, including eight photoreceptor neurons, four lens-secreting cone cells, seven optically insulating pigment cells and one mechanosensory bristle cell (Fig. 2). Three different types of pigment cells are present in each ommatidium. The primary pigment cells form the wall of the pseudocone chamber, which lies underneath the cornea, while the secondary and tertiary pigment cells define the hexagonal shape of the ommatidium (Fig. 2).

The rhabdomeres, membrane dense extensions of the photoreceptor neurons that contain the light gathering rhodopsins, are arranged in an asymmetric trapezoid within the center of each ommatidium (Fig. 1D and 2). The outer rhabdomeres R1 to R6 are grouped around the inner rhabdomeres R7 and R8 and have a noticeably larger diameter than the inner ones. The R7 rhabdomere lies on top of the R8 rhabdomere, therefore only one of these rhabdomeres is visible in a single cross section (Fig. 1C, D, and 2). Interestingly, ommatidia display a different chirality in the dorsal and ventral halves of the eye and are arranged in two fields with mirror image symmetry around the dorso-ventral midline, called the equator (Fig. 1C and 4D). The rhabdomeres R1, R2 and R3 are aligned perpendicular to the equator, with R1 being most equatorial and R3 being most polar at the tip of the trapezoid (Fig. 1D). The R4 rhabdomere lies just posterior to R3 and is noticeably closer towards the equator (Fig. 1D). R5 and R6 form the posterior border of the trapezoid with R5 being closer to the pole of the eye and R6 being closer to the equator (Fig. 1D). The mirror image orientation of the ommatidia is the direct consequence of ommatidial rotation, a precise 90° movement of the ommatidial precursor cells, which is discussed in detail in the following chapters. (For an in depth review on structure and development of the *Drosophila* eye see (Wolff and Ready, 1993)

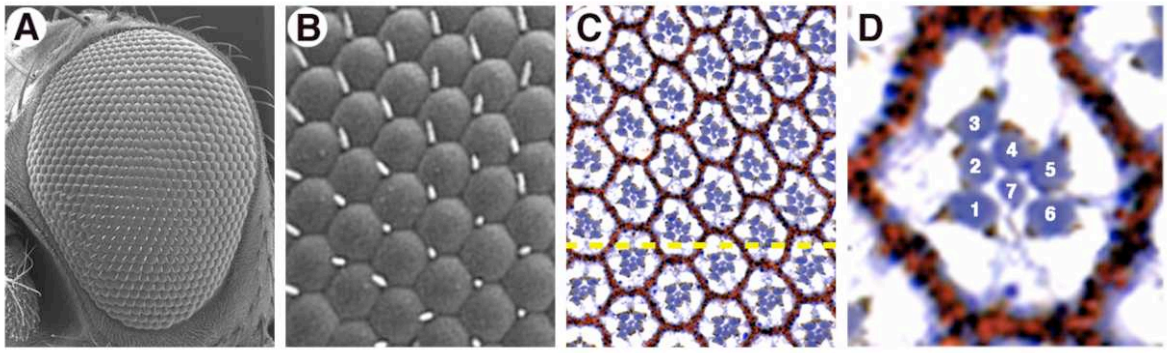

Figure 1. Structure of the adult *Drosophila* eye

(A, B) Scanning electron micrograph of a wild type *Drosophila* facet eye. **(A)** The adult eye is composed of a crystal like arrangement of approximately 750 single eye-units called ommatidia. **(B)** Enlargement of single ommatidia. The apical surface of the ommatidia is covered by the lens, which is secreted by cone and primary pigment cells. **(C, D)** Darkfield microscopic images of tangential sections through equatorial regions of the eye. **(C)** The optically insulating pigment cells (appearing in red) define the hexagonal shape of the single ommatidia. The photoreceptor rhabdomeres R1 to R7 (visible as blue round structures) are arranged in an asymmetric trapezoid in the center of each ommatidium. Opposite chirality of ommatidia in the dorsal and ventral half of the eye creates two fields of mirror image symmetry that meet at the equator (indicated by a yellow dashed line). **(D)** Enlargement of a single dorsal ommatidium. The rhabdomeres of the respective photoreceptors are indicated by white numbers. Note that the rhabdomeres of the outer photoreceptors R1 – R6 are larger in diameter than the central-most rhabdomere of the R7 cell. The rhabdomeres R1-R3 are aligned perpendicular to the equator, with R1 being more equatorial and R3 being more polar at the tip of the trapezoid. R4 lies posterior to R3 and is closer toward the equator. R5 and R6 form the posterior boarder of the trapezoid. In all panels, anterior is to the left and dorsal is up. (Scanning electron micrographs in A and B were kindly provided by Marek Mlodzik).

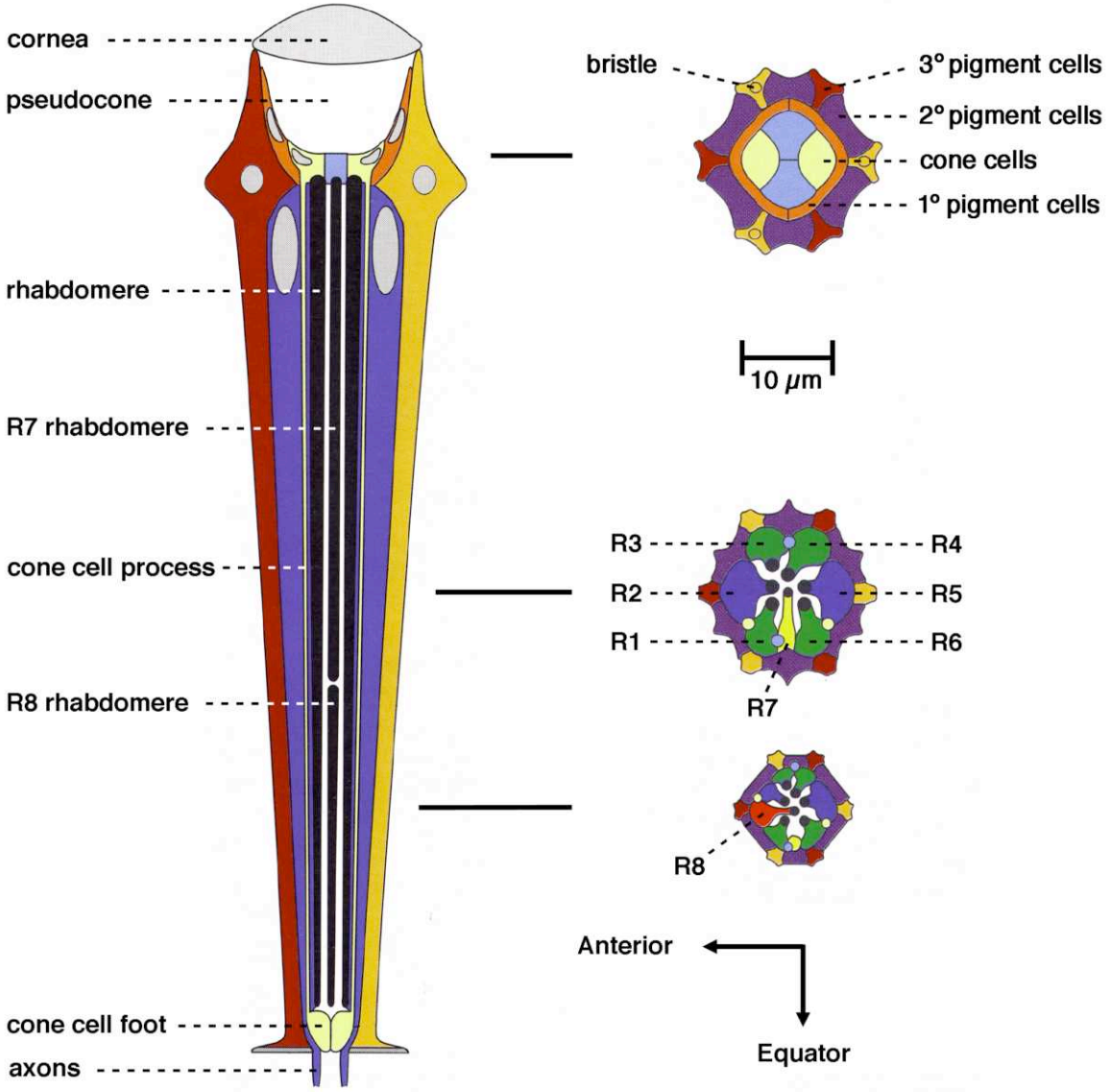

Figure 2. Cartoon of a single ommatidium

A longitudinal section (left) and three tangential sections taken at different levels of the ommatidium (right) are shown. Positions of the tangential sections are indicated by black lines. Note that although the cell-bodies of the photoreceptor neurons are arranged in a circular manner, their rhabdomeres extend differently towards the center of the ommatidium, thereby creating a characteristic asymmetric trapezoid. The R7 rhabdomere is extended between R1 and R6, whereas the underlying R8 rhabdomere is usually extended between R1 and R2. The cornea and the underlying pseudocone are extracellular secretions of cone cells and primary pigment cells. Secondary and tertiary pigment cells form the hexagonal shape of the ommatidia and optically isolate the single ommatidia from each other. The ommatidial taper contributes to the eye's curvature. Anterior is to the left and dorsal is up. (Modified after Wolff and Ready 1993)

The *Drosophila* life cycle

The life of the fruit-fly *Drosophila melanogaster* can be subdivided into four major phases: Embryonic development (first phase) is pursued by three larval stages (second phase), followed by pupation and metamorphosis (third phase), after which the adult fly, called imago, ecloses (fourth phase, Fig. 3). At 25ºC, embryonic development spans a period of 24 hours, during which the fertilized egg develops into the first instar larvae. Within the next 24 hours the second instar larvae develops and after another 24 hours the third larval instar ecloses. The third instar larval stage spans about 48 hours after which the larvae pupates. During pupation the body plan of the larvae is drastically rebuilt into the final organs and structures of the adult fly. Three to four days after pupation has begun, the imago ecloses out of the pupa case and becomes fertile within the next eight hours (Fig. 3).

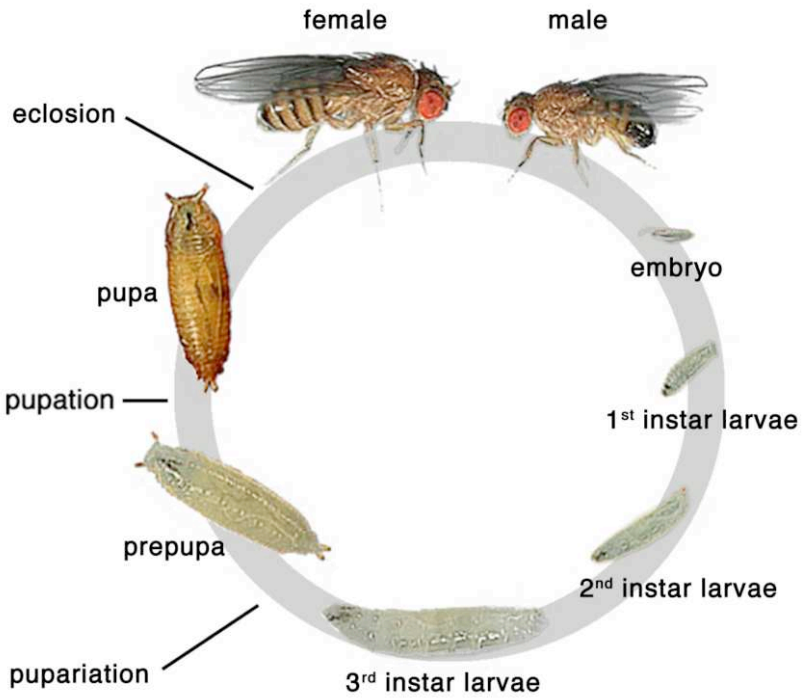

Figure 3. The *Drosophila* life cycle

At 25ºC the embryo develops over a period of 24h into the first instar larvae. First and second instar stages each span a period of 24h. The third instar stage spans about 48h after which the larvae pupariates. Three to four days later the imago hatches and becomes fertile within the next 8 hours. [Modified after FlyMove (http://flymove.uni-muenster.de/)].

Drosophila eye development – a brief overview

Almost all adult *Drosophila* structures derive from imaginal discs, single layered epithelia that invaginate from the ectoderm during embryonic development. The *Drosophila* eye develops from the eye-antennal disc (often simply called the eye disc), an imaginal disc that also gives rise to the antenna and most of the adult head (Fig. 4A). The origin of the eye disc can be traced back to a domain of dorsolateral ectoderm containing 6-23 cells (Garcia-Bellido and Merriam, 1969; Wieschaus and Gehring, 1976). Shortly before head involution, a connection between the later eye disc cells and the central nervous system is established in form of the optic stalk. Head involution folds the ectodermal cells reserved for eye and antennal development internally to form the eye-antennal disc. At this stage, the disc is a simple epithelial sac, with topologically intact apical and basal surfaces. The lumen of the disc opens into the pharynx and thus communicates with the outside.

During the first and second instars, the eye-antennal disc is un-patterned and proliferates. Asynchronous cell divisions increase the cell number during that period more than 10-fold, from about 130 at the end of the first instar to about 1300-1600 at the beginning of third instar (Becker, 1957). Pattern formation of the eye imaginal disc begins during the third larval instar. Four or five additional asynchronous cell divisions, that increase the cell number to roughly 10000, are necessary to create a pool of cells big enough for the subsequent differentiation events.

Unlike other tissues, the eye imaginal disc differentiates in a spatially graded manner. Starting at the posterior pole, a wave of cell differentiation sweeps toward the anterior of the eye disc. The front of this wave is marked by an indentation of the apical surface of the epithelium along its dorso-ventral axis called the morphogenetic furrow (MF). Every 1.5 – 2 hours a new column of evenly spaced ommatidial founder cells (R8 precursor cells) arises from the posterior margin of the MF. These founder cells differentiate into R8 cells just posterior to the MF and are the first photoreceptors to be specified. As the furrow progresses, seven other photoreceptor cells (R1 to R7) are recruited by the R8 cell in a stereotypical manner (see Fig. 5D for a cartoon of the differentiation events posterior to the MF). Once four additional photoreceptors (R5, R2, R3 and R4) have joined R8, these five-cell ommatidial pre-clusters begin rotating within the plane of the epithelium (Fig. 4C, 8 and 9). This morphogenetic movement is remarkable because it requires groups of cells to undergo a coordinated rotation of exactly 90° past their neighbors. Importantly, the unusual developmental progression of the eye disc allows the analysis of several stages of ommatidial maturation in a single imaginal disc - a stroke of luck for developmental biologists.

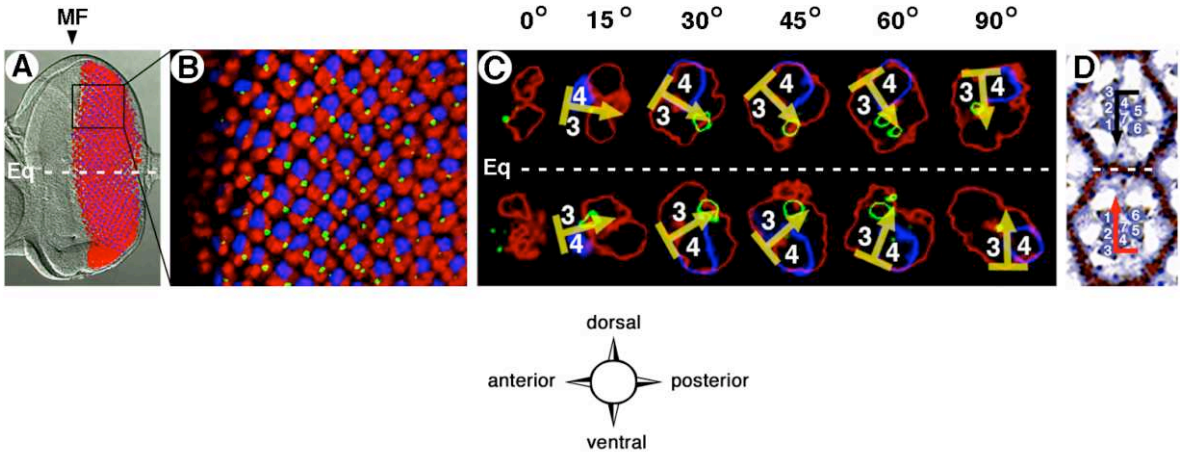

Figure 4. Development of the *Drosophila* eye

(A-C) Third instar eye imaginal discs showing ommatidial differentiation and rotation. **(A)** Eye imaginal disc stained with α-Elav (red, marking all photoreceptor precursors) and *mδ0.5-lacZ* (blue, highlighting the R4 precursors) shown as an overlay with a Nomarski optics bright-field image of the same disc. The position of the morphogenetic furrow (MF) is indicated by a black arrowhead and the equator (Eq) is represented by a white-dashed line. Note that the posterior half of the eye disc already has specified photoreceptor neurons, whereas the anterior half is un-patterned. **(B)** Higher magnification confocal image of boxed area in (A), also showing α-Boss staining (green, marking the central R8 cell in each cluster). For clarity the overlay of red and blue channels is shown in blue. (**C)** Semi-schematic presentation of ommatidial rotation (generated from actual ommatidial-clusters shown in (B) with the 'solarize' filter of Adobe® Photoshop®). Representative ommatidial clusters for the dorsal and ventral halves are shown. Colors are as in (B). Rotation angles of individual clusters are represented by yellow arrows and indicated above the panel. The 'base' of the arrow is aligned in parallel with the R3/R4 axis (white numbers) and the arrowhead points toward the central R8. Note that dorsal ommatidia rotate clockwise whereas ventral ommatidia rotate counter-clockwise. (**D)** Tangential section through the equatorial region of an adult Drosophila eye showing mature ommatidia of the dorsal and ventral half, respectively. The rhabdomeres of the photoreceptors R1-R7 are visualised in blue and indicated by white numbers. Ommatidial chirality and orientation is indicated by flagged-arrows (black arrow: dorsal ommatidium, red arrow: ventral ommatidium). In all panels anterior is to the left and dorsal is up.

Equator formation in the *Drosophila* eye

Correct specification of the equator is a prerequisite for MF initiation and subsequent patterning events (reviewed in Lee, 2002). Specification of the equator is triggered by the expression of the GATA transcription factor *pannier* (*pnr*) at the dorsal margin of the eye disc during embryogenesis (Ramain et al., 1993; Heitzler et al., 1996; Maurel-Zaffran and Treisman, 2000). Pnr stimulates the expression of *wingless* (*wg*), a Wnt family member, which, in concert with the secreted protein Hedgehog (Hh), specifies the dorsal half of the eye disc through induction of the three homeobox genes of the *Iroquois* complex (*Iro*-C, Gomez-Skarmeta et al., 1996; McNeill et al., 1997; Heberlein et al., 1998; Cavodeassi et al., 1999; Maurel-Zaffran and Treisman, 2000). *Iro*-C expression in turn limits the expression of the glycosyltransferase Fringe (*fng*) to the ventral part of the eye disc, as it represses *fng* dorsally (Cho and Choi, 1998; Dominguez and de Celis, 1998; Cavodeassi et al., 1999). While *Iro*-C expression displays a sharp expression boundary between the dorsal and the ventral half of the eye disc, the mechanism by which this boundary is established, is poorly understood. Fringe modifies the transmembrane receptor Notch by adding N-acetylglucosamine to O-linked fucose residues (Bruckner et al., 2000; Moloney et al., 2000). This modification increases Notch's (N) affinity for its ligand Delta, whereas it decreases its affinity for an alternative ligand, Serrate. Both Notch ligands are expressed in non-overlapping domains in the eye disc. Whereas Delta is expressed in the dorsal half of the eye disc, Serrate is limited to the ventral half (Cho and Choi, 1998; Dominguez and de Celis, 1998; Papayannopoulos et al., 1998). The domains of Delta and Serrate expression are thought to be specified through Hh and Wg signalling originating from peripodial membrane cells (which cover the eye disc epithelium, Cho et al., 2000). Fringe activity in the ventral compartment limits Notch activation to the midline where modified ventral Notch is exposed to dorsal Delta and unmodified dorsal Notch exposed to Serrate. Notch activity at the dorso-ventral midline defines the equator and is both necessary and sufficient to initiate differentiation, when exposed to the secreted protein Hedgehog (Hh), which is expressed at the posterior disc margin (see Fig 5A, B for a schematic representation of the key events leading to equator specification)

Initiation and progression of the morphogenetic furrow

The secreted protein Hh is critical for initiation and progression of the MF. In the third instar eye disc, Hh is initially expressed at the posterior margin and, as mentioned above, triggers the initiation of the MF where it overlaps with Notch activity at the equator (Dominguez and Hafen, 1997; Royet and Finkelstein, 1997; Borod and Heberlein, 1998). During progression

of the MF, Hh is strongly expressed in the newly differentiating photoreceptors R2 and R5 (and weaker in other cells of the precluster), from where it diffuses to promote differentiation of more anterior cells (Heberlein et al., 1993; Ma and Moses, 1995). Hh promotes differentiation by activating the expression of the proneural gene *atonal* (*ato*, Borod and Heberlein, 1998; Greenwood and Struhl, 1999) a basic loop helix transcription factor required for the formation of the founder R8 photoreceptor (Jarman et al., 1994). Atonal is first expressed in a broad stripe anterior to the MF, then refined to proneural clusters of cells and later to single R8 photoreceptor-precursors (Jarman et al., 1994; Dokucu et al., 1996; reviewed in Treisman and Heberlein, 1998). The restriction of Ato expression to single R8 photoreceptor-precursors is in part mediated through the homeodomain transcription factor Rough (Ro Kimmel et al., 1990; Dokucu et al., 1996) and later refined through Notch mediated lateral inhibition (Cagan and Ready, 1989; Baker and Zitron, 1995). Ro is expressed in a pattern complementary to that of Ato and has been shown to repress the transcription of *ato* (Dokucu et al., 1996). Thus, Hh regulates both the formation and the spacing of R8 photoreceptor precursors.

Besides Hh, the secreted TGF-β orthologue Decapentaplegic (Dpp) is critical for initiation and progression of the MF (Heberlein et al., 1993). Loss of either *hh* or *dpp* function at the posterior margin of an early eye disc abolish furrow initiation and both genes have been shown to function partially redundant during MF progression (reviewed in Lee, 2002). It is generally thought that one of the key functions of *dpp* is to restrict the expression domains of the secreted growth factor *wg*, which is expressed at the dorsal and ventral margins of the eye disc prior to MF initiation (Wiersdorff et al., 1996; Royet and Finkelstein, 1997). Wg has been shown to counteract furrow initiation and progression and its presence at the lateral margins is critical to prevent ectopic furrows from initiating (Ma and Moses, 1995; Treisman and Rubin, 1995). (See Fig. 5B, C for a schematic representation on initiation and progression of the MF).

Cell fate specification in the *Drosophila* eye

As mentioned above differentiation of ommatidia posterior to the MF occurs in a stepwise assembly of photoreceptor, cone and pigment cells (reviewed in Nagaraj, 2002). R8 is the first photoreceptor to differentiate and its correct specification through *ato* is critical for all subsequent patterning events. This is illustrated by the phenotype of *ato* null mutants, in which photoreceptor differentiation is impaired (Jarman et al., 1994). In addition, it has been shown that signalling via the Epidermal growth factor receptor (Egfr) is essential for the development of photoreceptors. Clones of Egfr mutant tissue fail to develop photoreceptors with the exception of R8 (Xu and Rubin, 1993; Dominguez et al., 1998; Baker and Yu,

2001). Conversely, mutations in the *argos* (*aos*) gene, a secreted inhibitor of Spitz (Spi), the main activating ligand of Egfr signalling in the eye, cause the differentiation of extra photoreceptors (Freeman et al., 1992). The mechanism through which Egfr signalling controls photoreceptor development are, however, not fully understood (For a review on the multiples roles of Egfr in the eye see Kumar, 2002). Besides a general requirement for Egfr, the specific expression of transcription factors in the respective photoreceptor precursors is critical for correct cell fate determination. Specification of R2 and R5 requires the function of the Ro gene (Saint et al., 1988; Tomlinson et al., 1988). Ro appears to be a repressor of Ato as loss of Ro function leads to ectopic Ato expression in R2/R5 (Dokucu et al., 1996). Conversely, misexpression of Ro causes loss of Ato in R8 (Dokucu et al., 1996). R3 and R4 are the last two photoreceptors to be specified within the 5-cell precluster. Specification of R3/R4 requires the function of the *sevenup* (*svp*) gene, which encodes two transcription factors of the Orphan family of nuclear receptors (Mlodzik et al., 1990). Svp is first expressed in R3/R4 and later also in R1/R6 (Fig. 17B-B''). In *svp* mutants, R3/R4 and R1/R6 are transformed to R7-like photoreceptors and the misexpression of *svp* causes complex cell fate changes (Hiromi et al., 1993). Although in the early five-cell precluster R3 and R4 appear equivalent, these cells adopt asymmetric positions in more mature ommatidia and thereby create chirality of the ommatidial. As will be discussed in more detail later, Notch signalling is critical for proper differentiation of R3/R4. Loss of Notch activity causes the R3/R4 pair to adopt R3/R3 fate, while gain of Notch function results in R4/R4 symmetric clusters (Cooper and Bray, 1999; Fanto and Mlodzik, 1999). With the specification of R8, R2/R5 and R3/R4, the five-cell precluster is established.

Specification of all remaining cell types requires an additional round of synchronized cell division, known as the second mitotic wave. The subsequent patterning events leading to specification of R1/R6, R7, cone and pigment cells have therefore been described as the second wave of morphogenesis (reviewed in Nagaraj, 2002). Interestingly, correct cell fate specification during this second wave of morphogenesis requires the function of Lozenge (LZ), a Runt domain transcription factor, which is expressed anterior to the furrow. Lz appears to regulate all transcription factors known to be required during the second wave of morphogenesis (Daga et al., 1996; Flores et al., 2000; Xu et al., 2000). Loss of *lz* function causes either loss of expression of these transcription factors or their ectopic up-regulation. The first cells to differentiate during the second wave of morphogenesis are R1/R6. Beside Svp, specification of R1/R6 requires also the homeodomain transcription factors BarH1 and BarH2 (Higashijima et al., 1992). In addition, the expression of the Phyllopod (Phyl) transcription factor, which is induced by the Ras/Raf/MAPK pathway, plays a critical role for the specification of R1/R6 (Chang et al., 1995; Dickson et al., 1995).

The last photoreceptor to be specified is R7. One of the key gene products for R7 specification is the Sevenless (Sev) receptor tyrosine kinase (RTK, Banerjee et al., 1987; Hafen et al., 1987). Several elegant genetic experiments showed that Sev mediates nuclear signalling via the Ras/Raf pathway (reviewed in Daga and Banerjee, 1994; Simon, 1994; Zipursky and Rubin, 1994; Dickson, 1995). Although broadly expressed, loss of Sev only affects R7 fate (Banerjee et al., 1987; Tomlinson et al., 1987). Activation of Sev is mediated by a membrane bound ligand, Bride of Sevenless (Boss), which is exclusively expressed in R8 (Kramer et al., 1991; Van Vactor et al., 1991). Similar to Sev, mutations in Boss only affect R7 cell fate. Boss is required in R8 in a non-cell autonomous manner to activate Sev in the adjacent R7 cell (Reinke and Zipursky, 1988). Sev activates the Ras/Raf pathway, which results in the transcription of *phyl* in R7 (Chang et al., 1995; Dickson et al., 1995). Phyl subsequently binds to Seven in absentia (Sina), a factor essential for R7 cell fate (Carthew and Rubin, 1990). The Phyl/Sina complex then promotes the degradation of Tramtrack (Ttk88), a negative regulator of neuronal differentiation (Kauffmann et al., 1996). In addition, Notch signalling is also required for proper R7 differentiation. Loss of the Notch ligand Delta (Dl) from the neighboring R1/R6 cells transforms R7 to an R1/R6 cell type (Cooper and Bray, 2000; Tomlinson and Struhl, 2001). Conversely, ectopic expression of Notch in R1/R6 converts these cells into R7-like cells (Tomlinson and Struhl, 2001).

Like the photoreceptors, the non-neuronal cone cells are specified by a unique combination of transcription factors including DPax-2, Prospero and Cut (Kauffmann et al., 1996; Fu and Noll, 1997). Furthermore, a certain level of Ras signalling is critical for correct cone cell specification (Gaul et al., 1992; Lai and Rubin, 1992).

The last class of cells to be specified in the eye are the pigment cells. Specification of these cells requires the transcription factors BarH1 and DPax-2, and a combination of Egfr and Notch signalling as well as signals from neighboring cone cells (Miller and Cagan, 1998). Loss of Egfr function results in loss of pigment cells and ectopic expression of Egfr causes an excessive specification of these cells (Freeman, 1996).

In summary a small number of transcription factors in combination with only two signalling pathways -- Notch and RTK's (Egfr/Sev) -- are sufficient to specify all cell types posterior to the morphogenetic furrow.

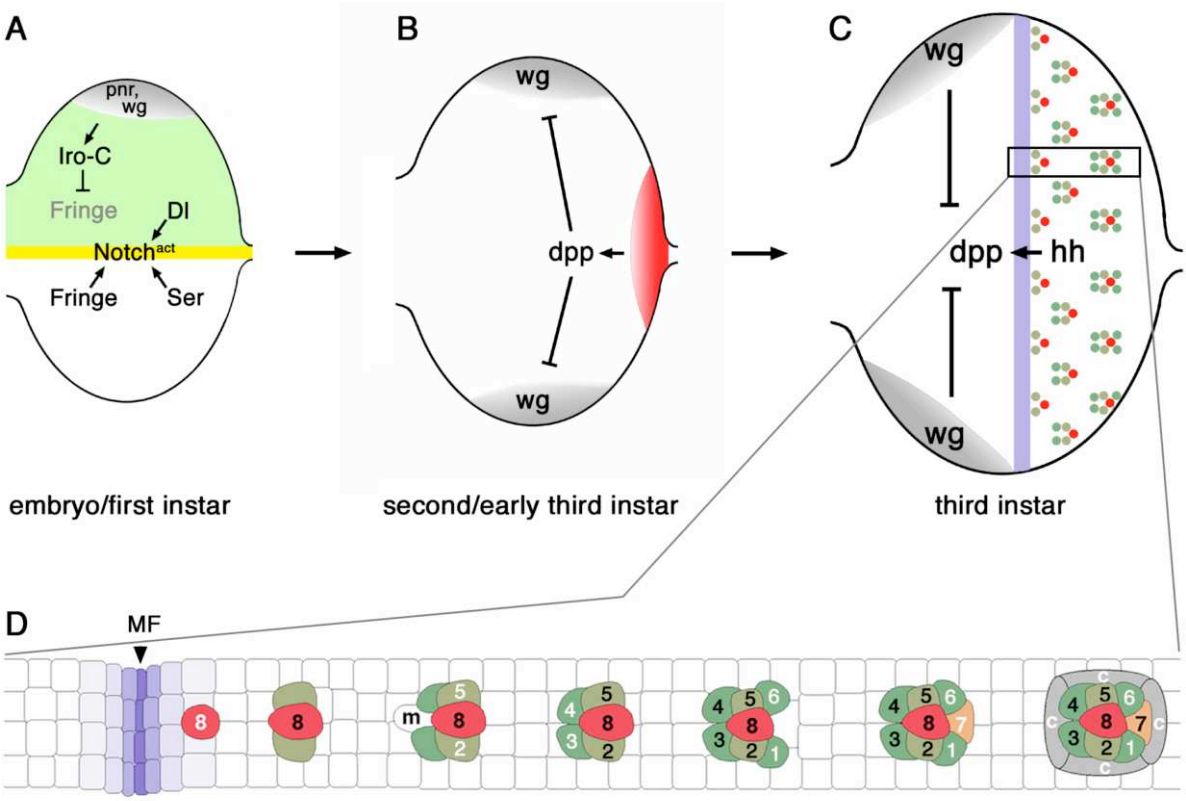

Figure 5. Specification of the equator and progression of the morphogenetic furrow

(A) Cartoon of the key signalling events leading to specification of the equator. Expression of Pannier (Pnr) at the dorsal margin of the eye disc triggers the expression of Wingless (Wg), which in turn induces the expression of the Iroquois complex (Iro-C) in the dorsal half of the eye (green). Iro-C activity represses the glycosyltransferase Fringe dorsally. Fringe-mediated modification of Notch (N) in the ventral half of the eye increases Notch's affinity for Delta (Dl) and decreases its affinity for Serrate (Ser). This leads to N activation only at the equator (yellow), where modified ventral N is exposed to Dl (which is expressed in the dorsal half of the eye) and unmodified dorsal N is exposed to Ser (which is expressed in the ventral half of the eye). **(B, C)** Cartoons illustrating initiation and progression of the morphogenetic furrow. Wingless (Wg) inhibits ectopic furrow initiation at the margins and is restricted by Decapentaplegic (Dpp), which is expressed in response to Hedgehog (Hh) signalling at the posterior margin of the eye disc. Hh and Dpp are both required for initiation and progression of the morphogenetic furrow (MF, shown in blue in C and D). During furrow progression Hh is expressed in the developing photoreceptors from where it diffuses to promote differentiation of more anterior cells (see text for detail). **(D)** Schematic representation of photoreceptor differentiation posterior to the morphogenetic furrow. The first photoreceptor to be specified is the founder R8 (shown in red). After R2/R5 and R3/R4 have been specified, the five-cell precluster is established. The mystery cell (m), which is initially part of the precluster, is later on excluded and does not adopt neuronal cell fate. During a second wave of morphogenesis R1/R6, R7, cone and pigment cells are specified (see text for detail). For simplicity, ommatidial rotation is not indicated in this cartoon. Anterior is left and dorsal is up in all figures. (Figures A-C are modified after Lee and Treisman and figure D is modified from Volker Wiersdorff)

Establishment of epithelial planar polarity in the *Drosophila* eye

Proper function of most tissues requires a polarization of cells. Most epithelial structures show an obvious polarization along their apical-basal axis. However, very often an additional polarization of cells or groups of cells within the plane of the epithelium can be observed. This phenomenon is referred to as epithelial planar cell polarity (PCP, reviewed in Eaton, 1997; Mlodzik, 2002a; Strutt, 2003; Fanto and McNeill, 2004). Obvious examples of such polarized structures are feathers in birds, scales in fish and the regular organization of hairs in the exocuticle of insects. Furthermore, planar polarity is evident in many neuroepithelia, such as in the precise alignment of stereocilia bundles in the inner ear epithelium. Planar polarization is also evident in internal organs, for example in the oviduct, where the orientation of cilia allows the directional transport of the egg. In the *Drosophila* eye, epithelial planar polarity is evident in the mirror-like arrangement of ommatidia, which are polarized with respect to both the anterior-posterior and the dorso-ventral axes (Fig. 1C,D and 4D). The anterior-posterior polarization is established through the progression of the morphogenetic furrow (Fig. 5D), whereas the dorso-ventral polarization is achieved, as ommatidia establish their chirality and subsequently rotate 90° within the plain of the eye imaginal disc (Fig. 4C, 7 and 8; reviewed in Reifegerste and Moses, 1999; Adler, 2002; Mlodzik, 2002b; Strutt, 2003; Fanto and McNeill, 2004). Genetic analysis of mutants affecting planar polarity in the eye has shown that correct cell fate specification of the R3/R4 pair is the critical step during chirality establishment and also determines the direction of rotation (Cooper and Bray, 1999; Fanto and Mlodzik, 1999). Young five-cell ommatidial pre-clusters that arise from the MF are initially bilateral symmetric and face the same direction (Fig. 5D). Chirality is established as the initially equivalent cells of the R3/R4 pair adopt distinct cell fate. In wild-type eyes, the cell closer to the equator will adopt R3 fate, while the other cell will adopt R4 fate. Experiments from several groups have shown that the R3 cell fate is specified via Frizzled (Fz) signalling, whereas the R4 cell fate is specified through Notch signalling (Fanto and Mlodzik, 1999; Tomlinson and Struhl, 1999; Cooper and Bray, 2000). Notch activity in R4 (and therefore the R4 cell fate decision) can be visualised with an *mδ0.5lacZ* reporter transgene (Cooper and Bray, 1999). Expression of this transgene is first detected at low levels in the 4th column behind the morphogenetic furrow, where it is expressed in either the R3 or the R4 precursor or in both cells (Fig. 7A). This initially weak and variable expression, which most likely reflect the actual specification process, is refined to strong expression in only the R4 cell from column 6 on (Fig. 7A). By this stage the R4 cell fate, and therefore the chirality of the ommatidial cluster, is established and ommatidia have initiated their rotation. In addition to the role of Notch in R4, genetic screens have identified several genes that are required for planar polarity establishment in most if not all tissues.

These genes are often classified as ‘core’ or ‘primary’ polarity genes and include Frizzled (Fz), a seven-pass transmembrane protein of the Wnt receptor family (Gubb and Garcia-Bellido, 1982; Vinson and Adler, 1987; Vinson et al., 1989; Adler et al., 1990), Dishevelled (Dsh), a multidomain protein essential for Fz signal transduction (Klingensmith et al., 1994; Theisen et al., 1994; Krasnow et al., 1995), Flamingo (Fmi, also called Starry night), an atypical cadherin with seven transmembrane domains (Chae et al., 1999; Usui et al., 1999), Strabismus (Stbm, also called Vang Gogh), a protein with four predicted transmembrane domains (Wolff and Rubin, 1998), Prickle-spiny-legs (Pk-Sple), a LIM domain protein (Gubb and Garcia-Bellido, 1982; Gubb et al., 1999) and Diego (Dgo), an ankyrin domain protein (Feiguin et al., 2001). In the eye, mutations in each of these genes can cause alterations of ommatidial polarity (examples for *fz* and *dsh* are shown in Fig. 6). Ommatidia can be flipped along the A/P axis or along the D/V axis (Fig. 6D and E respectively) or they can lose their chirality, as the R3/R4 cells adopt either R4/R4 or R3/R3 fate, and thereby become symmetrical ommatidia (Fig. 6F and G). In addition, ommatidia can both under- and overrotate (Fig. 6B, C). All of these phenotypes are visible in strong alleles of the core PCP genes, suggesting that these genes control all aspects of planar polarity in the eye (see Fig. 6B and C for examples of *fz* and *dsh*). In addition, several genes have been identified that perturb only certain aspects of PCP or show only a phenotype in certain tissues. Loss of *four jointed* (*fj*), *fat* (*ft*) or *dachsous* (*ds*) for example, only lead to D/V flips (Zeidler et al., 1999; Rawls et al., 2002; Yang et al., 2002), whereas mutations in *nemo* (*nmo*, Choi and Benzer, 1994), *roulette* (*rlt*, Choi and Benzer, 1994), *laminin A* (*lamA*, Henchcliffe et al., 1993b), *scabrous* (*sca,* Chou and Chien, 2002), *rhoA* (Strutt et al., 1997) and *Drok* (Winter et al., 2001) mainly seem to affect ommatidial rotation (discussed in detail in the next chapter). The fact that ommatidial chirality and rotation are established around the dorso-ventral midline of the eye led to the hypothesis that a polarizing signal emanates from the equator. This yet to be identified polarizing signal, often referred to as ‘Factor X’, is thought to diffuse equally to both the dorsal and the ventral half of the eye. Factor X is proposed to bind and activate the Fz receptor, resulting in a gradient of Fz activity, high at the equator and low at the poles of the eye (reviewed in Adler, 2002; Fanto and McNeill, 2004). As ommatidia emerge from the morphogenetic furrow, the presumptive R3 cell is closer to the equator than the presumptive R4 cell and therefore will be activated at slightly higher levels by Factor X. In agreement with this hypothesis, genetic mosaic studies have shown that the cell with higher Fz activity within the R3/R4 precursors will become R3 (Zheng et al., 1995; Tomlinson and Struhl, 1999). Fz signalling in the R3 precursor has been shown to upregulate the transcription of Delta, which subsequently activates Notch signalling in the neighboring R4 precursor, leading to its specification as an R4 photoreceptor (Cooper and Bray, 1999; Fanto and Mlodzik, 1999). Two models have been proposed for the signalling

events downstream of Fz in R3. The first model implicates a pathway consisting of Dsh and components of the Jun-N-terminal kinase (JNK) pathway. JNK signalling has been found to promote Dl transcription in R3 (Weber et al., 2000) and mutant alleles of JNK pathway components have been found to suppress polarity defects caused by the overexpression of Fz or Dsh (Boutros et al., 1998; Boutros and Mlodzik, 1999). However, with the exception of the MAPKKKK Misshapen (Paricio et al., 1999) the planar polarity phenotypes of JNK pathway components are very weak, suggesting that these proteins may be at least partially redundant with other signalling components (Weber et al., 2000). An alternative model proposes that the specific localisation of PCP genes within the R3/R4 pair modulate Notch activity and ultimately contribute to the cell fate decisions between R3 and R4 (Strutt and Strutt, 2002).

One candidate for Factor X is the secreted protein Fj, which is expressed in an equatorial-polar gradient in the eye disc (Zeidler et al., 1999; Yang et al., 2002). However, mutations in *fj* produce only mild polarity phenotypes, suggesting that *fj* might act redundantly with other factors (Zeidler et al., 1999; Zeidler et al., 2000). Furthermore, *fj* does not interact genetically with *fz* and seems to regulate its own expression even in a *fz* mutant background, which is hard to explain if these proteins would in fact be a ligand-receptor pair (Zeidler et al., 1999; Zeidler et al., 2000; Adler, 2002). *fj*, *ft* and *ds* all display very similar phenotypes and have recently been proposed to act in concert to promote long range patterning in the eye (Adler, 2002; Yang et al., 2002). Ft has been shown to promote R3 cell fate in a *fz*-dependent manner, whereas *ds* promotes R4 cell fate in a *ft*-dependent manner. Ds is expressed in a gradient with its high point at the pole and is thought to inhibit Ft, which is uniformly expressed, in a concentration dependent manner. This leads to a gradient of Ft activity, which is high at the equator and low at the poles. In addition, in mosaic analysis *fj* promotes R3 cell fate in a *ds*-dependent manner, suggesting that *fj* functions upstream of *ds* to modulate its function (Adler, 2002; Yang et al., 2002).

One of the most exciting developments in the polarity field has been the finding that the core planar polarity proteins are asymmetrically localised within the cells in which PCP is established (reviewed in McNeill, 2002; Strutt, 2003; Fanto and McNeill, 2004). In the eye, these proteins show a striking asymmetric localisation at the apical membranes of R3/R4, whereas they appear evenly distributed or absent from other cells posterior to the furrow. The boundary between the R3 and the R4 cell has lately become the center of attention for many researchers in the field. It is believed that signalling across this boundary ultimately leads to specification of R4 and therefore ommatidial chirality. Interestingly, through clonal analysis it is possible to correlate localisation of a core PCP gene with its requirement for either R3 or R4 cell fate. Fz, for example is positively required in R3. In mosaic ommatidia where the clonal boundary separates the R3 and R4 cell, the Fz^+ cell

always develops as R3 and the Fz^- cell as R4. The same is true for Dsh and Dgo. An analysis of the protein localisation of these genes revealed, that they localise, at a certain developmental stage, strongly to the membrane of R3, where it directly contacts the R4 cell, and on the apical and polar membranes of R4. However, these proteins are absent from the equatorial membrane of R4. In contrast, Stbm and Prickle are required in R4. Both proteins localise to the equatorial membrane of R4 and also to the equatorial membrane of R3, in a pattern opposite to that of Fz, Dsh and Dgo. Fmi, required in both cells, is thought to be localised to both sides of the R3/R4 boundary. Fmi staining in a third instar eye imaginal disc is shown as an example of PCP protein localisation in Fig. 7B. By column 8, all core PCP proteins become strongly enriched at R4 membranes in a horseshoe-like pattern.

In summary, the current model of PCP establishment in the eye predicts that signalling across the membrane of the presumptive R3/R4 cells during the five-cell precluster stage leads to cell fate specification of R3/R4 and ultimately defines chirality of ommatidia and the direction of rotation. This process is thought to involve the core planar polarity genes as well as Delta/Notch signalling, and can be visualised by the specific localisation pattern of the polarity genes and by the Notch dependent *mδ-0.5lacZ* reporter (Fig. 7).

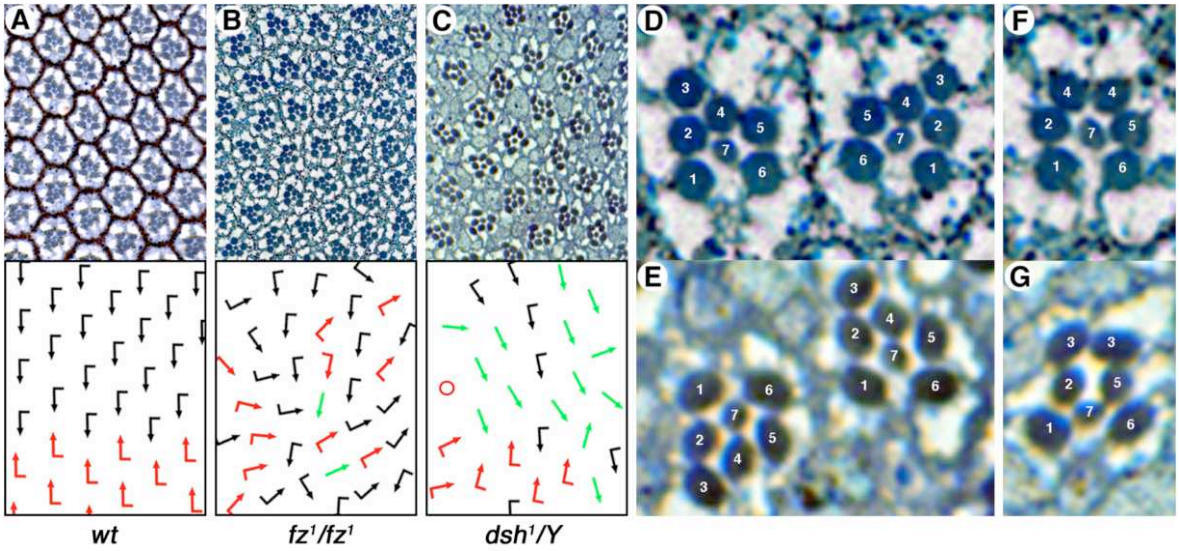

Figure 6. The eye phenotype of planar polarity mutants

(A-C) Tangential sections through equatorial regions of adult *Drosophila* eyes with schematic presentations indicating ommatidial chirality and rotation below the sections. Dorsal ommatidia are represented by black arrows and ventral ommatidia by red arrows. Symmetrical ommatidia are indicated by green arrows. Circles represent ommatidia with missing photoreceptors. (**A)** *wt*. (**B)** *fz*^{1}/*fz*^{1}. Note that in *fz*^{1} mutant eyes ommatidia with dorsal and ventral chirality are distributed randomly throughout the eye and that some ommatidia have lost their chirality and become symmetrical. **(C)** *dsh*^{1}/*Y*. In *dsh*^{1} hemizygous males many ommatidia are either R3/R3 or R4/R4 symmetric or show inverted chirality. **(D-G)** examples of polarity defects as seen in *fz*^{1} or *dsh*^{1} eyes. **(D)** A common phenotype in polarity mutants are anterior-posterior inverted ommatidia. The left ommatidium displays correct dorsal chirality, whereas the right ommatidium is inverted along the A/P axis. **(E)** Example of an ommatidium that is flipped along the dorsal-ventral axis (left) and a correct dorsal ommatidium (right). **(F, G)** Examples of symmetrical ommatidia. Ommatidia can either be R4/R4 symmetric (F) or R3/R3 symmetric (G). *fz*^{1} and *dsh*^{1} sections were kindly provided by Marek Mlodzik.

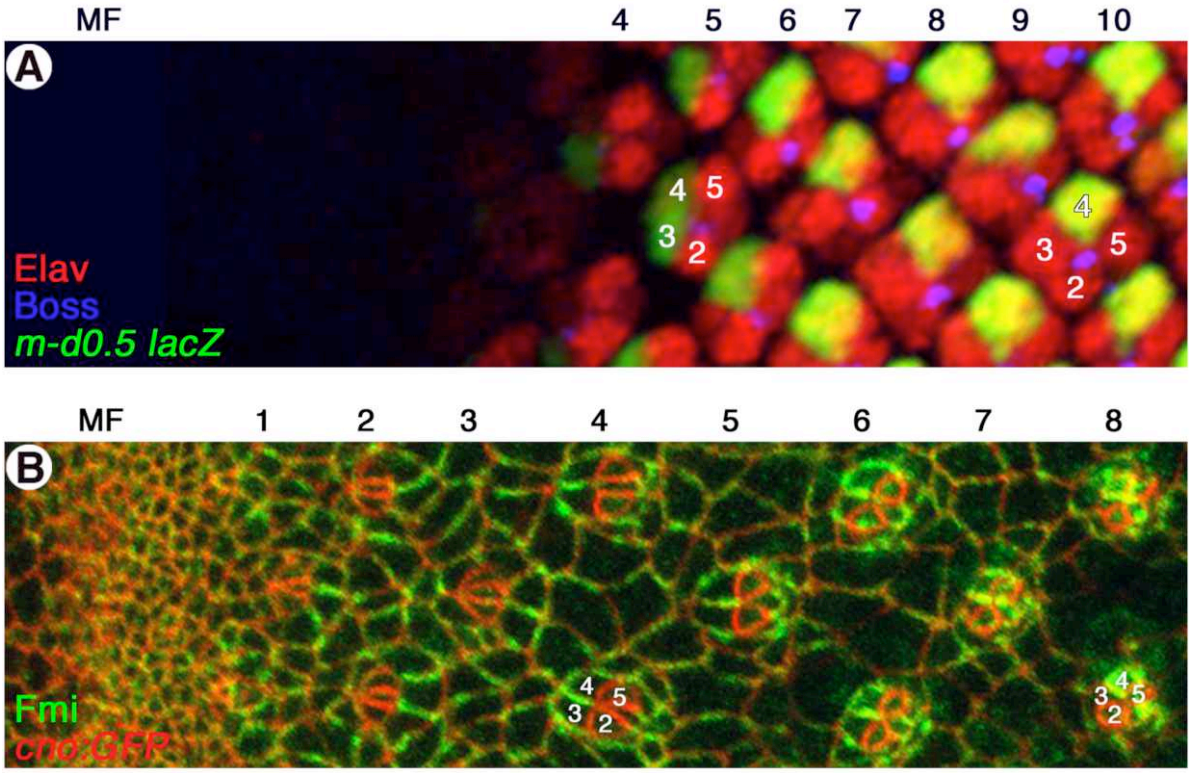

Figure 7. Polarity establishment in the eye disc can be visualised by different cellular markers

(A, B) Confocal images of third instar eye imaginal discs. The position of the morphogenetic furrow (MF) is indicated above each panel, as are the respective columns. The position of the photoreceptor cells R2/R5 and R3/R4 are indicated in selective ommatidial clusters by white numbers. Anterior is to the left and dorsal is up in both images. **(A)** The cell fate decision of the R3/R4 pair and hence ommatidial polarity can be visualised on the nuclear level using an *mδ0.5-lacZ* reporter transgene (green), which reflects Notch activity and indicates the R4 cell fate. Elav (red) marks all photoreceptors and Boss (blue) highlights the central R8. Note that by column six the R4 cell fate is specified, as mδ0.5-lacZ expression is restricted to only the R4 cell. **(B)** Alternatively, polarity establishment at the apical surface of the disc can be shown by the asymmetric localisation of the core planar polarity genes, here shown for Flamingo (Fmi, green). *cno:GFP* highlights the membranes of all cells and is strongly enriched in R2/R5. Posterior to the MF Fmi is initially uniformly distributed around the membranes of all cells. By column 4, Fmi becomes enriched at the membranes in both cells of the R3/R4 pair. Starting at column 6, Fmi gets depleted from the membranes in R3 and enriched at R4 membranes. By column 8, Fmi is strongly enriched in R4 and almost completely depleted from R3 membranes.

Ommatidial rotation

Ommatidial rotation is commonly described as the last step of polarity establishment in the eye (Reifegerste and Moses, 1999; Mlodzik, 2002b). However, in contrast to well studied earlier events such as the Fz-mediated chirality within the R3/R4 pair (Cooper and Bray, 1999; Fanto and Mlodzik, 1999; Tomlinson and Struhl, 1999), ommatidial rotation is a rather poorly understood process. Only a few genes have been identified that specifically affect ommatidial rotation. The most prominent of these genes is *nemo* (*nmo*), the founding member of the Nemo-Like-Kinases (NLK's), a Serine/Threonine kinase-subfamily distantly related to MAP-kinases. In homozygous *nmo* mutants, ommatidia initially rotate normally, but then arrest at a 45° angle, suggesting that *nmo* is required for the second 45° of rotation (Choi and Benzer, 1994). Although NLKs have been implicated in TGF-β, NFκB, JNK and Wnt signalling, the relationship of nemo to these pathways remains obscure in *Drosophila* (Martin-Blanco, 2000; Verheyen et al., 2001; Mirkovic et al., 2002; Zeng and Verheyen, 2004). A second gene that appears to specifically affect ommatidial rotation is *roulette* (*rlt*). Prior to this thesis, the *rlt* locus had not been characterised. In mutants homozygous for *rlt,* ommatidia either under-rotate (less than 90°) or over-rotate (more than 90°, Choi and Benzer, 1994). Interestingly, *nmo* is epistatic to *rlt*, as *nmo/rlt* double mutants display the *nmo* phenotype. These results suggested that *rlt* is required downstream of *nmo* for the accurate completion of the rotation process (reviewed in Reifegerste and Moses, 1999; Mlodzik, 2002b). In addition, mutations in *laminin A* (*lamA*) have been found to disrupt ommatidial rotation (Henchcliffe et al., 1993a). However, this is only true for certain allelic combinations of *lamA* in which the phenotype is pleiotropic and not fully penetrant. *LamA* is a secreted component of the extracellular matrix and does not appear to exclusively affect rotation, as the number and arrangement of cone and pigment cells are often altered in *lamA* mutants (Henchcliffe et al., 1993a). In addition, a recent report identified the secreted protein *scabrous* (*sca*) as an important regulator of rotation (Chou and Chien, 2002). Sca is produced in the MF as well as in developing R8 cells and is thought to be transported via actin-based cellular extensions to more posterior columns, where it is required to control the stop of ommatidial rotation by antagonizing *nmo* activity (Chou and Chien, 2002). As mentioned above, ommatidial rotation is also clearly affected in most mutants of the core planar polarity genes. However, these genes are usually not classified as rotation genes since they primarily affect the R3/R4 cell fate decision. Although the R3/R4 cell fate decision has been shown to determine the direction of rotation, the rotation process as such is not generally impaired in mutants of the core PCP genes nor do the ommatidia show an obvious tendency to either under- or over-rotate (reviewed in Mlodzik, 2002b). However,

mutations in *rhoA* and *Drok* appear to affect predominantly the rotation aspect during polarity establishment (Strutt et al., 1997; Winter et al., 2001; Strutt et al., 2002).

To date, cell motility during the actual rotation process has not been studied and publications correlating rotation angles of ommatidia with their developmental stages or their relative distance posterior to the MF, have been inconsistent (compare Choi and Benzer, 1994; Reifegerste and Moses, 1999; Chou and Chien, 2002). Due to this inconsistency it seems necessary to accurately evaluate the rotation angles and correlate these angles with the developmental stage of the respective ommatidia (especially to determine an average ommatidial rotation angle for each column posterior to the MF). I started to evaluate the rotation angles of ommatidial clusters in third instar eye imaginal discs using several marker combinations. An example of such an eye disc and the respective ommatidial rotation angles is shown in Fig. 9. My results, though preliminary, permit four general conclusions. First, ommatidia generally do not initiate their rotation prior to column 4. Second, ommatidia undergo a rapid initial 45° rotation from the 4th to the 8th column. Third, over the next eight columns ommatidia continue their rotation approximately four times slower (compared to their rapid initial rotation) and reach an average angle of 75° ± 14° by column 16. Fourth, over the next 6-8 columns ommatidia progressively continue their rotation until they reach their final 90° position. Thus, ommatidial rotation can be described as a two-step process, in which a fast initial 45° rotation is followed by a slow second 45° rotation step.

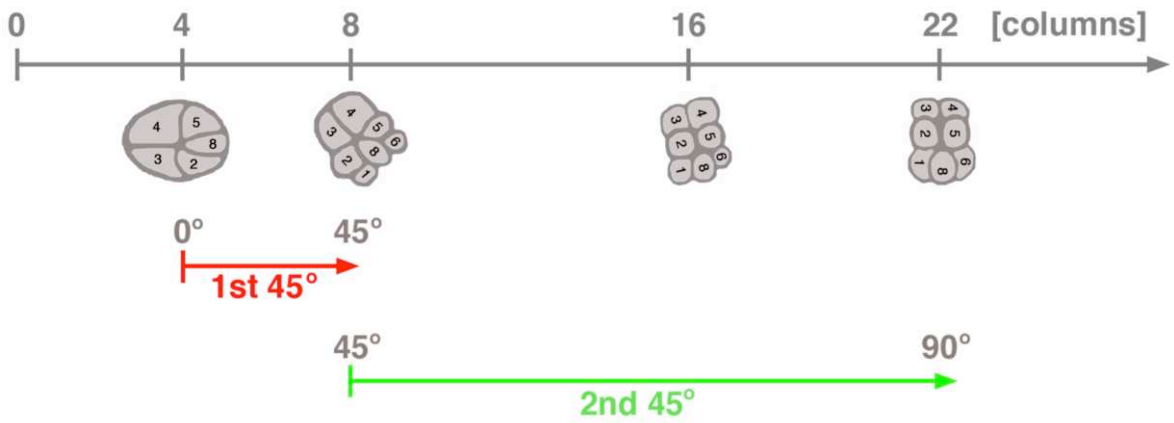

Figure 8. Ommatidial rotation is a two-step process

Schematic representation of ommatidial rotation angles as they are observed in a third instar eye imaginal disc (compare with Fig. 9). Ommatidia rotate in two 45° rotation-steps. A rapid initial rotation is usually initiated by column 4 and completed by column 8, where most clusters have reached 45° (indicated by the red arrow). Ommatidia then continue their rotation at a slower rate, until they reach their final 90° (indicated by the green arrow). Cartoons of typical ommatidia from columns 4, 8, 16 and 22 are shown as they rotate in a 3rd instar eye imaginal disc. Respective photoreceptors are indicated by black numbers.

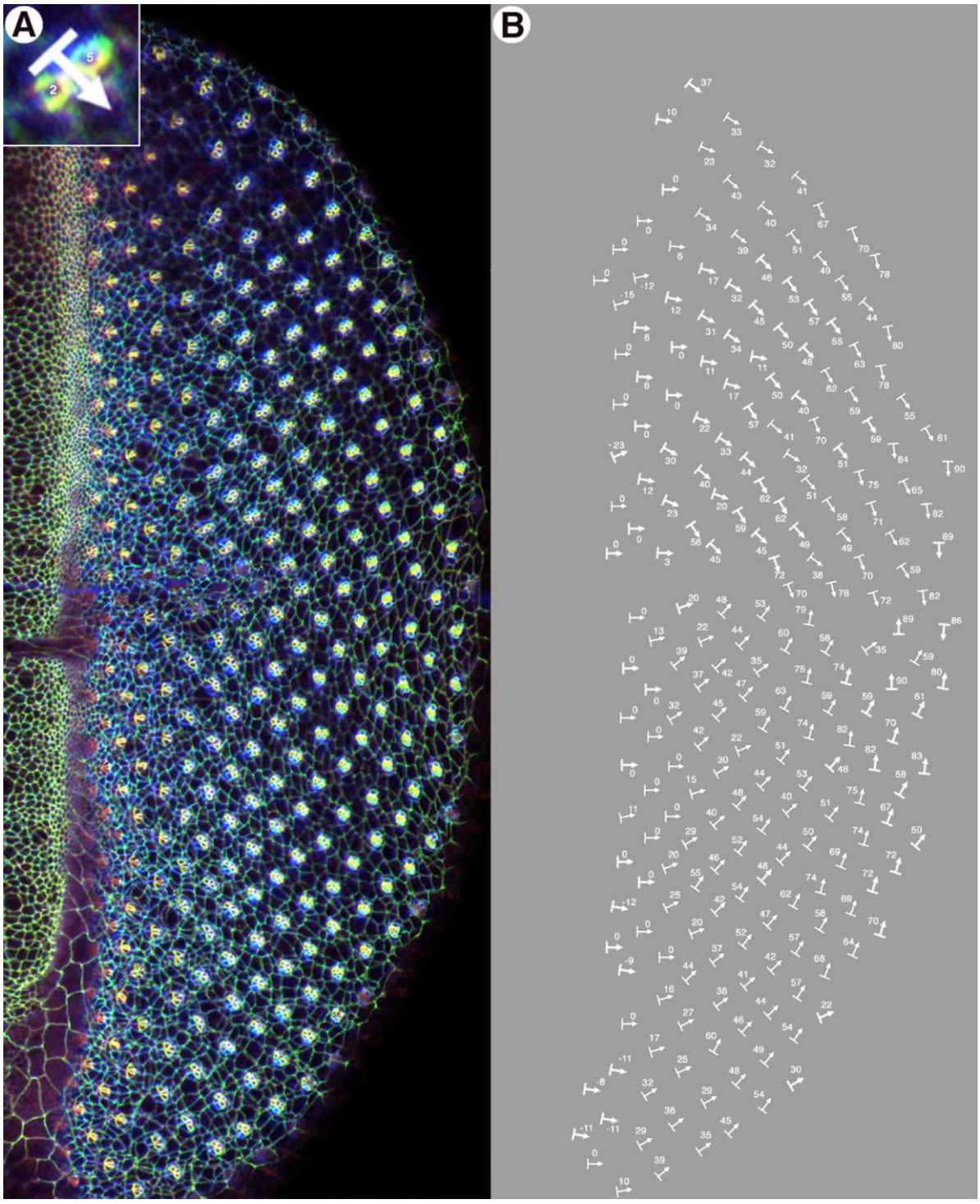

Figure 9. Ommatidial rotation as it occurs in a third instar eye imaginal disc

Confocal image of a third instar eye imaginal disc expressing a *cno:GFP* transgene (green) and stained for DE-cadherin (red) and Flamingo (blue). Cno:GFP highlights cell borders on the level of the adherense junctions and is strongly enriched in R2/R5, where it colocalises with DE-cadherin. Flamingo becomes strongly enriched in R4 by column 8 (see Fig. 7B for a detailed description of Fmi localisation). Ommatidial rotation angles are measured as shown in the enlarged insert in A), with the base of the arrow being parallel to the R2/R5 axis. **B)** Schematic representation of ommatidial rotation angles in the same disc.

A brief introduction to the Egfr signalling pathway

A substantial part of the work presented in this thesis is centered around Egfr signalling. This chapter therefore introduces the main components of the *Drosophila* Egfr pathway and outlines the key signalling mechanisms relevant for eye development (for in depth reviews see Casci and Freeman, 1999; Bogdan and Klambt, 2001; Shilo, 2003). The *Drosophila* genome encodes a single epidermal growth factor receptor that is equally similar to all four of its mammalian orthologues (the ErbB receptor family). The Drosophila EGF receptor (DER) is therefore considered to be a member of the family of prototypical receptors from which the mammalian ErbB genes evolved (Wadsworth et al., 1985; Schejter et al., 1986; Shilo et al., 1986). *Drosophila* Egfr is a type Ia transmembrane protein consisting of an extracellular ligand-binding domain, a hydrophobic membrane-spanning region and a cytoplasmic tail with intrinsic receptor tyrosine kinase activity. In its unstimulated form Egfr is present at the plasma membrane as a monomer. Upon ligand binding, monomeric receptors dimerize, leading to a trans-autophosphorylation of their cytoplasmic tails (Ullrich and Schlessinger, 1990). The phosphorylated tyrosine residues provide docking sites for various adaptor proteins containing Scr-homology (SH2) or phosphotyrosine binding (PTB) domains (Pawson and Scott, 1997). These adaptor proteins then activate the Ras/Raf/MAPK signal transduction cascades (see Fig. 10 for a schematic representation of the key signalling components). In contrast to mammals, where ErbB receptors are known to utilise several intracellular effector cascades (reviewed in Kazlauskas, 1994), *Drosophila* Egfr signalling almost always passes through Ras (Casci and Freeman, 1999).

Our understanding of the Egfr signal transduction pathway is greatly influenced by studies on another RTK, the *sevenless* (*sev*) gene. Pioneering work in the early 90's revealed that Sev utilises the Ras/Raf/MAPK signal transduction cassette (Simon et al., 1991; Dickson et al., 1992; Olivier et al., 1993; Simon et al., 1993; Biggs et al., 1994; Brunner et al., 1994b). The same conserved Ras/Raf/MAPK cassette was later shown to signal downstream of Egfr (Diaz-Benjumea and Hafen, 1994). Besides the Ras/Raf/MAPK signalling cassette, many additional molecules have been shown to transmit or regulate Egfr signalling. A list of these genes indicating their function and relevant references is given in Table 1. Although the biology of the core elements of this pathway is well understood, the epistatic relationship and/or exact role of many of the additional factors regulating Egfr signalling is not established in sufficient detail. I will therefore focus my description of Egfr signalling components on the well-established core proteins of this pathway and only introduce other factors if they are of direct relevance to my work.

Ligands activating the Egf receptor

Four secreted ligands have been shown to bind to and activate the Egf-receptor. The most prominent ligand is Spitz (Spi), a TGF-α like growth factor that is the major Egfr ligand in most developmental contexts (Rutledge et al., 1992). Spi is produced as an inactive transmembrane precursor and only becomes an active ligand after its EGF domain is proteolytically cleaved and released from the cell surface (Freeman, 1994b; Schweitzer et al., 1995b). Processing of Spi is the main mechanism by which Egfr signalling in *Drosophila* is regulated, since both the Egf receptor and Spitz are ubiquitously expressed. A second ligand, Keren, is closely related to Spi and is regulated in a similar manner (Reich and Shilo, 2002). Keren may complement Spi's activity in certain tissues, but since no mutants of Keren have been described, this has yet to be confirmed. A third Egfr ligand, Gurken, is also a TGF-α-like growth factor, but its expression is limited to the female germline (Neuman-Silberberg and Schupbach, 1993). Vein, the fourth ligand, is a neuregulin-like molecule which, in addition to the core EGF domain, also contains immunoglobulin repeats (Schnepp et al., 1996). Vein is produced as an active ligand and its secretion does not require the ligand processing machinery that processes Spi, Keren and Gurken.

The Egfr ligand processing machinery

One of the most exciting insights that refined our understanding of Egfr signalling comes from a number of recent papers clarifying the biochemical function of the ligand processing machinery - namely Star (S) and Rhomboid (Rho) proteins (Wasserman et al., 2000; Urban et al., 2001; Urban et al., 2002; reviewed in Klambt, 2002; Shilo, 2003). S and Rho functions are best studied in Spi processing, but Keren and Gurken appear to be processed in a similar manner by these proteins. The first regulated step in Spitz processing is its trafficking from the endoplasmatic reticulum (ER) to the Golgi apparatus (Golgi). This step is controlled by S, a novel type II transmembrane protein that serves as a cargo receptor for Spi (Kolodkin et al., 1994; Lee et al., 2001; Tsruya et al., 2002). In the Golgi the inactive Spi transmembrane precursor is cleaved by Rho, a novel type of sevenpass-transmembrane serine protease (Urban et al., 2001; Urban et al., 2002). Cleaved Spi is then transported to the plasma membrane, from which it is then released. In contrast to Spi and Star, which are both widely expressed, Rho expression is extremely dynamic and exactly correlates with Egfr-induced MAPK activation (Gabay et al., 1997). It is therefore believed that Rho expression is the limiting step of DER activation in the eye imaginal disc (Shilo, 2003, summarized in Fig.11).

Signalling components downstream of Egfr

Ligand binding leads to a dimerisation of receptor monomers and subsequently to an autophosphorylation in trans on tyrosine residues in their cytoplasmic tails (Ullrich and Schlessinger, 1990). The phosphorylated tyrosine residues provide docking sites for various adaptor proteins with SH2 or PTB domains (Pawson and Scott, 1997). The most prominent of these adapter proteins is Downstream of receptor kinase (DRK), a GRB2 orthologue (Simon et al., 1993; Raabe et al., 1995). DRK binds to the cytoplasmic tail of Egfr via its SH2 domains and recruits the guanine nucleotide exchange factor Son of Sevenless (Sos, Rogge et al., 1991; Simon et al., 1991). Sos in turn stimulates the exchange of GTP for GDP on the small G-protein Ras1 (often simply called Ras, Simon et al., 1991). However, in order to exert its full enzymatic activity Ras requires the presence of the GTPase activating protein GAP1 (Gaul et al., 1992). Activated Ras subsequently signals via a Mitogen activated protein kinase (MAPK) cascade consisting of the serine/threonine kinase D-Raf (a MAPKKK, Dickson et al., 1992), the dual specific kinase Downstream suppressor of raf (Dsor or D-Mek, a MAPKK) that phosphorylates its substrate kinase at threonine and tyrosine residues (Tsuda et al., 1993) and Rolled (Rl, an ERK like MAPK, Biggs et al., 1994) that further transduces the signal to nuclear factors (Fig. 10).

Nuclear factors downstream of Egfr

Doubly phosphorylated Rolled is translocated into the nucleus, where it phosphorylates and thereby activates the ETS domain transcription factor Pointed P2 (Pnt Brunner et al., 1994a). Pnt P2 in turn activates the transcription of target genes (discussed below). In addition to PntP2, Rolled has another nuclear target – the transcriptional repressor Yan (also called Anterior open or Aop) which also contains an ETS domain (Lai and Rubin, 1992). Unphosphorylated nuclear Yan protein serves as a transcriptional repressor. Upon phosphorylation, Yan is translocated into the cytoplasm where it is rapidly degraded (O'Neill et al., 1994; Rebay and Rubin, 1995). Thus, Rolled regulates transcription at ETS binding sites by activation of Pnt and inactivation of Yan (Fig 10).

Egfr target genes

More than 200 ETS target genes have been identified in mammalian cell culture experiments. (For a general review on transcriptional regulation by MAPK signalling cascades and on ETS target genes see Sementchenko and Watson, 2000; Yordy and Muise-Helmericks, 2000; Yang et al., 2003). In contrast, surprisingly little is known about the direct target genes of the ETS transcription factor Pointed in *Drosophila*. DER signalling in the embryo was shown to have primary and secondary target genes (Gabay et al., 1996). A

high level of DER activity in the ventral-most cells of the embryo triggers expression of a set of primary target genes encoding Ventral nervous system defective (vnd), Fasciclin III and Pointed P1. Interestingly, the pointed gene contains two promoters separated by 50 kb, which generate two alternative transcripts: Pointed P1 and Pointed P2. Pointed P1 acts as a constitutively active transcriptional activator, while Pointed P2 requires phosphorylation via the MAPK Rolled to become activated (Klambt, 1993; Brunner et al., 1994a; O'Neill et al., 1994). Pointed P1 regulates the transcription of secondary target genes such as *orthodenticle*, *argos* and *tartan* (Gabay et al., 1996). One of the few established target genes in the eye is *phyl*, a gene required for proper development of R1/R6 and R7 (Chang et al., 1995; Dickson et al., 1995). In addition, Rhomboid expression was found to be regulated in response to DER signalling (Sapir et al., 1998; Wasserman and Freeman, 1998). As mentioned above Rho expression is the critical step for ligand processing and subsequent DER activation as both receptor and ligand are widely expressed. In addition, it has recently been shown that Argos, Kekkon-1 and Sprouty - three negative regulators of Egfr activity - are direct targets of Ras/MAPK/Pointed signalling (discussed below).

Negative regulators of Egfr signalling

In recent years it has become clear that negative regulators of Egfr play a key role in controlling the complex signalling profiles required for developmental pattern formation (reviewed in Casci and Freeman, 1999; Bogdan and Klambt, 2001; Shilo, 2003). One negative regulator of Egfr activity is the secreted protein Argos (Aos). Aos contains an atypical EGF motif and was long believed to be an inhibitory ligand for Egfr itself. However, a recent publication demonstrated that Aos directly binds to Spitz and downregulates Egfr activity by ligand sequestration (Klein et al., 2004). A second negative regulator is Kekkon-1, a single pass transmembrane protein containing immunoglobulin and leucine-rich repeats. In contrast to Argos, Kekkon-1 binds directly to the extracellular domain of the EGF receptor. Sprouty (Sty) is a third inhibitor of Egfr signalling. However, in contrast to Aos or Kekkon-1, Sty is not specific for Egfr and might inhibit all RTK-mediated signalling. Sty binds to DRK and to RasGAP1. RasGAP1 inhibits Ras function by converting GTP bound Ras into the inactive GDP bound stage. Sty is thus believed to downregulate Ras function by recruiting GAP1 to the active signalling complex and by sequestering DRK away from the receptor (Casci et al., 1999). As mentioned above Aos, Kekkon-1 and Sty are all direct transcriptional targets of the Egfr signalling pathway and form a negative feedback loop to restrict its activity (Casci and Freeman, 1999; Shilo, 2003). Interestingly, each of these negative regulators uses a different mechanism to downregulate signalling activity and each factor works in a different range. Aos inhibits activation of Egfr in a non cell-autonomous

manner, as it has been shown to diffuse several cell diameters away from its source. Kekkon-1 is localised to the cell surface and might inhibit Egfr in the same or in directly adjacent cells. In contrast, Sty inhibits Ras signalling in a strictly cell autonomous manner (Fig. 11).

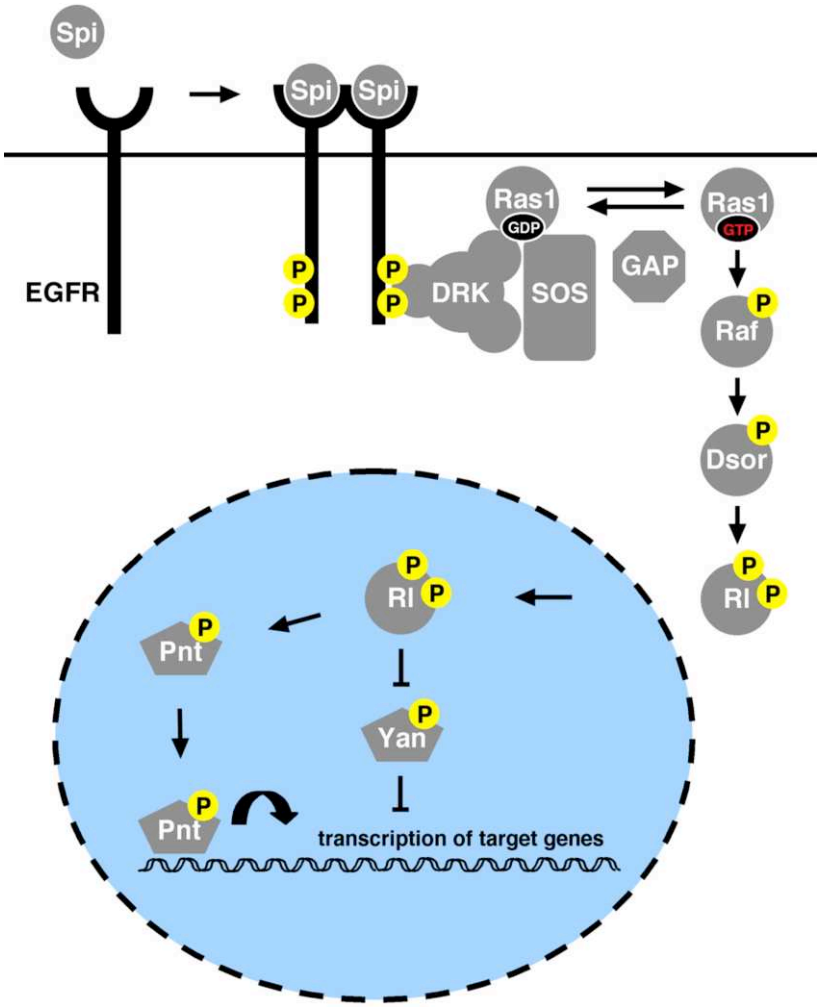

Figure 10. The Egfr signal transduction pathway in *Drosophila*

This cartoon shows a simplified scheme of the core Egfr pathway components. Factors whose exact role or position is still uncertain are, for clarity, not shown. (For a full list of signalling components and relevant references see Table 1). Upon ligand binding, monomeric Egf receptors dimerize, which leads to a phosphorylation in trans of their cytoplasmic tails on several tyrosine residues. The phosphorylated tyrosines provide docking sites for various adaptor proteins like DRK, which in turn recruits the Guanine nucleotide exchange factor SOS. SOS stimulates the exchange of GTP for GDP on the small GTP'ase Ras1, which subsequently signals via a conserved MAPK cascade consisting of the serine/threonine kinase Raf (a MAPKKK), the dual specific kinase Dsor (a MAPKK) and RI (an ERK like MAPK). Upon activation, RI translocates to the nucleus where it activates the ETS domain transcription factor Pnt P2. In addition to Pnt P2, RI also phosphorylates the transcriptional repressor Yan. Upon phosphorylation Yan translocates to the cytoplasm, where it is rapidly degraded. Thus Rolled regulates transcription at ETS binding sites by activation of Pnt and inactivation of Yan.

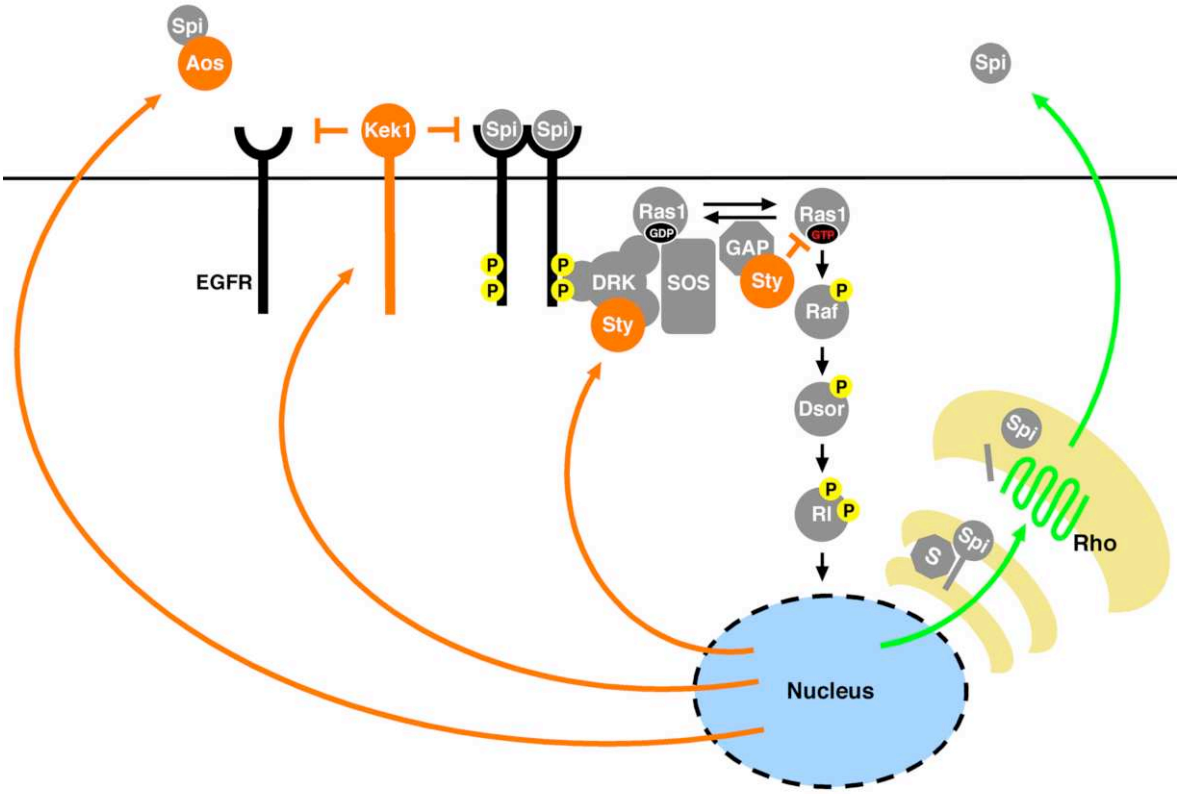

Figure 11. Feedback loops induced by high level Egfr signalling

High-level Egfr signalling induces several negative and positive feedback loops. With Aos, Kek1 and Sty, three negative regulators of Egfr signalling have been found to be direct transcriptional targets of the Ras/MAPK pathway (shown in orange). All three negative regulators use a different mechanism to repress signalling activity. The secreted protein Aos inhibits activation of Egfr in a non cell-autonomous manner, as it has been shown to diffuse several cell diameters away from its source. Kekkon-1 is expressed at the cell surface and might inhibit Egfr in the same or in directly adjacent cells. Sty inhibits Ras signalling in a strictly cell autonomous manner as it sequester DRK away from the receptor and recruits the negative regulator GAP to the active signalling complex. A positive feedback loop is primarily mediated via elevated Rho expression (shown in green). Rho expression is the limiting step of Spi processing and subsequent DER activation, as both the receptor and its ligand are widely expressed. On it's way from the ER to the Golgi, membrane bound Spi is chaperoned by S, its cargo receptor. In the ER, the Spi-transmembrane precursor is proteolytically cleaved by the serine protease activity of Rho and subsequently secreted as an active ligand.

Table 1. *Drosophila* genes involved in Egfr/Ras signalling

Gene	Function	Reference
Activating Egfr ligands:		
Spitz	TGF-α homologue, main activating ligand in the eye	(Rutledge et al., 1992; Freeman, 1994b)
Gurken	TGF-α homologue	(Neuman-Silberberg and Schupbach, 1993)
Keren	TGF-α homologue	(Reich and Shilo, 2002)
Vein	Neuregulin-like	(Schnepp et al., 1996)
Ligand processing machinery:		
Star	Chaperon, required for ligand transport from the ER to the Golgi	(Kolodkin et al., 1994; Lee et al., 2001)
Rhomboid	Atypical intra-membrane serine protease, require for ligand processing	(Bier et al., 1990; Urban et al., 2001; Urban et al., 2002)
Signalling factors:		
Corkscrew	SH2-domain protein tyrosine phosphatyase	(Allard et al., 1996; Perkins et al., 1996)
Downstream of receptor kinase (DRK)	SH2-SH3-SH2 adapter protein (Grb2 homologue)	(Simon et al., 1993), (Raabe et al., 1995)
Son of sevenless	Guanine nucleotide exchange factor	(Rogge et al., 1991; Simon et al., 1993)
Gap1	GTPase activating protein	(Gaul et al., 1992)
Ras1	GTPase	(Simon et al., 1991)
RasGAP (p120)	GTPase activating protein	(Cleghon et al., 1998; Feldmann et al., 1999)
D-Raf	MAPKKK	(Dickson et al., 1992)
Ksr	Kinase	(Therrien et al., 1995)
Connector enhancer of Ksr (Cnk)	Raf binding protein	(Therrien et al., 1998)
Leonardo	14-3-3 adapter protein	(Kockel et al., 1997; Li et al., 1997)
Dsor (D-Mek)	Serine/Threonine MAPKK	(Tsuda et al., 1993)
Rolled	MAPK	(Biggs et al., 1994)
PP2A	Serine/Threonine protein phosphatase	(Karim et al., 1996; Wassarman et al., 1996)
Twins	Regulatory subunit of PP2A	(Uemura et al., 1993; Shiomi et al., 1994)
Shc	Adapter protein	(Lai et al., 1995; Li et al., 1996)
Disabled	PTB-domain protein, putative adapter protein	(Le and Simon, 1998)
Daughter of sevenless	PH-domain protein	(Herbst et al., 1996; Raabe et al., 1996)
Nuclear factor:		
Pointed	ETS-domain transcription factor	(Brunner et al., 1994a)
Yan	ETS-domain transcription factor, negative regulator of EGFR signalling	(Lai and Rubin, 1992)
Phyllopod	Nuclear protein	(Chang et al., 1995; Dickson et al., 1995)
Prospero	Homeo-domain protein	(Kauffmann et al., 1996)
Negative regulators of Egfr signalling:		
Argos	Secreted protein, binds and sequesters Spitz, negative regulator	(Freeman et al., 1992; Schweitzer et al., 1995a; Klein et al., 2004)
Kekkon-1	Membrane bound inhibitory ligand of EGFR	(Musacchio and Perrimon, 1996; Ghiglione et al., 1999)
Sprouty	Membrane associated, binds and inhibits Gap1 and Drk	(Hacohen et al., 1998; Casci et al., 1999)
Small wings	PLCγ, negative regulator of Ras	(Thackeray et al., 1998)
D-Cbl	Docking protein, negative regulator	(Hime et al., 1997; Meisner et al., 1997)
Cofactors:		
Canoe	Multidomain protein localised to adherense junctions	(Matsuo et al., 1997)

II
Results

The *roulette* phenotype

rlt was identified as a spontaneous mutation causing a rough-eye phenotype (Choi and Benzer, 1994). Flies homozygous for the *rlt* locus are viable and fertile and aside from the roughened eye structure no other phenotype is obvious. Tangential sections through adult eyes reveal severe defects in ommatidial rotation (Fig. 12A), whereas overall ommatidial architecture and cell fate specification seem largely normal. Most ommatidia in *rlt* eyes display a wt complement of photoreceptors as well as pigment and cone cells (Fig. 12A and B). A small number of ommatidia, however, have one extra outer photoreceptor (Fig. 12A and C). The percentage of ommatidia with extra photoreceptors varies from eye to eye but is on average 6.1 ± 4.1% (out of 1065 ommatidia in seven eyes scored). This finding is in general agreement with published data, in which 17% (out of 545 ommatidia in 4 eyes scored) extra photoreceptors are reported (Choi and Benzer, 1994), although in my analysis the percentage of extra photoreceptors appears to be smaller (Fig. 12E). A very small fraction of ommatidia 1.6 ± 1.5% (17 out of 1065 ommatidia in seven eyes scored) appear to be symmetrical and 0.5 ± 0.5% (5 out of 1065 ommatidia in seven eyes scored) of ommatidia seem to have inverted chirality (Fig. 12D and E). Neither symmetrical ommatidia nor ommatidia with inverted chirality have been previously reported in *rlt* eyes, but their contribution to the overall phenotype is almost negligible.

In contrast to wt eyes, in which all ommatidia are rotated 90º with respect to the equator, ommatidial rotation angles in *rlt* eyes show a very broad distribution (Fig. 12F and G). Interestingly, ommatidia that under-rotate (less than 90º) or over-rotate (more than 90º) are frequently observed (Fig. 12G). An analysis of the rotation angles of 634 ommatidia from 4 eyes homozygous for *rlt* revealed that over- and under-rotated ommatidia are present at about the same percentage, with 40.7% of ommatidia being under-rotated (less than 80º) and 38.5% of ommatidia being over-rotated (more than 100º). For this analysis, ommatidia that were rotated between 80º and 100º were counted as wt-oriented ommatidia since a 10º variation to either side is generally considered a ‘wobble’ rather than a mis-rotation. The distribution of rotation angles in *rlt* eyes are not random, but rather resemble a Gaussian distribution in which the highest peak (21.1 ± 4.2%) represents ommatidia that have rotated between 80º and 100º. The slopes of this distribution are formed by under and over-rotated ommatidia with decreasing percentages as rotation angles get more extreme (Fig. 12G).

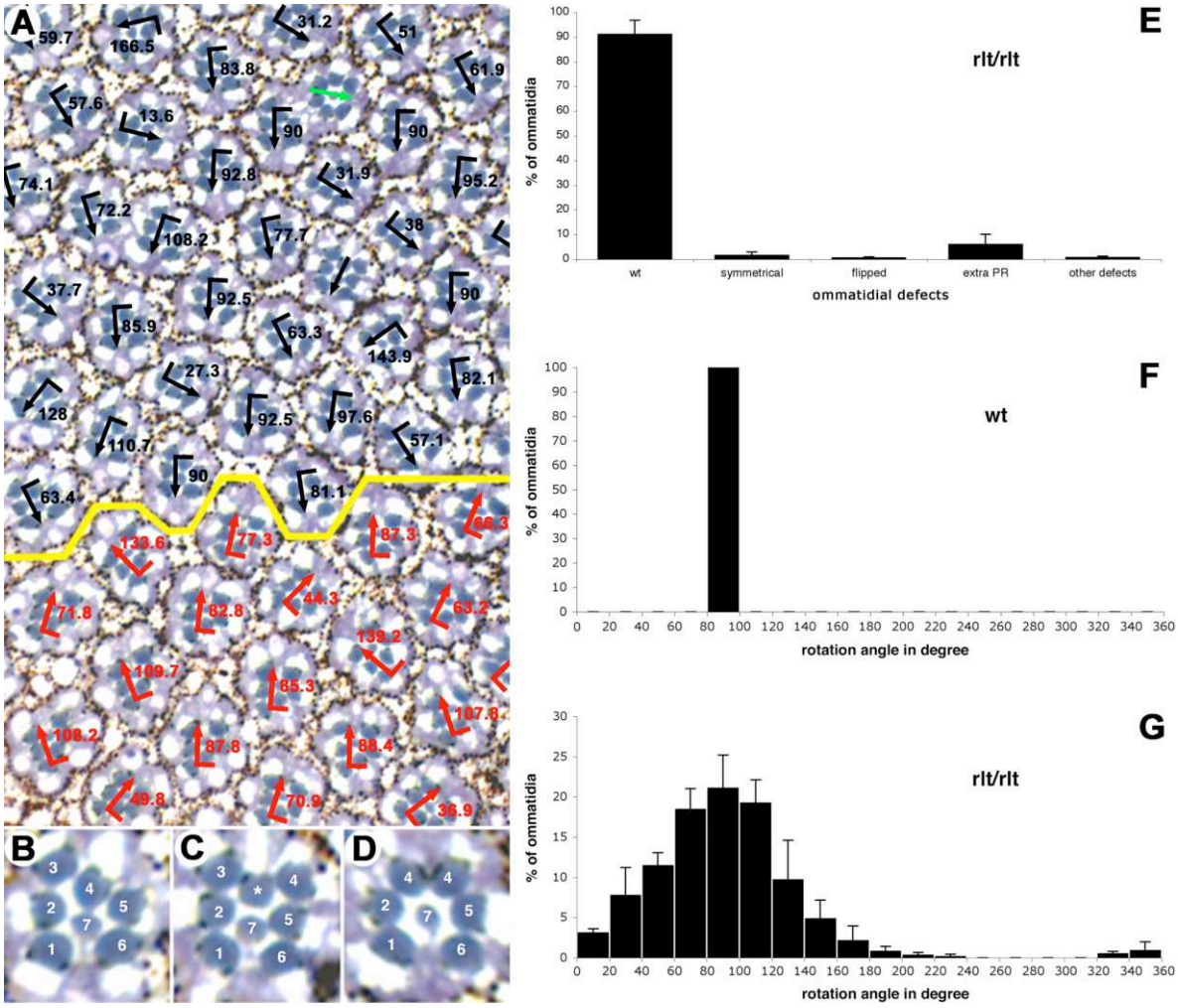

Figure 12. The *roulette* phenotype

(A-D) Tangential sections through an adult *rlt* eye. **(A)** A large section around the equator (yellow line) with schematic representation of ommatidial rotation angles by arrows. Flagged arrows indicate ommatidia with a wt complement of photoreceptors and numbers the respective rotation angle. Dorsal ommatidia are represented by black arrows and ventral ommatidia by red arrows. Ommatidia with an extra photoreceptor are indicated by non-flagged arrows and symmetrical ommatidia are represented by green arrows. **(B)** Example of a typical ommatidium from (A) with a *wt* complement of PRs. **(C)** Single ommatidium from (A) displaying an extra PR indicated by a star. **(D)** Rare example of a symmetrical ommatidium of the R4/R4 type from (A). **(E)** Diagram indicating ommatidial defects in *rlt* eye. **(F, G)** Evaluation of rotation angles in *wt* and *rlt* eyes. Note that ommatidia in *wt* eyes rotate 90°, whereas ommatidia in *rlt* eyes show a broad range of rotation angles, resembling a Gaussian distribution.

roulette is a rotation-specific allele of the secreted Egfr inhibitor *argos*

The *roulette (rlt)* locus was originally described as a spontaneous mutation on the third chromosome. However, the mutation was only roughly mapped and the responsible gene was not identified (Choi and Benzer, 1994). To map the *rlt* region more precisely, I screened overlapping deficiencies for non-complementation of the rough eye phenotype. The smallest non-complementing deficiency Df(3L) st7P allowed me to restrict the *rlt* locus to 73A2-73A7, on the left arm of the third chromosome (Fig. 13).

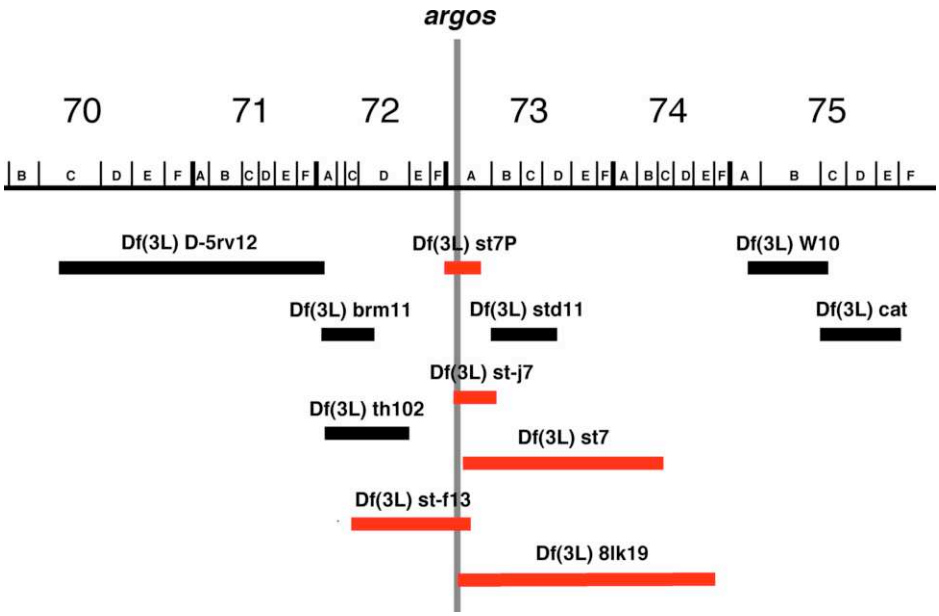

Figure 13. Deficiency mapping of the *roulette* locus

Deficiencies complementing *rlt* are shown in black. Deficiencies that fail to complement *rlt* are shown in red. The region of non-complementation could be restricted to 72A2-73A7 on the left arm of the third chromosome. The vertical grey line at 73A2 indicates the genomic location of the *argos* gene.

Complementation analysis with candidate genes within this region revealed that alleles of the secreted Egfr inhibitor *argos* (*aos*, Freeman et al., 1992) failed to complement *rlt* (Fig. 14C). Trans-heterozygous mutant combinations of *rlt/aos*^{W11}, *rlt/aos*$^{\Delta 7}$ and *rlt/Df(3L)st7P(aos*$^{-}$*)* displayed very similar phenotypes with rotation defects resembling homozygous *rlt* eyes (Fig. 14 B, C, D and not shown). In addition, the extra photoreceptor phenotype seen in a small number of *rlt* ommatidia is enhanced in *rlt/aos*^{W11}, *rlt/aos*$^{\Delta 7}$ and *rlt/Df(3L)st7P(aos*$^{-}$*)* combinations (Fig. 14 B, C, D and not shown). This is intriguing, as the most prominent phenotype of strong *aos* alleles (like *aos*^{W11}) and *aos* null clones (like *aos*$^{\Delta 7}$) is 1-2 extra photoreceptors per ommatidium due to a lack of inhibition of Egfr activity during early photoreceptor specification (Freeman et al., 1992). Thus, genetically *rlt* behaves as a hypomorphic loss-of-function allele of *aos.*

The genetic behavior of *rlt* as a hypomorphic loss-of-function allele strongly suggested that the associated ommatidial rotation phenotype is caused by the lack of Argos protein. To test this hypothesis, I attempted to rescue *rlt* with an *aos* transgene. A *sev-aos* transgene, which drives expression of *aos* under the control of the *sevenless* enhancer in a pattern overlapping with the endogenous *aos* expression pattern, had previously been shown to rescue the argos loss-of-function phenotype and had no dominant effect on eye development by itself (Freeman, 1994a). In fact, the *sev-aos* transgene was sufficient to completely rescue aos^{rlt} (Fig. 14E).

These results confirm that loss-of-*aos*-function is causing the ommatidial rotation defects associated with the *rlt* locus, and identify *rlt* as a rotation-specific hypomorphic allele of *aos*. Furthermore, the *sev-aos* rescue of *rlt* excludes the unlikely possibility of a trans-heterozygous-dominant interaction between *rlt* and *aos*. Hereafter, I will refer to the *rlt* allele as aos^{rlt}.

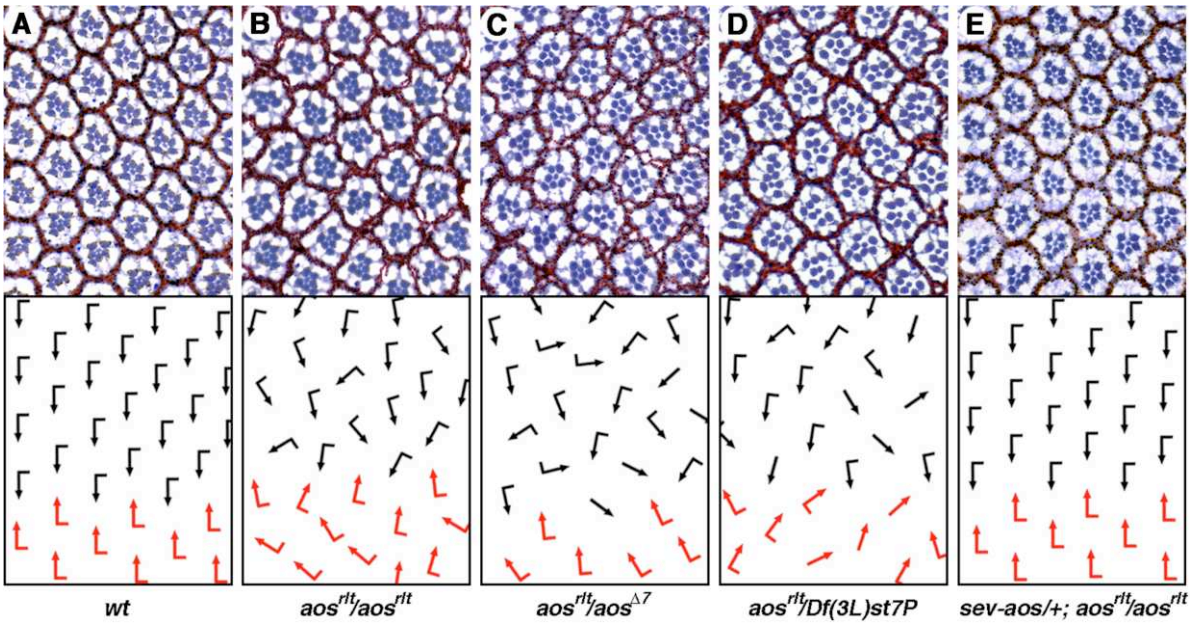

Figure 14. The *roulette* mutant is a rotation-specific allele of the secreted Egfr inhibitor *argos*

(A-E) Tangential sections through equatorial regions of adult *Drosophila* eyes with schematic presentations indicating ommatidial rotation below the sections. Dorsal ommatidia are indicated with black arrows, and ventral ommatidia are indicated with red arrows. Ommatidia with a wt number of photoreceptor cells are represented by a flagged arrow, whereas ommatidia with extra photoreceptors are indicated with a non-flagged arrow. **(A)** *wt*, the two chiral forms of ommatidia in the dorsal and ventral halfs are rotated 90° with respect to the equator. **(B)** aos^{rlt}/aos^{rlt}, note the broad range of rotation angles. **(C, D)** $aos^{rlt}/aos^{\Delta 7}$ and $aos^{rlt}/Df(3L)st7P$ eyes, respectively. Note that ommatidial rotation defects are similar to aos^{rlt} and that the number of ommatidia with extra photoreceptors is increased. **(D)** $aos^{rlt}/Df(3L)st7P$, ommatidial rotation defects are similar to aos^{rlt}/aos^{rlt} and the number of extra photoreceptors is increased. **(E)** sev-aos/+; aos^{rlt}/aos^{rlt} flies show completely rescued ommatidial rotation and architecture. In all panels anterior is to the left and dorsal is up.

Molecular characterisation of the *roulette* locus

The molecular characterisation of *rlt* was guided by genetic evidence, suggesting that *rlt* was a regulatory allele of *aos*. As mentioned above, aos^{rlt} behaves as a hypomorphic allele in the eye and, in contrast to other alleles of *aos*, the *rlt* mutation does not show obvious developmental defects in other tissues (Freeman et al., 1992; Choi and Benzer, 1994). Regulatory mutations often affect the non-coding region of a gene without altering the coding sequence. I therefore analysed the genomic region of the *aos* gene in homozygous *rlt* flies using overlapping PCR primer sets in hope of finding a difference in one of the PCR products. Two of the overlapping primer sets resulted in PCR products that were approximately 1kb larger than in the *wt* control (not shown). Sequencing of these PCR products revealed a truncated P-element inserted within the 5' untranslated region (5' UTR) of the *aos* gene, 570bp upstream of the translation start side (Fig. 15 and 16).

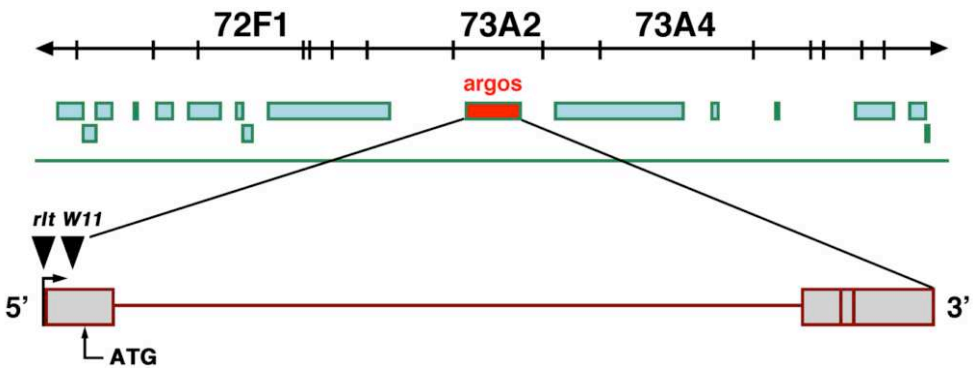

Figure 15. Position of *roulette* and the $argos^{W11}$ P-element insertions within the 5'UTR of *argos*

Schematic representation of the genomic organization of the *argos* gene. The 5' - 3' orientation is indicated. The four exons of the *argos* gene are represented by red-boxed rectangles. The large first intron is represented by a red line. Black arrowheads indicate the position of *rlt* and *w11* P-element insertions within the 5' UTR of the *argos* gene. The *rlt* P-element is situated 570bp upstream of the translation start side and the W11 P-element 544bp, respectively. The translation start site is indicated with ATG.

```
1     CACAGACACG CACATACCGG CAGCGACGCG AGCAGCGCAC TTCTCTGCCG GCTTCAACGG CTCTCGTTCG
71    CCGCGCGCTG TTCGTTTTTG GATTTTCTGT TTGATCCATG ATGAAATAAC ATAAGGTGGT CCCGTCGGCA
141   AGAGACATCC ACTTAACGTA TGCTTGCAAT AAGTGCGAGT GAAAGGAATA GTATTCTGAG TGTCGTATTG
211   AGTCTGAGTG AGACAGCGAT ATGATTGTTG ATTAACCCTT AGCATGTCCG TGGGGTTTGA ATTAACTCAT
281   AATATTAATT AGACGAAATT ATTTTTAAAG TTTTATTTTT AATAATTTGG AGTTTCCAAT TAACTTTTGT
351   TTTTGATTTT TAATTTCAAT TTTTTTGTTG AAGTACTTAA TTCTAAAATA TATTCTAATT TTAAAATAAA
421   AAGATTTTAC TTGTTTATCA ACATCGACGT TTCGCGCTGC TAATATTAAT TTTTCCTTTA CATTATTGTC
491   TTTTTTATTT ATTTATTGTC TTTTTATGTC CACATCTGAT AACCATCTGT ACAAAGTCGT ACGACTGGGC
561   AAAGGAAATC CTTTTTTGTA CAGATGGTTA TACGCTCGAG GGCCTGCGGT GTGGAGACAA ATAGCTGTAG
631   AAATGTCGTC GGAATTGAAC GTAGCTCTTT GTCCACCATT CTTCAGTATC CGTATCTGCG TGTCCGTGAA
701   GATTTTGCGT AGAGACTCCT CCAACTGTTG AGACTCCCTC AGCTGCTGCT CTAAACGACG CATTTCGTAC
771   TCCAAAGTAC GAATTTTTTC CCTCAAGCTC TTATTTTCAT TAAACAATGA ACAGGACCTA ACGCACAGTC
841   ACGTTATTGT TTACATAAAT GATTTTTTTT ACTATTCAAA CTTACTCTGT TTGTGTACTC CCACTGGTAT
911   AGCCTTCTTT TATCTTTTCT GGTTCAGGCT CTATCACTTT ACTAGGTACG GCATCTGCGT TGAGTCGCCT
981   CCTTTTAAAT GTCTGACCTT TTGCAGGTGC AGCCTTCCAC TGCGAATCAT TAAAGTGGGT ATCACAAATT
1051  TGGGAGTTTT CACCAAGGCT GCACCCAAGG CTCTGCTCCC ACAATTTTCT CTTAATAGCA CACTTCGGCA
1121  CGTGAATTAA TTTTACTCCA GTCACAGCTT TGCAGCAAAA TTTGCAATAT TTCATTTTTT TTTATTCCAC
1191  GTAAGGGTTA ATGTTTTCAA AAAAAAATTC GTCCGCACAC AACCTTTCCT CTCAACAAGC AAACGTGCAC
1261  TGAATTTAAG TGTATACTTC GGTAAGCTTC GGCTTACGAC GGGACCACCT TATGTTATTT CATCATGGTT
1331  TGATCAGTTC GAAAAGTGAG TTGGTCGAGC GAACAACGAT AGAGCGAGGG CAGAGTAACC GAGGCGATAC
1401  GATACGATAT AATATAGCAT CGGTACCATT GGGTATACGT TCCAGGAGCG AAAGAAAAGA CGAAAACGAG
1471  ACGAGACGAA AGGCCACCGG AGACAGCGAC GTCGCGGGTG TTAAGTTACT AAATAGCAAA CAGAAACTAC
1541  CGACCACCGA CCGATTGCAG TGAATGAAAT ATCCAATAAT TTCGAGTGAC ATTGGCCACA AATCAATCGA
1611  TCGTTCGATT TGAAACCTGA TTTGTAGAGT TCGTTTCTGC CAGTGTGTGT GTGCATGTAA GCCATGGGTT
1681  CTGGGCGAGC GAGGGAGATA GAGCGAGAAC ACTGATTCGA CTCGATTCGA TTCGATTCGA TTGGATTTGA
1751  TTCGAATTCA ATTACAAAAT TCATTGAGTG TCAATTACAA ACCGCAAGAA AACAACACGC ACGGAGATTC
1821  GGAAAGATCC CAAGATCCAA ATACAAGATC CAGATCCAGA TTCTCGAACA TCCAGAGATC CCAGCCAGAG
1891  TCAGAGTCAT AAATCATGCC TACGACATTG ATGTTGCTGC CGTGCATGCT GCTGTTGCTG CTGACCGCCG
```

Figure 16. Molecular characterisation of the *roulette* allele

Letters represent the sequence of the *argos* 5' UTR in homozygous *rlt* flies. Underlined sequences indicate the position of PCR primers used to detect the truncated P-element sequence (bp1-19 5' aos II primer, bp 1361-1380 3' aos I primer). Blue bold letters indicate the putative transcriptional start side of the *aos* gene. Orange letters represent the truncated P-element sequence inserted 570bp upstream of the start codon. Orange dotted lines indicate the inverse terminal repeats of the P-element. The position of the *W11* P-element is indicated with a black arrowhead. Red bold letters represent the start codon.

Intriguingly, the truncated P-element sequence recovered from the genomic PCR was inserted within the proposed transcriptional start site of the *aos* gene, just 26bp upstream of the P-element insertion that is responsible for the strong hypomorphic phenotype of the aos^{W11} allele, (which is inserted 544bp upstream of the ATG, Fig. 15 and 16). A BLAST search with the inserted sequence showed high similarity to P-element transformation vectors. Both, the 5' and the 3' inverse terminal repeats of the P-element vector are present, but the recovered sequence is shorter than usual in P-element vectors. Therefore, sequences in the center of the recovered P-element are likely to be truncated.

Eye imaginal discs mutant for *argos* exhibit ommatidial rotation defects

Despite the fact that ommatidial rotation occurs during third instar and early pupal stages, previous studies mainly focused on the analysis of adult eye sections to investigate rotation. In order to determine if the ommatidial rotation defects seen in adult *aos*^{rlt} eyes have already occurred at the time when chirality is established and rotation is initiated, I analysed eye imaginal discs mutant for *aos*^{rlt} or the strong hypomorph *aos*^{w11} using markers that highlight cell-type identity and orientation of each cluster (Fig. 18, 19 and 20). I found three marker combinations to be particularly helpful. To determine the R3/R4 cell fate decision and chirality of ommatidia, a monoclonal antibody against the neuronal antigen Elav (Robinow and White, 1991) which stains the nuclei of all developing photoreceptors, was used in combination with an *mδ0.5-lacZ* reporter-transgene (Cooper and Bray, 1999) which specifically highlights the R4 photoreceptor (Fig. 17A-A''). To study the initial 45° of ommatidial rotation an *svp-lacZ* enhancer trap (Mlodzik et al., 1990) was used in combination with the anti-Elav antibody (Fig. 17B-B''). The *svp-lacZ* enhancer trap is expressed at the time when rotation is initiated and later is also expressed in R1/R6 and R7 (Fig. 17B'). For the second 45° rotation step, an antibody against the geneproduct of the the homeobox gene *bar* (Higashijima et al., 1992) is of particular value, since it specifically marks R1 and R6 (Fig. 17C-C''). Bar, in combination with Elav or an anti-Boss antibody, which stains the central R8 cell (Kramer et al., 1991), is an excellent marker to determine rotation angles of ommatidial clusters from columns 10 or 11 on. An overview of the markers used in this study is shown in Fig. 17

As previously mentioned, the core planar polarity genes primarily affect the cell fate specification of R3 and R4 and thus chirality and subsequent direction of rotation. Therefore, a classical planar polarity phenotype in the eye is a combination of symmetrical, flipped and misrotated ommatidia (Adler, 2002; Mlodzik, 2002b; Fanto and McNeill, 2004). *aos*^{rlt} displays only a negligible percentage of symmetrical or flipped ommatidia and thus does not exhibit a classical polarity phenotype in adult eye sections. However, it cannot be excluded that the ommatidial rotation defects in adult *aos*^{rlt} eye are caused by initial defects in chirality establishment that might be corrected at a later stage in development. I therefore investigated cell fate specification of R3 and R4 in *aos*^{rlt} eye imaginal discs using the *mδ0.5-lacZ* reporter transgene as a marker.

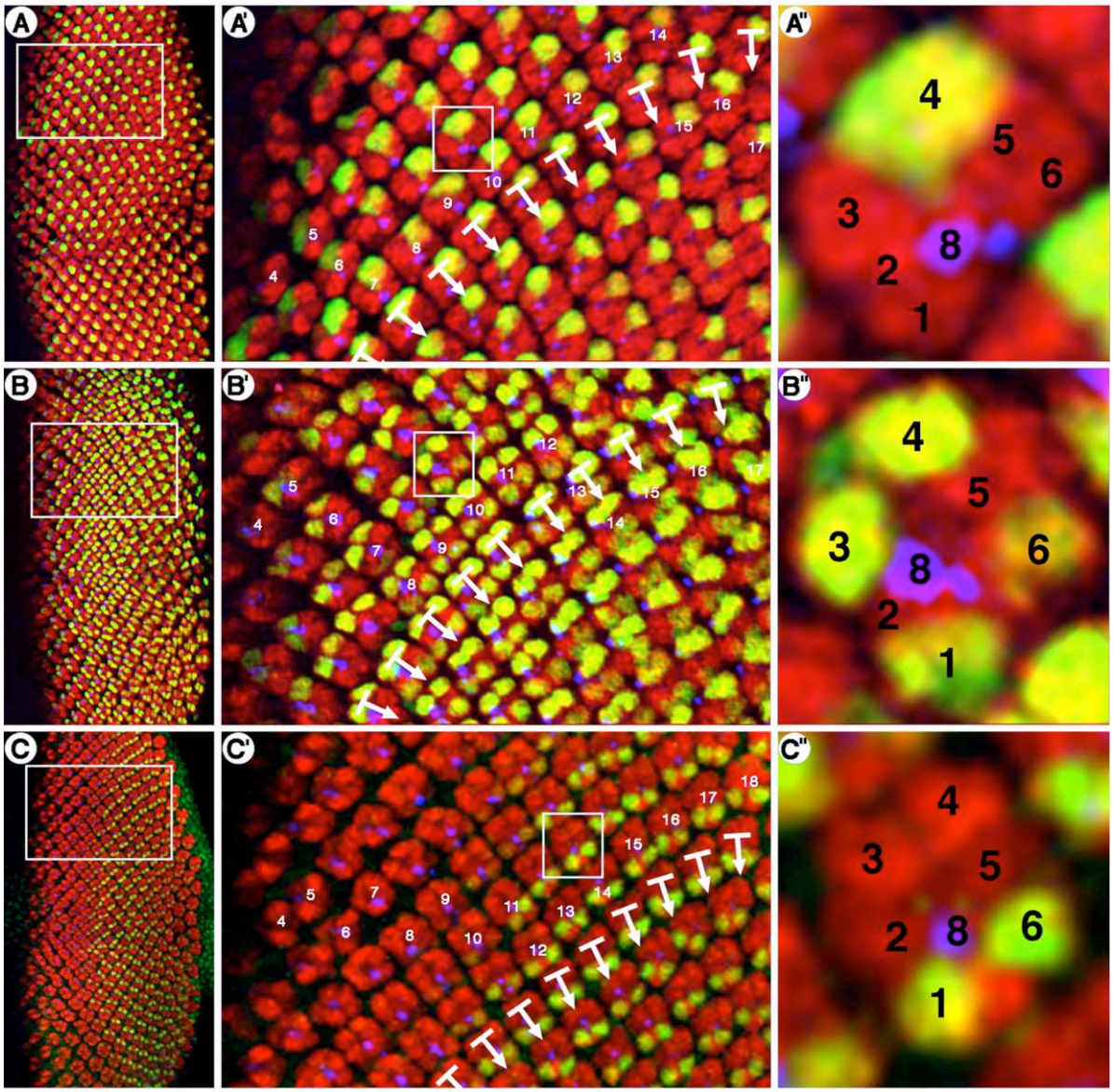

Figure 17. Useful marker combinations to study chirality and rotation of ommatidia in imaginal discs

All panels show third instar eye imaginal discs stained with different marker combinations to highlight chirality and orientation of ommatidia. In all panels anterior is left and dorsal is up. Left panels show large areas of discs stained with respective marker combinations. Middle panels are enlargements of boxed areas in left panels. White arrows indicate ommatidial orientation and white numbers indicate respective columns. Boxed areas in middle panels show a single ommatidium and are enlarged in right panels. Numbers indicate respective photoreceptors. **(A-A'').** A combination of an *mδ0.5-lacZ* reporter-transgene, as a indicator for adopted R4 cell fate (green) with an antibody against Elav marking all photoreceptor neurons (red) and an anti-Boss antibody highlighting the central R8 cell (blue), is particularly valuable to determine if ommatidia have adopted correct chirality. **(B-B'')** Expression of the *svplacZ* enhancer trap, shown in green, is an excellent marker for the first 45° of ommatidial rotation, since it is initially expressed in R3/R4 pair (and later on also in R1/R6 and R7). It is nicely complemented with anti-Elav (red) and anti-boss antibodies (blue). **(C-C'')** The second 45° of ommatidial rotation can be studied with an antibody against Bar which specifically stains R1/R6 in combination with anti-Elav or anti-Boss antibodies.

The *mδ0.5-lacZ* transgene is a Notch responsive reporter expressed exclusively in R4 and reliably reflects the R4 cell fate (Cooper and Bray, 1999). Fz signalling in the R3 precursor has been shown to activate the transcription of the Notch ligand Delta, which in turn signals to the Notch receptor in the neighboring R4 precursor, leading to specification of the R4 cell fate (Fanto and Mlodzik, 1999). Not surprisingly, eye imaginal discs mutant for aos^{rlt} did not reveal severe defects in R3/R4 specification and ommatidial chirality. The *mδ0.5-lacZ* expression pattern was largely similar to the wild type control (Fig. 18), with only R4 expressing *mδ0.5-lacZ* in most clusters. In some rare cases, young clusters close to the morphogenetic furrow did show weak *mδ0.5-lacZ* expression in R3 and R4 (Fig. 18B' green arrows), but this could also be observed in the wt control and is thought to reflect the initial chirality decision. In some clusters *mδ0.5-lacZ* expression was also seen in an extra cell which, judged by position, was neither an R3 nor R4 cell. However, these cells co-stain with Elav and are therefore likely to represent extra photoreceptor cells occasionally observed in adult aos^{rlt} eyes. (Fig. 18B' red arrow). In some cases, however, the extra *mδ0.5-lacZ* expressing cells did not co-stain with Elav and therefore most likely do not represent photoreceptors (Fig. 18B' blue arrow).

To study if initiation of rotation is affected in aos^{rlt} eye imaginal discs, I recombined the *svp-lacZ* enhancer trap on the aos^{rlt} chromosome. As shown above, the *svp-lacZ* enhancer trap is a good marker for the R3/R4 photoreceptor pair and allows one to determine rotation angles of early ommatidial clusters. Interestingly, no striking difference could be observed between aos^{rlt} discs and the *wt* control. Initiation of rotation seems essentially normal judged by the relative regular *svp-lacZ* pattern and only a small number of ommatidia appeared misrotated (Fig. 19). However, the analysis of the second 45° rotation step showed that discs mutant for *aos* do exhibit ommatidial rotation defects (Fig. 20). For this experiment, in addition to aos^{rlt}, I also investigated the strong hypomorphic aos^{W11} allele. As mentioned previously, aos^{W11} is caused by insertion of a P-lacZ enhancer trap vector in the 5' UTR of the *aos* gene (Fig. 15). The aos^{W11} P-lacZ insertion drives expression of β-galactosidase under control of the *aos* promotor and thus unfortunately cannot be used in combination with the *mδ0.5-lacZ* or the *svp-lacZ* markers. I therefore investigated the second 45° rotation step, using Bar in combination with antibodies to either Elav or Boss. Fortunately, aos^{W11} can be kept as a homozygous stock at 18°C, which facilitates the analysis of imaginal discs. In the wild type control, Bar shows a fairly regular 'fishbone-like' pattern, whereas in aos^{rlt} or even more in aos^{W11}, several misrotated ommatidia can be observed (Fig. 20). Given the strong adult rotation defects in adult eyes, it is however surprising that aos^{rlt} discs display a relatively mild phenotype, whereas aos^{W11}

discs exhibit a large number of ommatidia that are severely misrotated (compare Fig. 20B' and B'' with 20C' and C'').

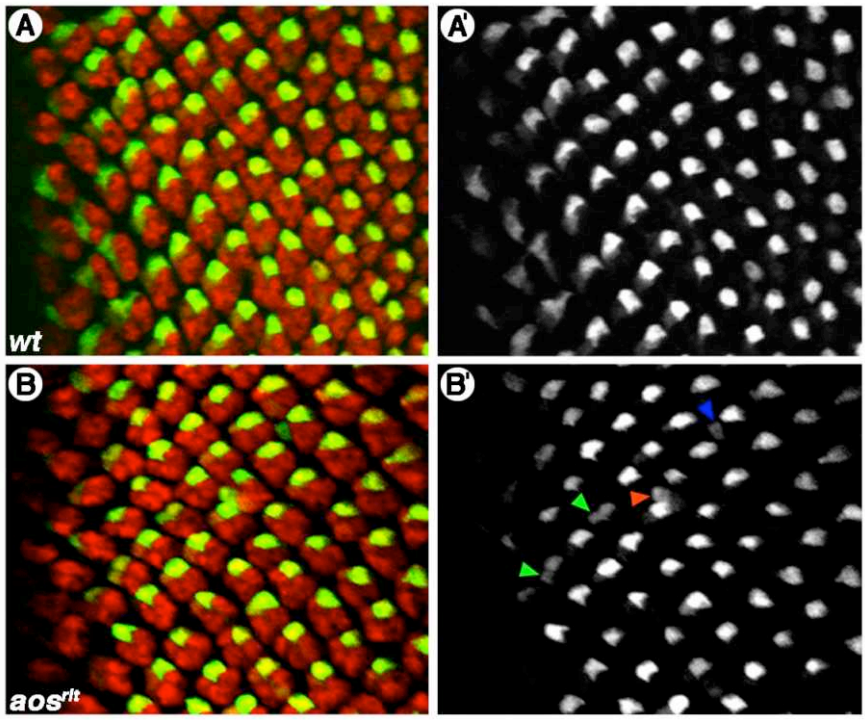

Figure 18. The R3/R4 cell fate decision is largely unaffected in *aos^{rlt}* eye imaginal discs

(A-B') Third instar eye imaginal discs stained for *mδ0.5-lacZ* reporter expression (green) as a marker for R4 cell fate, in combination with an antibody against the Elav protein (red), which highlights all developing photoreceptor neurons. **(A', B')** shows the green channel (*mδ0.5-lacZ* reporter expression) only. **(A, A')** *wt*. The *mδ0.5-lacZ* reporter highlights only R4 in each cluster. **(B, B')** *aos^{rlt}*. *mδ0.5-lacZ* expression is largely normal. However in rare cases, weak expression is found in R3 and R4 (green arrowheads). The red arrowhead indicates *mδ0.5-lacZ* expression in additional cells which, judged by position, are neither an R3 nor an R4 cell. However, the cell co-stains with Elav and is therefore likely to represent an extra photoreceptor cell occasionally observed in adult *aos^{rlt}* eyes. The blue arrowhead represents an extra *mδ0.5-lacZ* positive cells that does not co-stain with Elav.

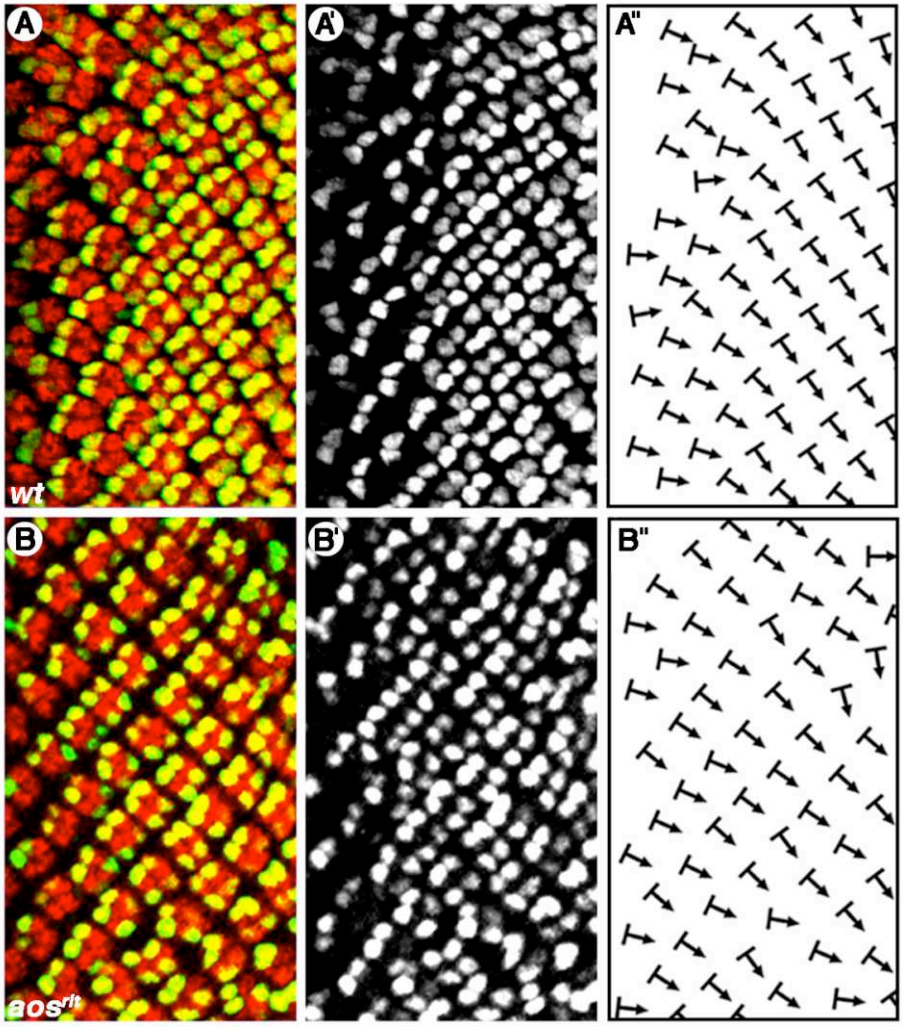

Figure 19. Initial ommatidial rotation is not severely disturbed in *aos^{rlt}* discs

(A, B) Third instar eye imaginal discs stained for *svp-lacZ* (green) in combination with an antibody against the Elav protein (red), which highlights all developing photoreceptor neurons. *svp-lacZ* is expressed in the R3/R4 pair as ommatidial rotation is initiated and in older ommatidial clusters, is also expressed in R1/R6 and R7. **(A', B')** shows the green channel (*svp-lacZ* expression) only. **(A''- B'')** Schematic representation of ommatidial orientation by arrows indicating actual rotation angles. The base of each arrow is aligned in parallel to the R3/R4 pairs. The arrowhead points between R1/R6. **(A-A'')** *wt*. **(B-B'')** *aos^{rlt}*. Only a small number of *aos^{rlt}* ommatidia are misrotated with respect to their developmental stage and their neighbors.

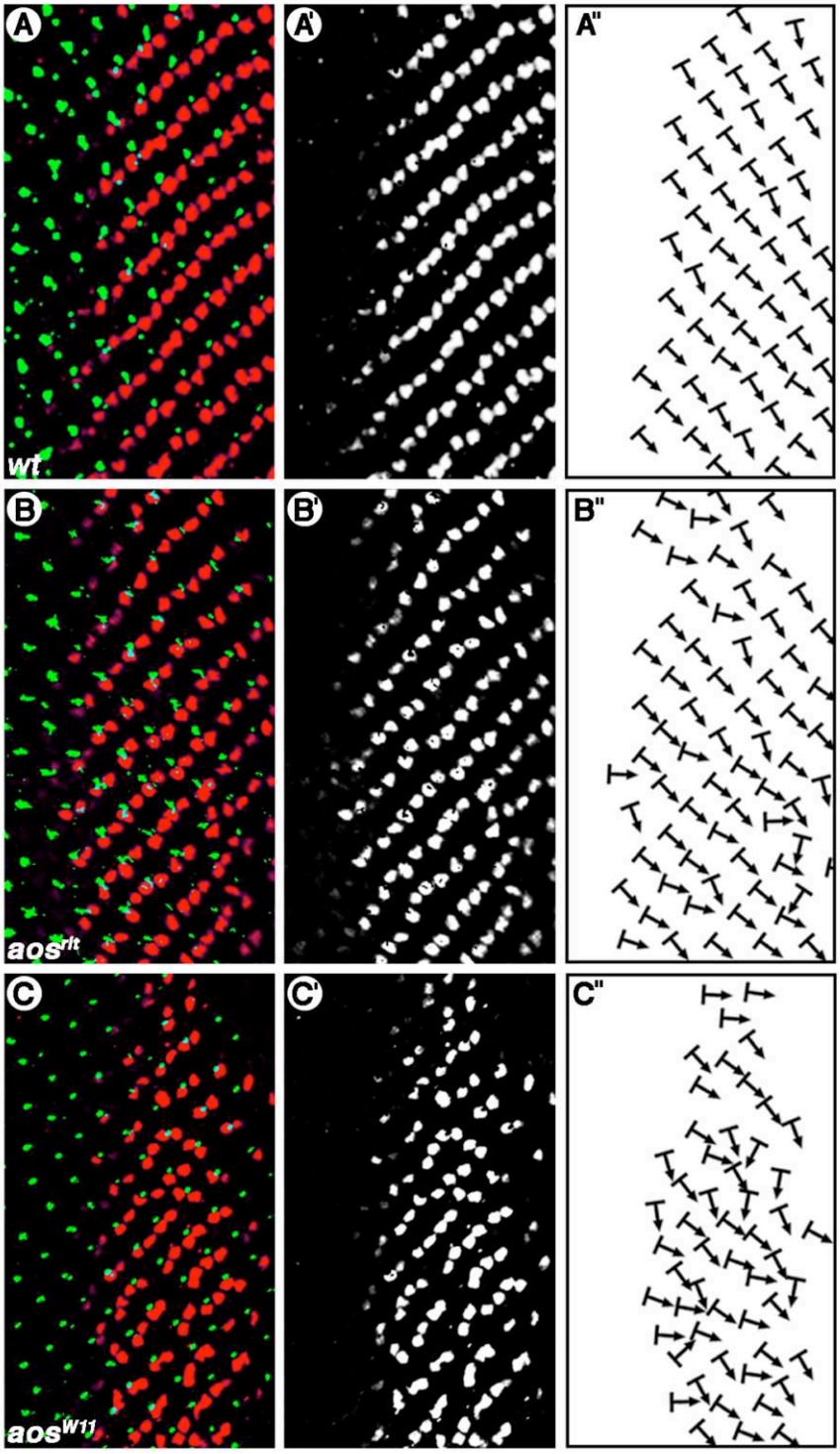

Figure 20. Eye imaginal disc mutant for *aos* exhibit ommatidial rotation defects

(A-C) Third instar eye imaginal discs stained with antibodies against Bar highlighting R1/R6 (red) and Boss marking R8 (green). **(A'-C')** Shows the red channel (Bar) only. **(A''- C'')** Schematic representation of ommatidial orientation by arrows indicating actual rotation angles. The base of each arrows is aligned in parallel to the R1/R6 pairs and the Boss staining is used as a reference for the middle of the ommatidial clusters. **(A-A'')** *wt*. **(B-B'')** aos^{rlt}. **(C-C'')** aos^{W11}. The Bar staining shows a relatively regular, 'fishbone-like' pattern in the wt control, whereas in aos^{rlt} and more prominently in aos^{W11} many ommatidia are misrotated. Both under and over-rotated ommatidia can be observed.

Ommatidial rotation is controlled by Egfr signalling

The identification of *rlt* as a rotation specific allele of *aos,* combined with the findings that Aos is a secreted inhibitor of Egfr signalling (Schweitzer et al., 1995a; Klein et al., 2004) strongly suggested a direct function for Egfr in ommatidial rotation. I thus investigated the phenotype of *Egfr* mutant eyes. The analysis of *Egfr* in the process of ommatidial rotation is complicated by the fact that strong *Egfr* mutants are lethal. Furthermore, null clones generated in the eye are not informative since *Egfr* is required for multiple processes prior to ommatidial rotation, including the specification of all photoreceptors except R8 (Dominguez et al., 1998; Kumar et al., 1998; Baker and Yu, 2001). In Egfr null clones, ommatidial assembly is therefore impaired preventing the analysis of ommatidial rotation. However, several hypomorphic alleles of *Egfr* have been described (Clifford and Schupbach, 1989), which are semi-viable and allow the analysis of ommatidial rotation. Eyes trans-heterozygous for the mild *Egfr* loss-of-function alleles top^{1}/top^{EC20} for example, are mildly rough and reveal prominent rotation defects in addition to the expected loss of photoreceptors in a small number of ommatidia. Interestingly, the top^{1}/top^{EC20} phenotype is more severe in the anterior portion of the eye whereas posterior regions often show only a very mild phenotype. Strikingly, anterior regions that exhibit a more severe loss of photoreceptors are adjacent to more posterior regions in which most ommatidia are misrotated but have a full complement of photoreceptors (Fig. 21A). This demonstrates that rotation defects are not caused by compromised ommatidial architecture or by defective packaging of ommatidia in these regions. A similar phenotype is also observed in top^{1}/top^{1} homozygous eyes (Fig. 21B). These results clearly show that a reduction in *Egfr*-activity due to mild loss of function alleles perturbs ommatidial rotation and that a certain level of *Egfr* signalling is required to control this process. In top^{1}/top^{EC20} trans-heterozygous flies ommatidia can under or over-rotate. However, over-rotated ommatidia are more frequently observed than under-rotated ommatidia (17.7 ± 4.2% over-rotated vs. 6.6 ± 3.5% under-rotated). This is in contrast to aos^{rlt} eyes in which over and under-rotated ommatidia are found in roughly the same percentage (40.7% under-rotated vs. 38.5 over-rotated). Overall, the top^{1}/top^{EC20} phenotype is milder than the aos^{rlt} phenotype, with 75.7 ± 7.5% of ommatidia rotated correctly.

To examine the effects of elevated *Egfr*-signalling on ommatidial rotation, I expressed an activated form of Egfr (*UAS-λ-top,* Queenan et al., 1997) under control of the *mδ0.5-Gal4* enhancer. The *mδ0.5-Gal4* enhancer drives expression of Gal4 in the R4 precursor at the time planar polarity signalling takes place and ommatidia begin to rotate (see Fig. 18). Tangential sections through *mδ0.5-Gal4>UAS-λ-top* eyes exhibit rotation defects with under-and over-rotated ommatidia (Fig. 21 C). In summary, these results show that gain

and loss of Egfr signalling leads to misrotated ommatidia, implying a general function for Egfr in regulating ommatidial rotation.

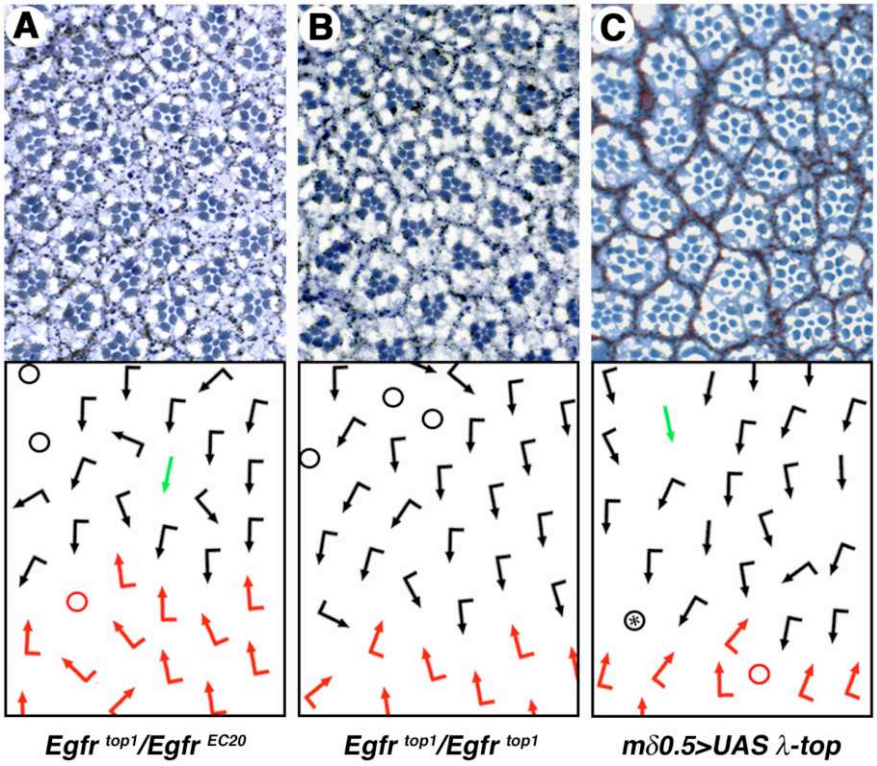

Figure 21. Loss and gain of Egfr function affects ommatidial rotation

(A-C) Tangential sections through equatorial regions of adult *Drosophila* eyes with schematic presentations indicating ommatidial rotation below the sections. Dorsal ommatidia are represented by black arrows, ventral ommatidia by red arrows. Flagged arrows represent ommatidia with a full complement of photoreceptors, whereas ommatidia with extra photoreceptors are indicated by straight arrows. Circles indicate ommatidia with missing photoreceptors and circles with a star indicate ommatidia with a severe gain of photoreceptors that cannot be scored for rotation. Symmetrical ommatidia are represented by green arrows. **(A)** *Egfr*^{top1}*/Egfr*^{EC20}, **(B)** *Egfr*^{top1}*/Egfr*^{top1}. Hypomorphic mutations in *Egfr* reveal ommatidial rotation defects. Note that in both allelic combinations photoreceptor loss is relatively mild whereas ommatidia with a full complement of photoreceptors are often misrotated. **(C)** *mδ0.5-Gal4>UAS λ-top*. Elevated Egfr signalling also perturbs ommatidial rotation.

Further evidence for an involvement of Egfr-signalling in ommatidial rotation comes from the analysis of *Star (S)* mutants (Fig. 22A and Table 2). The molecular function of *S*, for many years known as one of the main activators of Egfr-signalling in the Drosophila eye, has recently been uncovered (Kolodkin et al., 1994; Lee et al., 2001; Klambt, 2002; Tsruya et al., 2002; Shilo, 2003). The *S* gene encodes a transmembrane chaperon required to transport the TGFα homologue Spitz (Spi), the main activating ligand of Egfr in the eye, from the endoplasmatic reticulum to the Golgi apparatus (Golgi, Lee et al., 2001; Tsruya et al., 2002). *En route* to the Golgi, the Spi transmembrane precursor is then cleaved by Rhomboid proteases. Cleavage of Spi produces the active growth factor and is required for its secretion. Interestingly, Spi is uniformly expressed throughout the developing eye imaginal disc, and activation of Egfr is controlled by the timely and spatially restricted activity of the Spi processing machinery – mainly S and Rhomboid (Rho) proteins (reviewed in Shilo, 2003). As for most components of the Egfr pathway, null mutants of *S* are embryonic lethal and clones of null alleles generated in the eye do not develop photoreceptors others than R8 (Kolodkin et al., 1994) and are therefore not informative for the analysis of ommatidial rotation. Fortunately, *S* is haplo-insufficient for eye development and loss of one gene copy results in a mild rough eye phenotype due to a reduction in Egfr activation (Kolodkin et al., 1994). $S^{48.5}$/+ eyes are slightly rough and show a very mild loss of photoreceptors and in addition 9.6 ± 1.4% misrotated ommatidia (Fig. 22A and Table 2). Thus, *aos*, *Egfr* and *S,* three well characterised components of the Egfr pathway, revealed defects in ommatidial rotation in mutant alleles.

To further analyse if other known components of Egfr-signalling are also required for ommatidial rotation, I tested mutant alleles of various genes implicated in Egfr signalling for their ability to modify the dominant $S^{48.5}$/+ rotation-phenotype. In $S^{48.5}$/+ eyes, processing and subsequent secretion of Spi, the main activating ligand of Egfr in the eye, is compromised and thus Egfr signalling is reduced. I therefore expected mutant alleles of factors acting positively in the Egfr pathway to enhance the $S^{48.5}$/+ phenotype, whereas I expected negative regulators of Egfr signalling to suppress the $S^{48.5}$/+ phenotype. In fact, mutant alleles of *spi*, *Egfr*, *ras* and *pnt* did enhance the $S^{48.5}$/+ phenotype, whereas alleles of negative regulators such as aos^{rlt}, and *sty* were identified as suppressors. (Fig. 22 and Table 2). Interestingly, from the three tested Egfr ligands only alleles of *Spi* enhanced the rotation phenotype of $S^{48.5}$/+, whereas *vein* (*vn*) and *gurken* (*grk*) had no effect, suggesting that Spi is the main activating ligand in this context. The recently described Egfr ligand Keren could not be tested, since no mutant alleles are available to date.

***Star*$^{48.5}$/+ for all genes below**	**% misrotated ommatidia ± s.d.**	**moleculare function of gene**
oregon-R	9.6 ± 1.4	Wild type control
vein^{addC6}	10.0 ±3.3	Secreted ligand of Egfr
grk^{HK36}	3.1 ± 2.6	Secreted ligand of Egfr
spi^{1}	40.0 ± 3.7	Tgf-α homologue, main activating ligand of Egfr in the eye
spi^{259}	37.8 ± 13.4	Tgf-α homologue, main activating ligand of Egfr in the eye
Egfr^{top1}	41.5 ± 7.2	Epidermal growth factor receptor
ras^{e2F}	58.1 ± 4.6	Ras-GTPase
pnt^{07825}	59.0 ± 6.7	ETS-domain transcription factor
aos^{rlt}	3.7 ± 2.0	Secreted Egfr inhibitor
sty^{D5}	1.2 ± 0.5	Ras inhibitor

Table 2. Mutant alleles of several core Egfr pathway genes enhance the *S*$^{48.5}$/+ rotation phenotype in a dosage dependent manner

S$^{48.5}$ is haplo-insufficient for eye development; loss of one gene copy results in a rough eye phenotype with a mild loss of photoreceptors and misrotated ommatidia. All interactions are in heterozygous genotypes of the indicated genes. For all genotypes *n* is > 400 ommatidia from at least three eyes. The standard deviation (s.d.) is between eyes. Only ommatidia with a wild type complement of photoreceptors were scored. Ommatidia with an abnormal photoreceptor complement do not contribute to the total % of ommatidia analysed.

As demonstrated above, ommatidial rotation defects in *aos*^{rlt} eyes are the consequence of a reduction in Argos protein, which in turn leads to elevated Egfr signalling. Recently it was shown that Argos does not function as an inhibitory ligand for Egfr itself but instead directly binds to Spi and down-regulates Egfr signalling by ligand sequestration (Klein et al., 2004). Previous studies have shown that the rough eye phenotype of the *argos*^{257} allele is dosage-sensitive to Egfr signalling components (Sawamoto et al., 1996). I thus investigated if a reduction in Egfr signalling components could suppress the ommatidial rotation defects in homozygous *aos*^{rlt} eyes. To gain insight into the effector pathways involved in ommatidial rotation I analysed *aos*^{rlt} flies in a heterozygous background of *Egfr* or its downstream effectors. Strikingly, I found that the ommatidial rotation defects of *aos*^{rlt} eyes were suppressed in an *Egfr*^{top1}/+, *Ras*^{e2F}/+ and *pnt*$^{\Delta 88}$/+ background (Fig. 23B, C and E), arguing for a requirement of the conserved Ras/MAPK/Pnt cascade in rotation downstream of Egfr. This is further supported by the fact that *aos* is a direct transcriptional target of Pnt (Golembo et al., 1996), which is itself activated by the MAPK Rl (Brunner et al., 1994a). Surprisingly, removal of either one copy of a hypomorphic allele of *raf* (*raf*^{C110}) or a

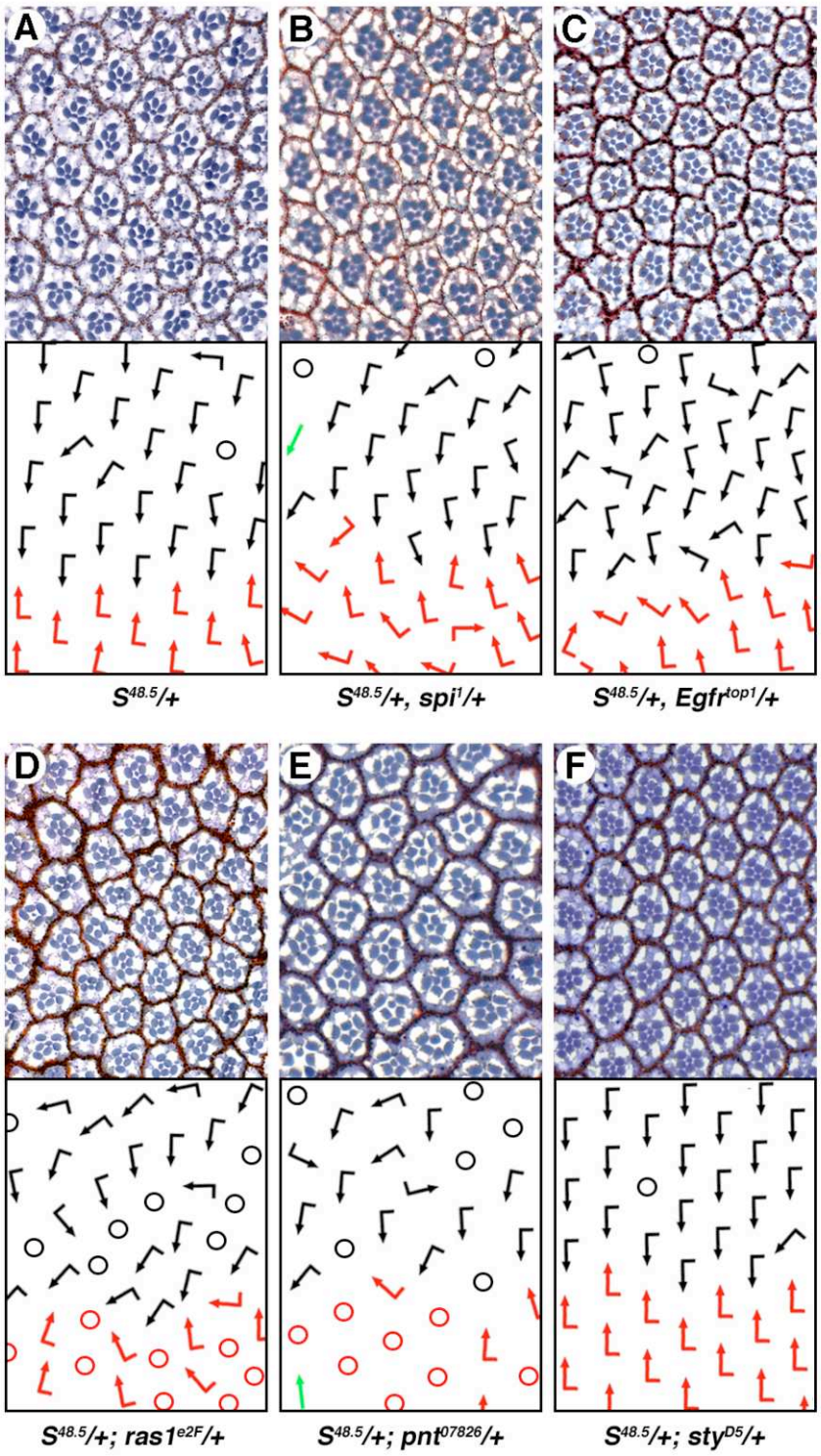

Figure 22. Rotation defects of the dominant $S^{48.5}$ allele are further enhanced by removal of one gene dosage of key Egfr signalling components

(A-F) Tangential sections through equatorial regions of adult *Drosophila* eyes with schematic presentations indicating ommatidial rotation below the sections. Dorsal ommatidia are represented by black arrows, ventral ommatidia by red arrows. Flagged arrows represent ommatidia with a full complement of photoreceptors, whereas ommatidia with extra photoreceptors are indicated by straight arrows. Circles indicate ommatidia with missing photoreceptors and symmetrical ommatidia are represented by green arrows. Genotypes are indicated below each panel.

deficiency that deletes *rl* (*Df(2R)rl*^{10A}) were not sufficient to suppress the rotation defects of *aos*^{rlt} (Fig. 23D and not shown), suggesting that these kinases are not rate limiting in this process. Since a previous study reported the nemo kinase as being epistatic to *rlt (nemo/rlt* double mutants display the nemo phenotype (Choi and Benzer, 1994), I investigated if removal of one copy of *nemo* could modify the *aos*^{rlt} phenotype. Strikingly, removal of one gene copy of *nemo* led to a suppression of rotation defects in *aos*^{rlt} (Fig. 23F), suggesting a link between Egfr signalling and the nemo kinase. Although pure speculation at this point, it is tempting to suggest that nemo might execute some function downstream of Egfr in ommatidial rotation.

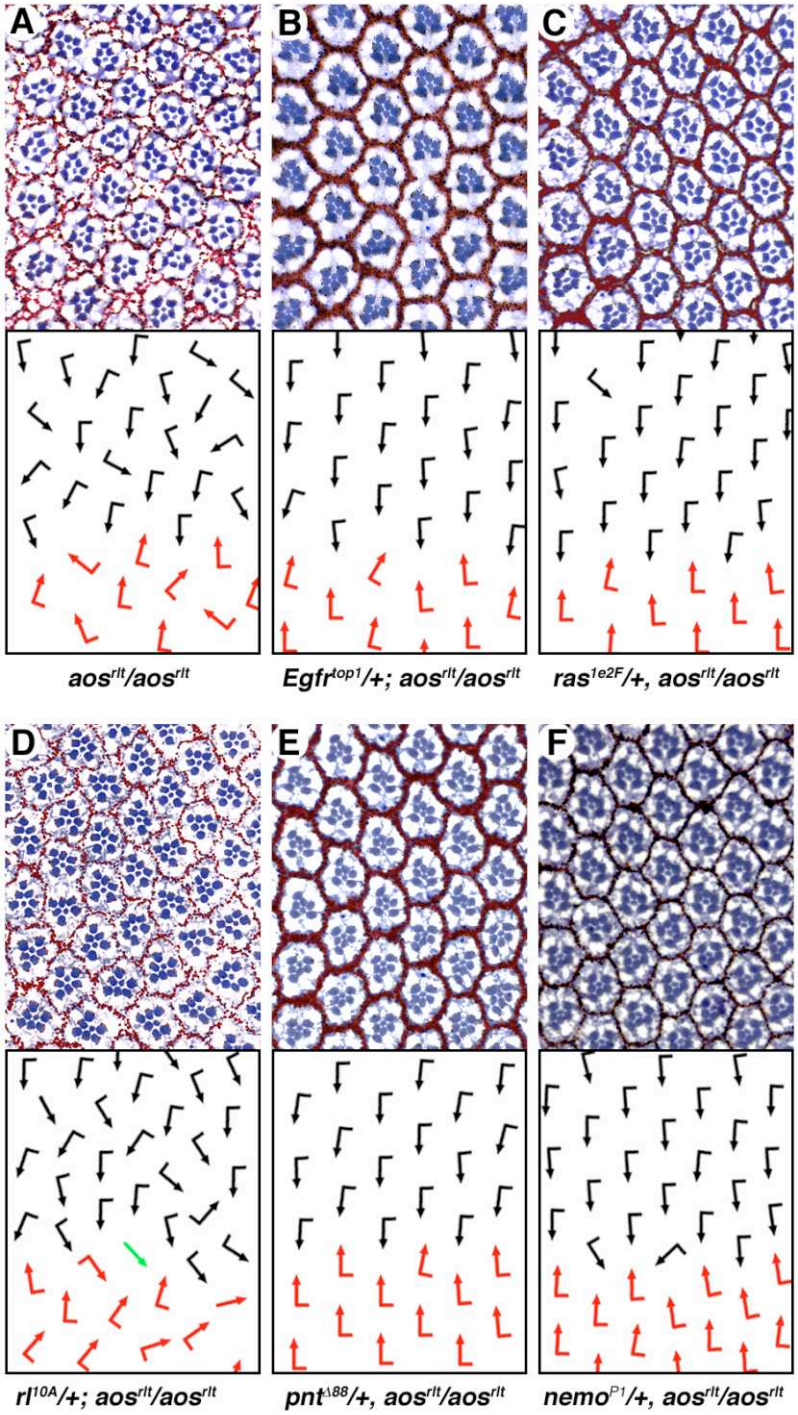

Figure 23. *aos*^{rlt} is dominantly suppressed by *Egfr*, *ras, pnt* and *nmo* but not by the MAPK *rl*

(A-G) Tangential sections through equatorial regions of adult *Drosophila* eyes with schematic presentations indicating ommatidial rotation below the sections. Dorsal ommatidia are represented by black arrows, ventral ommatidia by red arrows. Flagged arrows represent ommatidia with a full complement of photoreceptors, whereas ommatidia with extra photoreceptors are indicated by straight arrows. Symmetrical ommatidia are represented by green arrows. Genotypes are indicated below each panel. Note that loss of one gene copy of *Egfr*, *ras* or *pnt* and *nemo* does suppress aos^{rlt}, whereas the MAPK *rl* fails to do so, suggesting that *rl* is not rate limiting in this assay. The suppression of aos^{rl} by nemo indicates a link between the nemo kinase and the Egfr pathway.

Ras-effector loop mutations point towards an involvement of additional Egfr effectors beside the conserved Raf/MAPK/Pnt signalling cassette in ommatidial rotation

Although ommatidial rotation has not yet been studied on a cellular level, it seems obvious that this morphogenetic movement requires some, if not all, of the components used in other contexts of cellular motility. It appears essential that cells within the ommatidia adhere to one another more strongly than to surrounding non-ommatidial cells in order to allow the ommatidium to rotate as a unit. It further seems essential that cell-cell and cell-matrix adhesion between ommatidial cells and surrounding cells and/or the extracellular matrix must be modified in order to allow the ommatidial clusters to rotate. Furthermore, the actual rotation process must require some sort of cytoskeletal rearrangements, most likely mediated through the actin/tubulin-cytoskeleton. In addition, the direction of rotation must be determined to ensure that ommatidia rotate in the correct direction, which is most likely achieved by asymmetrical localisation of the components required for this morphogenetic movement. Given these requirements, I wondered if other effectors of Egfr beside the Raf/MAPK cascade might play a role in ommatidial rotation. The Ras GTPase is thought to be the main transducer of Egfr signalling in *Drosophila* (Casci and Freeman, 1999). In mammalian cell culture, however, Ras is known to utilise distinct effectors in different cellular contexts (Reviewed in Rommel and Hafen, 1998). In *Drosophila*, at least four different Ras effectors have been implicated in eye development. The best characterised is the MAPKKK Raf which mediates nuclear signalling via MAPK/Pnt (Dickson et al., 1992). In addition, Ras has been found to affect cell growth and/or cytoskeletal rearrangements via its effectors Phospho-inositol-3-Kinase (PI3K, Rodriguez-Viciana et al., 1996; Prober and Edgar, 2002), Rgl/Ral (Mirey et al., 2003) and Canoe/AF6 (Matsuo et al., 1997). Several point mutations have been identified within the Ras-effector loop (amino acids 34-41) that abrogate the binding to and activation by Ras of specific effectors (Fig. 24G, Joneson et al., 1996; Rodriguez-Viciana et al., 1997; Karim and Rubin, 1998). The specificity of certain Ras-effector loop mutations has been thoroughly tested in *Drosophila* imaginal discs (Prober and Edgar, 2002). Constitutively active Ras (Ras^{V12}) can bind and activate all known Ras effectors, whereas Ras^{V12S35} specifically binds and activates Raf and induces Ras/Raf/ERK specific transcriptional responses in wing and eye imaginal discs (Prober and Edgar, 2002). In cell culture, Ras^{V12G37} interacts specifically with RalGDS (resulting in activation of the Ral GTPase, Rodriguez-Viciana et al., 1997), PI3Kγ (Pacold et al., 2000) and PI3Kδ (Kinashi et al., 2000), but not with PI3Kα or Raf (Rodriguez-Viciana et al., 1997). In addition Ras^{V12G37} fails to induce Raf/ERK specific responses, but is capable of activating PI3K-specific read-outs in *Drosophila* eye and wing imaginal discs (Pacold et al., 2000;

Prober and Edgar, 2002). Its effect on Ral in *Drosophila* has not jet been established. Another variant, Ras^{V12C40} is reported to bind to PI3Kα, but not PI3Kγ, PI3Kδ, Raf or RalGDS in mammalian tissue culture (Rodriguez-Viciana et al., 1997) and is unable to induce either Raf/ERK or PI3K specific responses in *Drosophila* eye and wing imaginal discs (Prober and Edgar, 2002). However, unpublished data suggest Ras^{V12C40} might be specific for the Ras effector Canoe/AF6 in *Drosophila* eye imaginal discs (Ulrike Gaul, personal communication). Thus, I tested these Ras-effector loop mutations in constitutively active Ras^{V12} for their effects on ommatidial rotation.

Expression of Ras^{V12} in developing photoreceptor precursor cells using common eye specific drivers causes induction of many extra photoreceptors (Fortini et al., 1992) and thus does not allow the analysis of rotation (since the orientation of individual ommatidial clusters cannot be determined unambiguously in the presence of extra photoreceptor cells). To circumvent this problem Ras^{V12} and its effector loop isoforms were expressed in a limited subset of cells after these have already been determined as photoreceptors (mainly in R4) using the *mδ0.5-Gal4* driver (see Fig. 18 for the expression pattern of this driver). Ras^{V12} effects on photoreceptor number and fate were thus strongly reduced. To determine the full effect of activated Ras expression under the *mδ0.5-Gal4* control, I expressed constitutively active Ras^{V12} that activates all known Ras-effectors. This gave rise to eyes with some gain and loss of photoreceptors and severe misrotations (Fig. 24A). The equivalent expression of Ras^{V12S35}, which only activates Raf, also resulted in rotation abnormalities and occasional gain or loss of photoreceptors, again supporting a requirement of the Raf/MAPK cascade (Fig. 24B) in ommatidial rotation. Interestingly, expression of Ras^{V12G37} and Ras^{V12C40} also caused rotation defects (albeit weaker than Ras^{V12} or Ras^{V12S35}), suggesting an involvement of additional Ras-effectors in this process. In particular Ras^{V12G37}, in which Raf activation is abolished, resulted in clear rotation defects (Fig. 24C), suggesting that PI3K, Rgl/Ral or Canoe might play a role in this cell motility process. Interestingly, even Ras^{V12C40}, thought to retain only limited ability to stimulate Canoe/AF-6 (Ulrike Gaul, personal communication), showed mild rotation abnormalities (Fig. 24D). Moreover, expression of Ras^{V12C40} under the control of the *sevenless* (*sev*) promoter (in R3/R4, R1/R6 and R7) resulted in strong rotation defects, comparable to those seen with Ras^{V12G37} under *sev* control (Fig. 24E, F). Taken together, these data suggest an involvement of PI3K, Rgl/Ral or Canoe in ommatidial rotation.

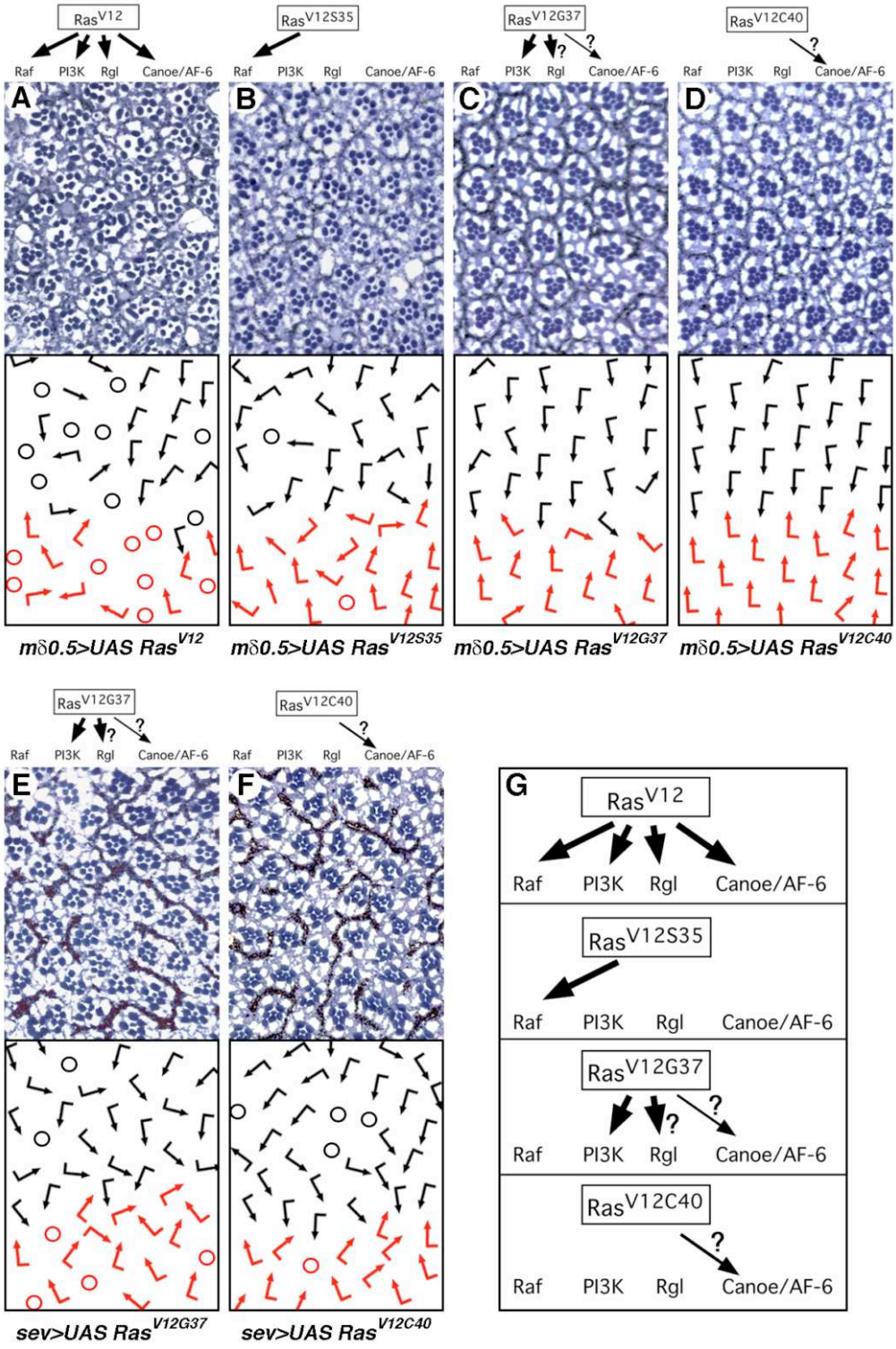

Figure 24. Expression of Ras-effector loop mutations causes ommatidial rotation defects

(A-F) Tangential sections through equatorial regions of adult *Drosophila* eyes with schematic presentations indicating ommatidial rotation below the sections. Dorsal ommatidia are represented by black arrows, ventral ommatidia by red arrows. Flagged arrows represent ommatidia with a full complement of photoreceptors, whereas ommatidia with extra photoreceptors are indicated by straight arrows. Loss of photoreceptors is indicted by circles. **(A)** mδ0.5-Gal4>UAS Ras^{V12}, **(B)** mδ0.5-Gal4>UAS Ras^{V12S35}, **(C)** mδ0.5-Gal4>UAS Ras^{V12G37}, **(D)** mδ0.5-Gal4>UAS Ras^{V12C40}, **(E)** sev-Gal4>UAS Ras^{V12G37}, **(F)** sev-Gal4>UAS Ras^{V12G40}. **(G)** Schematic representation of the effectors specificity in different Ras^{V12} effector-loop mutations.

Loss and gain-of-function Canoe disrupts ommatidial rotation

To further investigate the findings that mis-expression of the effector loop mutations Ras^{V12G37} and Ras^{V12C40} can cause ommatidial rotation defects, I analysed the implicated effectors PI3K, Ral and Cno more closely. Expression of UAS PI3K under control of the *mδ0.5-Gal4* driver failed to produce convincing rotation defects. Furthermore, clones of null alleles of PI3K are reported to affect growth, but not ommatidial rotation (Leevers et al., 1996), suggesting that PI3K might not be required in this process. In contrast, expression of an activated form of Ral (Sawamoto et al., 1999b), (discussed below), as well as *mδ0.5-Gal4>UAS-cno* results in severe ommatidial rotation defects (Fig. 25C), implying both Ral and Cno in this morphogenetic process. In order to test for a direct *cno* requirement in ommatidial rotation, I asked whether *cno* heterozygosity could modify the $S^{48.5}$/+ rotation phenotype. Strikingly, strong *cno* alleles did in fact enhance $S^{48.5}$/+ to a degree similar to that seen by removal of one copy of *spi* or *Egfr*. The $S^{48.5}$/+ phenotype is relatively mild in a wild type background (9.6 ± 1.4 % misrotated ommatidia), but loss of one copy of either cno^2 or cno^3 lead to 40.6 ± 8.0 % or 43.2 ± 8.7 % misrotated ommatidia, respectively (Fig. 25B, Table 3 and not shown)

Cno has been reported to localise to adherense junctions and is an essential component for junctional integrity (Takahashi et al., 1998; Matsuo et al., 1999). Furthermore, Cno is required for cone cell and photoreceptor differentiation and morphogenesis and clones of null or strong alleles cause a severe disorganization of the eye, impairing the analysis of ommatidial rotation (Miyamoto et al., 1995; Matsuo et al., 1997; Matsuo et al., 1999). However, the hypomorphic cno^{mis1} allele is subviable in trans to the strong alleles cno^2 or cno^3 with mildly rough eyes, allowing the analysis of ommatidial rotation. Strikingly, eye sections of these transheterozygous combinations (e.g. cno^{mis1}/cno^2) revealed, besides the previously reported photoreceptor morphogenesis defects, also rotation defects (Fig. 25D). I then asked whether the ommatidial rotation defects seen in adult cno^{mis1}/cno^2 eyes sections are already visible during imaginal disc development. An analysis of homozygous cno^{mis1}/cno^{mis1} discs revealed mild rotation defects similar to those seen in aos^{rlt} discs (Fig. 26). The discs were counterstained with anti-Elav (not shown) to verify that the photoreceptor complements were normal and that the observed rotation abnormalities were primary defects. In summary, these data suggest that Cno plays an important role in ommatidial rotation and most likely acts as an effector of Ras signalling in this context. However, further work will be necessary to understand how Cno transduces Ras-signalling and mediates cell motility in this context.

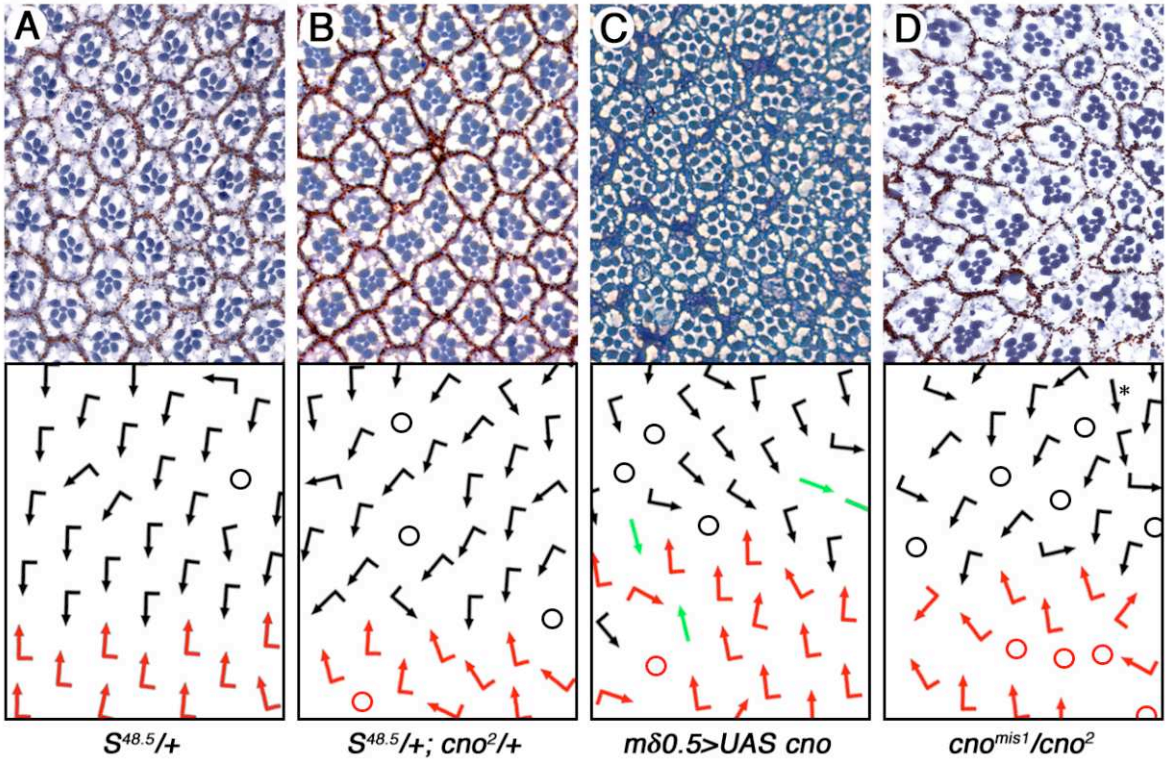

Figure 25. Cno is involved in ommatidial rotation

(A-D) Tangential section of adult eyes around the equatorial region, with corresponding schematic representation below each panel. Arrows and circles are as in previous figures. **(A, B)** Loss of one copy of *cno* dominantly enhances the *S48.5/+* phenotype, leading to severe rotation defects. **(C)** Expression of *UAS cno* under control of the *mδ0.5-Gal4* enhancer results in ommatidial rotation defects, a mild loss of photoreceptors and symmetrical ommatidia. **(D)** Transheterozygous cno^{mis1}/cno^{2} eyes exhibit defects in ommatidial rotaion.

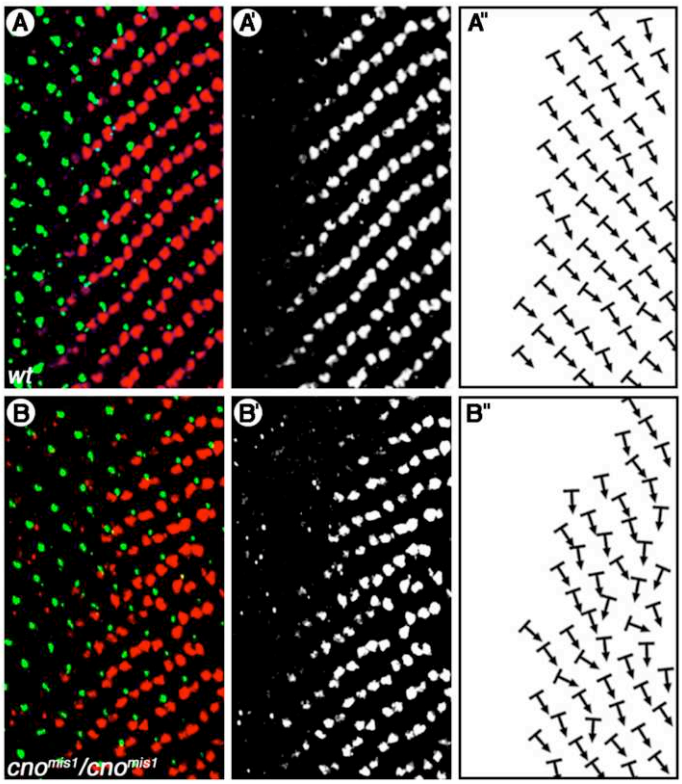

Figure 26. Eye imaginal discs mutant for *cno* exhibit defects in ommatidial rotation

(A, B) Third instar eye imaginal discs stained with antibodies against Bar highlighting R1/R6 (red) and Boss marking R8 (green). **(A'-B')** Shows the red channel (Bar) only. **(A''- B'')** Schematic representation of ommatidial orientation by arrows indicating actual rotation angles. The bases of the arrows are aligned in parallel to the R1/R6 pairs and the Boss staining is used as a reference for the middle of the ommatidial clusters. **(A-A'')** *wt.* **(B-B'')** cno^{mis1}/cno^{mis1}**.** The Bar staining shows a relative regular, 'fishbone-like' pattern in the wt control, whereas it is slightly disturbed in cno^{mis1}/cno^{mis1} discs, with some ommatidia being misrotated. Both under-and over-rotated ommatidia can be observed.

Canoe co-localises with DE-cadherin to adherense junctions during eye-imaginal disc development

In order to study Cno function and sub-cellular localisation during eye imaginal disc development, I constructed a C-terminally GFP tagged Cno fusion protein which I hereafter will refer to as Cno:GFP (see Materials and Methods). In order to study Cno localisation, I cloned the Cno:GFP construct into an expression vector that drives low level expression under control of the tubulin promoter (pCasper-tubulin), hereafter referred to as tub>Cno:GFP (see Materials and Methods). The pCasper-tubulin vector has been successfully used to study protein localisation of GFP fusion proteins since its low level expression rarely results in a dominant phenotype (Wu et al., 2004). Furthermore, I cloned the Cno:GFP construct in a pUAST expression vector (see Materials and Methods) that allows the induced expression of Cno:GFP if crossed to an appropriate Gal4 line (see Duffy, 2002 for a review on the Gal4 system in *Drosophila*). These constructs were then used to establish transgenic fly lines. A subsequent analysis of eye imaginal discs from tub>Cno:GFP flies revealed that Cno:GFP co-localises with DE-cadherin at adherense junctions and is enriched in a pattern complementary to Fmi (Fig. 27 and 28). Whereas Cno:GFP is localised to the same apical region as DE-cadherin and Fmi, it is more basal than that of Disc large (Dlg), a marker for the peripodial membrane, and just below Actin (Fig. 27). Cno:GFP, expressed under control of the tubulin promotor, is present at the apical membranes of all cells and is specifically enriched around the apical membranes of the photoreceptors R2 and R5 (Fig. 28). Two columns behind the morphogenetic furrow, Cno:GFP is enriched at the membranes of R2, R5 and R8 (Fig. 28B, F, J and N). In the 4th column, Cno:GFP localisation appears strongest in R2/R5 (Fig. 28C, G, K and O). Slightly later, between columns 6-8, Cno:GFP is also found at the membrane between R3/R4, while its R2/R5 specific enrichment remains most prominent (Fig. 28 D, H, L and P). From about column 8 on, Cno:GFP is also enriched around the membranes of R8 and more weakly around the posterior membranes of R4 (Fig. 28E, I, M and Q). The finding that Cno:GFP localises to adherense junctions in the eye imaginal disc is not surprising, since previous studies have also reported an association of Cno with markers of adherense junctions (Matsuo et al., 1999). However, it is noteworthy that Cno and DE-cadherin enrichment in the eye imaginal disc is complementary to that of the planar cell polarity genes, as shown here for Fmi in Fig. 28.

Although the cno:GFP localisation in the eye disc is striking, it does not prove functionality of the fusion protein. In order to test if the Cno:GFP construct encodes for a functional protein, I first tested if expression of Cno:GFP under the control of *mδ0.5-Gal4* or the *sevenless* enhancer could create a gain-of-function cno phenotype similar to that seen

with *UAS-cno*. In fact, the *UAS-cno:GFP* construct did produce a gain-of-function phenotype similar to that of *UAS-cno*, albeit slightly weaker (not shown), suggesting that the Cno:GFP fusion protein is biologically functional. In order to demonstrate that Cno:GFP can substitute for endogenous Cno, I am currently performing rescue experiments in which I attempt to rescue the strong cno^{2} allele.

In summary, the data presented above suggest that Cno co-localises with DE-cadherin to adherense junctions in the developing eye imaginal disc. Importantly, Cno and DE-cadherin are enriched in a pattern complementary to that of the planar polarity genes. The localisation pattern of Cno together with its gain- and loss-of-function rotation phenotype further suggests a critical role for adherense junctions in ommatidial rotation. This hypothesis is in line with experiments presented below, suggesting a key role for DE-cadherin in ommatidial rotation.

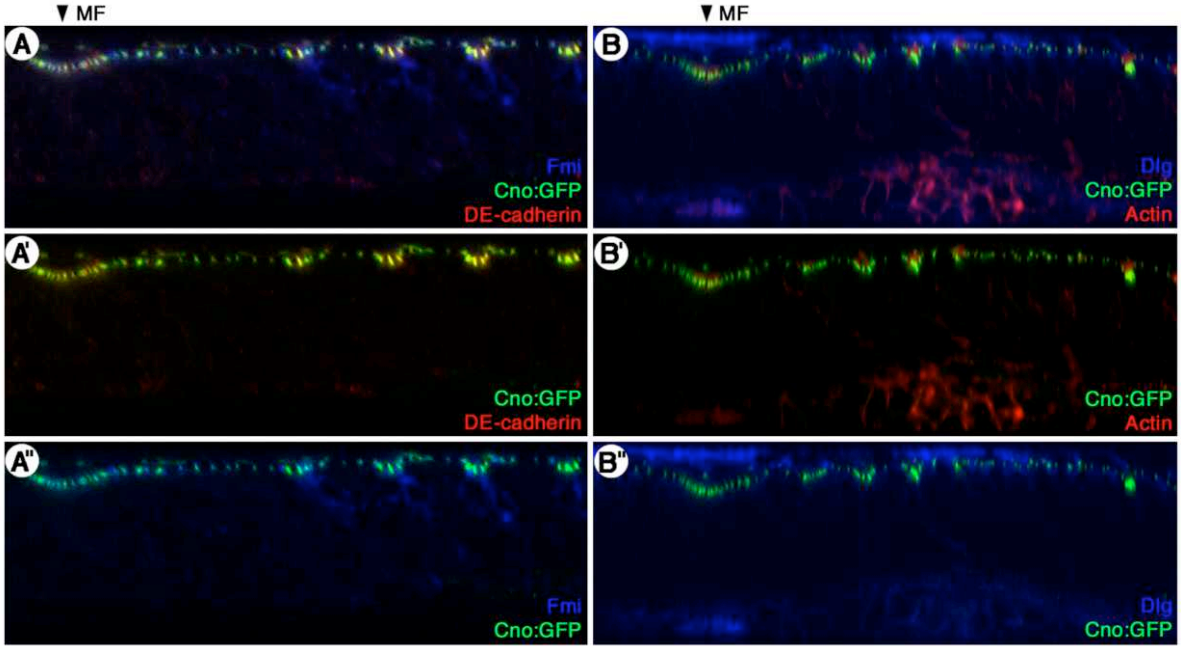

Figure 27. Cno:GFP co-localises with DE-cadherin apically to adherense junctions

(A-B'') Confocal Z-sections of third instar eye imaginal disc showing localisation of Cno:GFP with respect to several marker genes that are visualised by respective antibodies. The position of the morphogenetic furrow (MF) is indicated by a black arrowhead above the panels. Anterior is to the left and apical is up. **(A-A'')** Cno:GFP (green) co-localises with DE-cadherin, a marker for adherense junctions (red), but not with Fmi (blue) at apical membranes of the eye imaginal disc. **(B-B'')** Cno:GFP (green) is localised basally with respect to Dlg, a marker for the peripodial membrane (blue) and just below Actin (red).

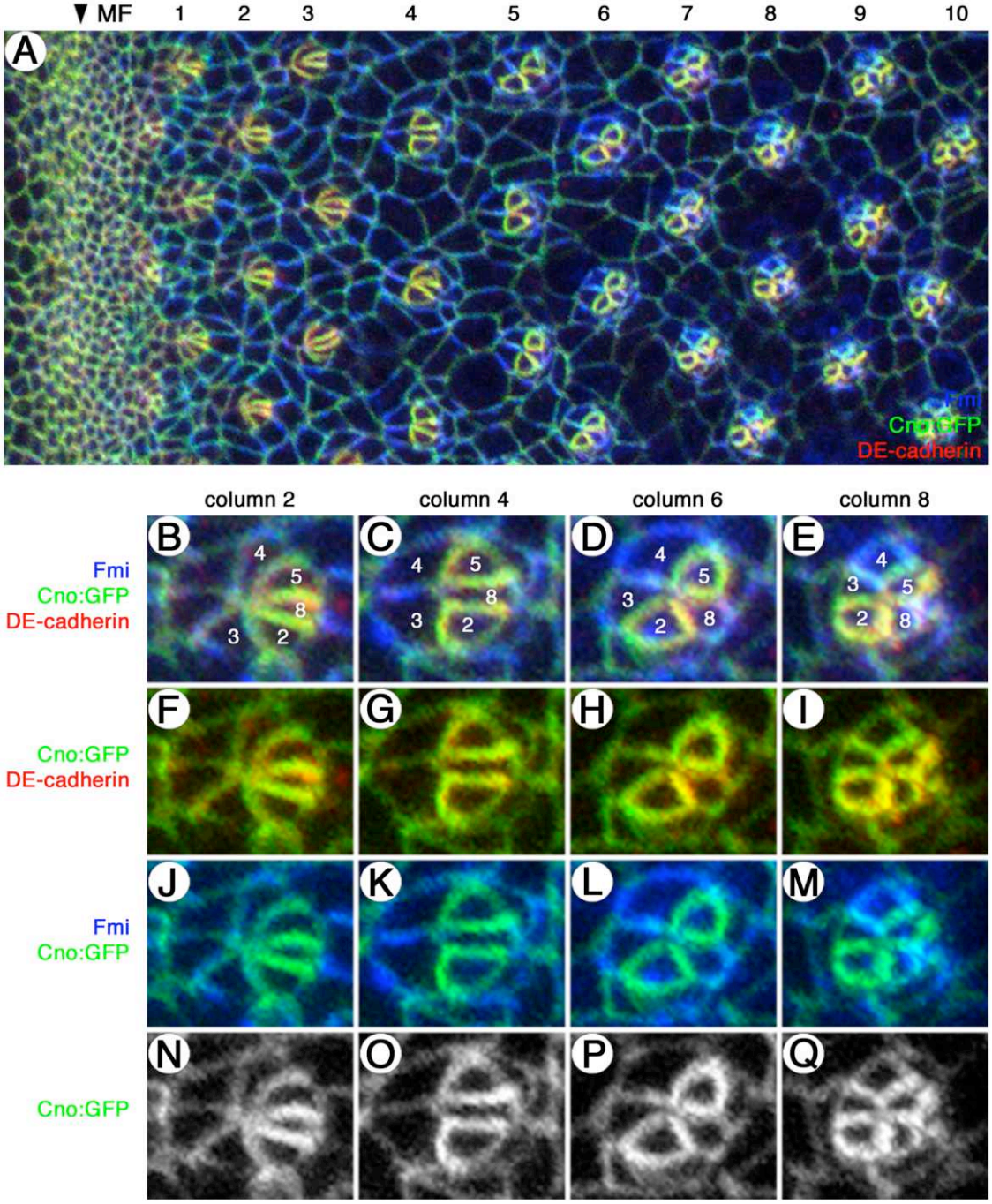

Figure 28. Cno:GFP is strongly enriched around the apical membranes of R2 and R5

(A-Q) Confocal images of third instar eye imaginal disc showing Cno:GFP localisation (green and single channel in N-Q). Discs were co-stained with antibodies against Flamingo (shown in blue) and DE-cadherin (shown in red). **(A)** Cno:GFP localises to the apical membranes of all cells but is strongly enriched in R2 and R5, where it co-localises with DE-Cadherin. The position of the MF is shown by a black arrowhead and black numbers indicate respective columns behind the MF. **(B-Q)** Enlarged single ommatidia from A, showing examples of columns 2 **(B, F, J, N)**, 4 **(C, G, K, O)**, 6 **(D, H, L, P)** and 8 **(E, I, M, Q),** respectively. The position of the photoreceptor pre-cursors R8, R2, R5, R3 and R4 is indicated by white numbers in the first panel of each column (B, C, D and E). By column 2, Cno:GFP shows an enrichment around the membranes of R2, R5 and R8 (B, F, J, N). From column 4 on Cno:GFP is strongly enriched in R2 and R5 (C, G, K, O). Examples from column 6 and 8 further show that Cno:GFP is also enriched at the membrane between R3 and R4 (D, H, L, P and E, I, M, Q).

A role for Ral in ommatidial rotation?

The Ras-like small GTPase Ral (in *Drosophila* also referred to as Rala) has been previously implicated in cytoskeletal rearrangements in *Drosophila* (Sawamoto et al., 1999a). To determine if Ral is also required for ommatidial rotation, I first re-examined a previously reported fly-stock in which an activated form of the human orthologue of Ral (Ral^{G23V}) is expressed under control of the GMR promotor (Sawamoto et al., 1999b). Tangential sections through GMR>Ral^{G23V} eyes displayed a very clean rotation phenotype, highlighting the potential of Ral in this process (Fig. 29A). For many years a loss of function analysis of *ral* was prevented by the lack of suitable alleles. However, three P-element induced mutants of *ral* have recently been described (Bourbon et al., 2002). Although these alleles have not yet been characterised in sufficient detail, they are lethal. I therefore recombined these alleles on FRT chromosomes in order to induce clones of *ral* mutant tissue in developing eye imaginal discs. (For a review on the FLP/FRT system see Theodosiou and Xu, 1998). Unfortunately, all three available *ral* alleles are P[w+] marked and therefore do not allow the identification of mutant tissue in adult eye sections unambiguously (since heterozygous and homozygous mutant tissue will be w^+ marked and therefore cannot be distinguished). In order to know exactly which cell is lacking *ral* function it will be necessary to either mutate the white gene of the P-element responsible for the mutation or to obtain new alleles that are in a white mutant background. I am currently designing a P-element excision screen in order to create null alleles of *ral* that lack the white gene. These can than be used for a careful clonal analysis. In the mean time I have induced unmarked *ey-FLP* clones of the available *ral* alleles to determine if loss of *ral* function would have any effect on eye development. In fact *ey-FLP* clones of the tested *ral* alleles PG89 and PL56 displayed a roughened eye structure. Tangential sections through these eyes revealed a mild loss of photoreceptors as well as problems with photoreceptor morphogenesis, but only occasional rotation defects (Fig. 29B-G). However, since it is impossible to distinguish between homozygous mutant and heterozygous areas in these eyes it is not clear if loss of *ral* function causes a general loss of photoreceptors, problems with rhabdomere morphogenesis or has an impact on ommatidial rotation. A detailed analysis of the adult eye phenotype can therefore not be performed until suitable alleles are generated.

I further investigated the effect of *ral* in the developing eye imaginal disc, where clones can be marked unambiguously using an *armadillo-lacZ FRT* chromosome. A preliminary analysis of *ey-FLP* induced clones of the ral^{PG89} allele indicated that loss of Ral function does not impair photoreceptor development in general, judged by the relatively normal Elav staining (Fig. 30A). However, some ommatidia were misrotated whereas others

showed Bar expression in only one cell of the R1/R6 pair (Fig. 30). In some cases it also seems as if the spacing between R1/R6 is abnormal (Fig. 30C).

Thus, at this point my preliminary results suggest that *ral* is required for photoreceptor cell fate specification and/or survival. Furthermore, *ral* function is most likely needed for proper rhabdomere morphogenesis. In addition, *ral* might also have an impact on ommatidial rotation since a small number of misrotated ommatidia can be seen in the developing eye disc and in adult sections of *ral* clones. However, these results are preliminary and further experiments are required to clarify the role of Ral in photoreceptor specification and its potential involvement in ommatidial rotation.

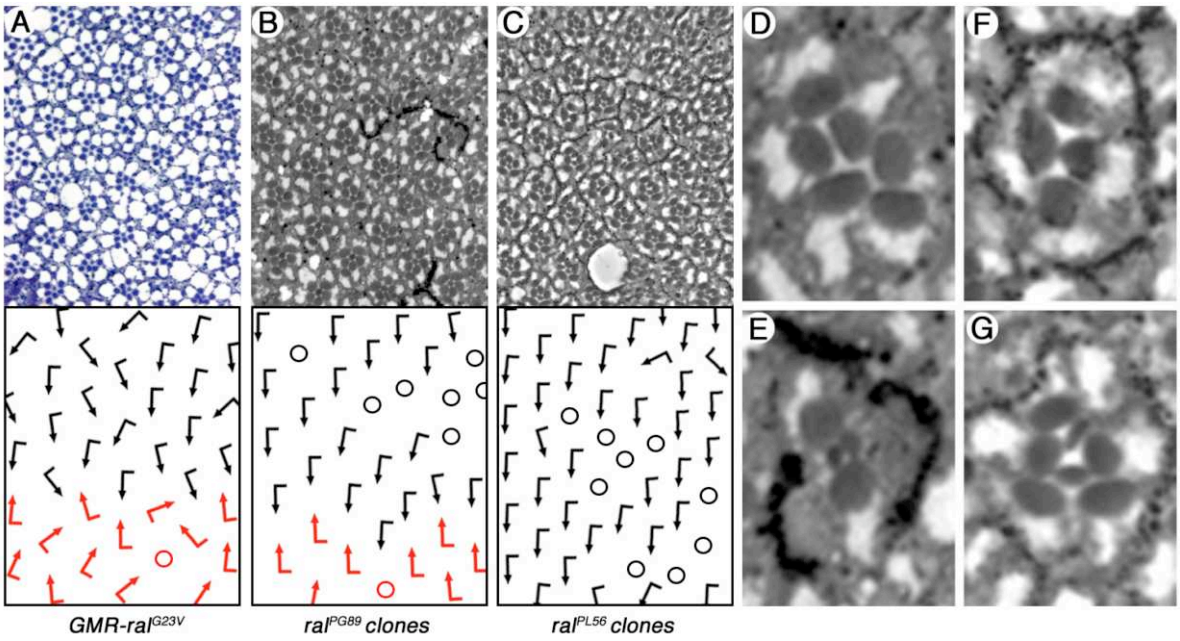

Figure 29. *ral* clones disrupt normal eye development

Tangential sections through adult eyes in which an activated form of Ral is expressed under control of the GMR promoter **(A)** or in which unmarked *ey-FLP* clones of *ral*^{PG89} and *ral*^{PG56} were induced **(B, C)**. Schematic representations are below each section. Black arrows represent dorsal ommatidia and red arrows ventral ommatidia. Flagged arrows indicate ommatidia with a full complement of photoreceptors, whereas circles indicate ommatidia with missing photoreceptors. Note that loss of photoreceptors, changes in rhabdomere morphology and rotation defects can be observed. **(D-G)** Enlargements of single ommatidia from B and C. **(D)** Example of a ommatidia in which the central R7 photoreceptor is lost. **(E)** Loss of several photoreceptors in an ommatidium of the same eye. Only two outer photoreceptor rhabdomers are visible. **(F)** Example of an ommatidia that lost two outer and the central R7 photoreceptor. **(G)** Illustration of an ommatidia in which the rhabdomere of the R4 photoreceptor displays an abnormal morphology.

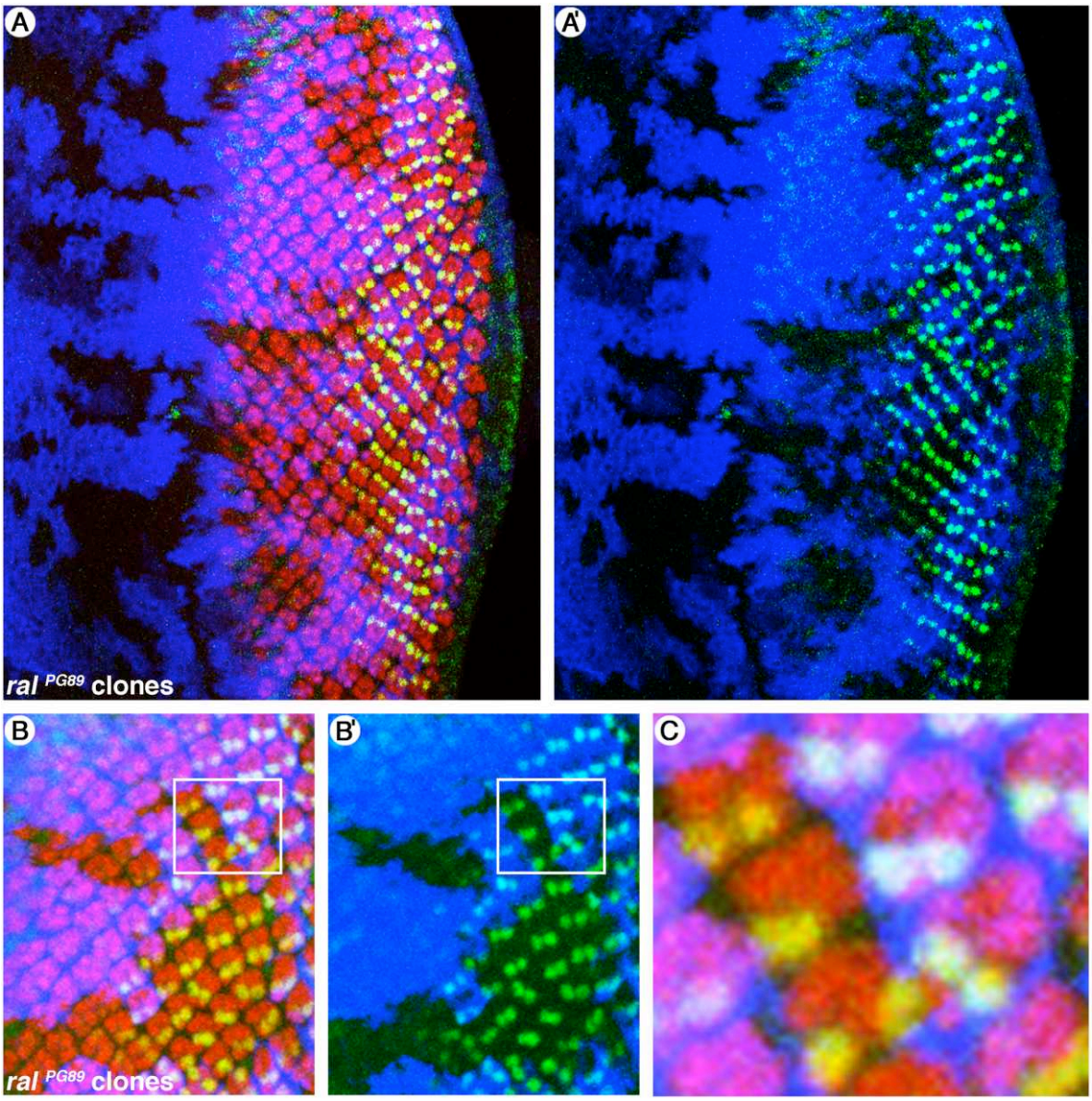

Figure 30. *ral* clones disturb normal eye imaginal disc development

(A-C) Third instar eye imaginal showing *ey-FLP* induced clones of *ral*^{PG89}. Clones are marked by the absence of *armadillo-LacZ* (blue). Anti-Elav (red) marks developing photoreceptor neurons and anti-Bar (green) indicates the position of the R1/R6 photoreceptor pair. **(A)** Overview of a whole disc. **(A')** The same disc showing the clonal marker (blue) and anti-Bar (green) channels only. Note that some ommatidia within the Rala mutant area have lost Bar staining in one photoreceptor of the R1/R6 pair and that a number of ommatidia appear misrotated. **(B)** Enlarged area from a different disc showing a *ral*^{PG89} clone. **(B')** Same area as in B showing the clonal marker (blue) and anti-Bar (green) channels only. **(C)** Enlargement of boxed areas in B and B' showing loss of Bar staining in the R6 photoreceptor of an ommatidium within *ral*^{PG89} mutant tissue. Anterior is left and dorsal is up in all panels.

Cell adhesion and cytoskeletal factors involved in Egfr mediated ommatidial rotation

To identify cell adhesion and cytoskeletal factors involved in ommatidial rotation, I performed two sets of experiments. First, candidate genes were tested for their ability to modify the $S^{48.5}/+$ rotation phenotype and second, I examined whether cell-adhesion components such as cadherins are mislocalised in aos^{rlt} or cno^{mis1} mutant eye imaginal discs.

I reasoned that a reduction in gene dosage of components required for ommatidial rotation would lead to a modification of the mild rotation phenotype displayed in the haploinsufficient $S^{48.5}/+$ allele, which exhibits 9.6 ± 1.4% misrotated ommatidia. As demonstrated previously, this is true for key components of Egfr signalling (see Fig. 22 and Table 2) and for strong alleles of *cno* (Fig. 25B and Table 3). In fact, I found that several factors implicated in adhesion or regulation of the cytoskeleton did modifiy the $S^{48.5}/+$ rotation phenotype substantially (summarized in Table 3). Among the strongest interactors were alleles of *DE-cadherin/shotgun* and the core planar polarity gene *fmi* (an atypical seven-transmembrane cadherin). DE-cadherin/shotgun enhanced the $S^{48.5}/+$ rotation defects to 40.6 ± 5.2% (shg^{2}) and *fmi* to 45.6 ± 7.3% (fmi^{E59}), 43.8 ± 7.4% (fmi^{E45}) respectively (Fig. 31B, C and Table 3). In contrast, Integrins and Laminins did not enhance the $S^{48.5}/+$ rotation phenotype (see Table 3). Among the tested motor-proteins, alleles of the non-muscle Myosin(II) heavy chain encoded by *zipper (zip),* as well as the non-muscle Myosin light chain encoded by *spaghetti-squash (sqh)* enhanced the $S^{48.5}/+$ rotation defects to 34.6 ± 4.7% (zip^{02957}), 19.3 ± 7.1% (zip^{1}), or 20.1 ± 9.9% (sqh^{PL91}), respectively (Table 3, Fig. 31D and not shown). Alleles of *crinkled (ck)*, an orthologue of Myosin VIIa, as well as alleles of *kinesin-heavy chain (khc)* had no effect (Table 3). Furthermore, I found that genes involved in the regulation of the actin-cytoskeleton also modified the $S^{48.5}/+$ rotation phenotype. Among these were several genes that function together in actin polymerisation and or de-polymerisation and are known to regulate cell motility in several contexts (for reviews see Pollard and Borisy, 2003; Paavilainen et al., 2004). For example, *chickadee (chic)*, the *Drosophila* orthologue of Profilin promotes the elongation of actin filaments on barbed ends. Twinstar (Tsr), the *Drosophila* orthologue of the actin depolymerising factor Cofilin promotes actin depolymerisation at pointed ends and serves long actin filaments. I also found alleles of the actin monomer sequestering protein Twinfilin (Twf) and the phosphatase Slingshot (Ssh) to genetically interact with $S^{48.5}$. Interestingly, *chic*, *tsr* and *twf* enhance the rotation defects of $S^{48.5}$/+ to 21.9 ± 6.0% ($chic^{01320}$), 27.8 ± 9.6% (tsr^{k05633}) and 23.4 ± 5.0% ($Df(3R)su^{Hw7}[twf]$), respectively, whereas an allele of the phosphatase Ssh (which de-phosphorylates Cofilin) almost completely suppresses the $S^{48.5}$ rotation

phenotype 0.4 ± 0.4% (*ssh*^{01207}, Table 3 and Figure 31F, G and H). In addition, I found that alleles of the adenylyl cyclase-associated protein Capulet (Capt) as well as the septin Peanut (Pnut) enhance the *S*$^{48.5}$*/+* rotation phenotype to 34.2 ± 8.9% (*capt*^{06955}), 24.6 ± 5.9% (*pnut*^{XP}), 20.1 ± 11.3% (*pnut*^{02502}), respectively (Fig. 31E and not shown). I also tested genes previously implicated in ommatidial rotation for their ability to modify the *S*$^{48.5}$*/+* rotation phenotype and found that *nemo* enhanced the rotation defects of *S*$^{48.5}$*/+* to 19.8 ± 6.6% (*nmo*^{P1}), whereas *scabrous* (*sca*) and *Drok* had no significant effect (see Tabel 3).

In summary, I have identified several genes as modifiers of the mild *S*$^{48.5}$*/+* rotation phenotype that can be grouped according to their biological function into four classes: cadherins, (*DE-cadherin* and the atypical cadherin *fmi*), motor proteins (non-muscle Myosin heavy and light chain), genes involved in actin polymerisation/depolymerisation and components of the actin cytoskeleton (Chic, Tsr, Twf, Ssh, Pnut and Capt). Cno and Nmo can be grouped together as 'signalling components' and would form a fourth class.

***Star*$^{48.5}$*/+* for all genes below**	**% misrotated ommatidia ± s.d.**	**molecular function of gene**
oregon-R	9.6 ± 1.4	Wild type control (baseline)
canton-S	10.5 ± 1.0	Wild type control (baseline)
Cadherin family members:		
shg^{2}	40.6 ± 5.2	DE-Cadherin
fmi^{E59}	45.6 ± 7.3	Atypical Cadherin, classical polarity gene
fmi^{E45}	43.8 ± 7.4	Atypical Cadherin, classical polarity gene
Integrin and extracellular matrix components:		
mys^{null}	4.4 ± 2.6	Integrin β-subunit
mys^{1}	7.7 ± 3.8	Integrin β-subunit
wb^{09437}	13.2 ± 3.1	Laminin
wb^{4418}	7.2 ± 0.6	Laminin
Motor proteins:		
zip^{02957}	34.6 ± 4.7	Non-muscle Myosin II heavy chain
zip^{1}	19.3 ± 7.1	Non-muscle Myosin II heavy chain
sqh^{PL91}	20.1 ± 9.9	Non-muscle Myosin light chain
ck^{13}	5.4 ± 2.2	Myosin VIIa
khc^{8}	10.4 ± 5.7	Kinesin heavy chain
khc^{k13314}	2.9 ± 2.0	Kinesin heavy chain
Actin polymerising/depolymerising factors and components of the actin cytoskeleton:		
capt^{06955}	34.2 ± 8.9	Adenylyl cyclase-associated protein with actin & microtubuli binding activity, involved in actin filament polymerization and or depolymerisation
pnut^{XP}	24.6 ± 5.9	Septin, actin & microtubuli binding activity, involved in actin filament polymerization and or depolymerisation
pnut^{02502}	20.1 ± 11.3	

chic^{01320}	21.9 ± 6.0	Profilin, actin filament polymerization and or depolymerisation
tsr^{k05633}	27.8 ± 9.6	Cofilin/actin depolymerising factor
twf Df(3R)su^{Hw7}	23.4 ± 5.0	Actin monomer sequestering protein
ssh^{01207}	0.4 ± 0.4	Cofilin phosphatase, required for actin filament polymerization and or depolymerisation
ena^{02029}	7.8 ± 3.0	VASP homolog, actin filament polymerization and or depolymerisation
karst^{01318}	5.6 ± 1.1	β-Heavy spectrin, actin & microtubuli binding activity
Adherense junction associated proteins:		
arm^{XM19}	12.4 ± 5.7	Armadillo/β-cathenin, localised to adherense junctions
cno^{2}	40.6 ± 8.0	Ras-effector multidomain protein with actin binding capability, localised to adherense junctions
cno^{3}	43.2 ± 8.7	
Genes implicated in ommatidial rotation		
nmo^{P1}	19.8 ± 6.6	MAPK family member, controls ommatidial rotation
sca^{BP1}	9.8 ± 3.1	Secreted factor implicated in ommatidial rotation
Drok^{1}	7.8 ± 5.7	Rho-Kinase, planar polarity gene
Drok^{2}	4.9 ± 4.0	Rho-Kinase, planar polarity gene
Others:		
N^{73}	7.4 ± 3.7	Notch-receptor
aPKC	13.3 ± 6.8	Atypical protein kinase C, establishment and maintenance of epithelial polarity
baz^{11}	26.1 ± 4.0	aPKC binding, PDZ-domain protein, establishment and maintenance of epithelial polarity
baz$^{815-8}$	7.2 ± 5.2	
hdc^{Fus-6}	22.8 ± 6.7	Cell differntiation factor, required for terminal branching of trachea

Table 3. Summary of genetic interactions with *S*$^{48.5}$*/+*

Mutant alleles of several cell adhesion and cytoskeletal factors enhance the *S*$^{48.5}$/+ rotation phenotype in a dosage dependent manner, revealing their requirement in ommatidial rotation. Among the strongest enhancers are the cadherin family members (e. g. *shg* and *fmi*) and the ras effector *cno*. The motor-protein non-muscle myosin heavy and light chain and the actin polymerising/depolymerising factors as well as components of the actin cytoskeleton lead to a mild but consistent enhancement of the rotation defects in *S*$^{48.5}$/+ eyes. All interactions are in heterozygous genotypes of the indicated genes. For all genotypes, *n* is > 400 ommatidia from at least three eyes. The standard deviation (s.d.) is between eyes. Only ommatidia with a wt complement of photoreceptors were scored. Ommatidia with an abnormal photoreceptor complement do not contribute to the total % of ommatidia analysed.

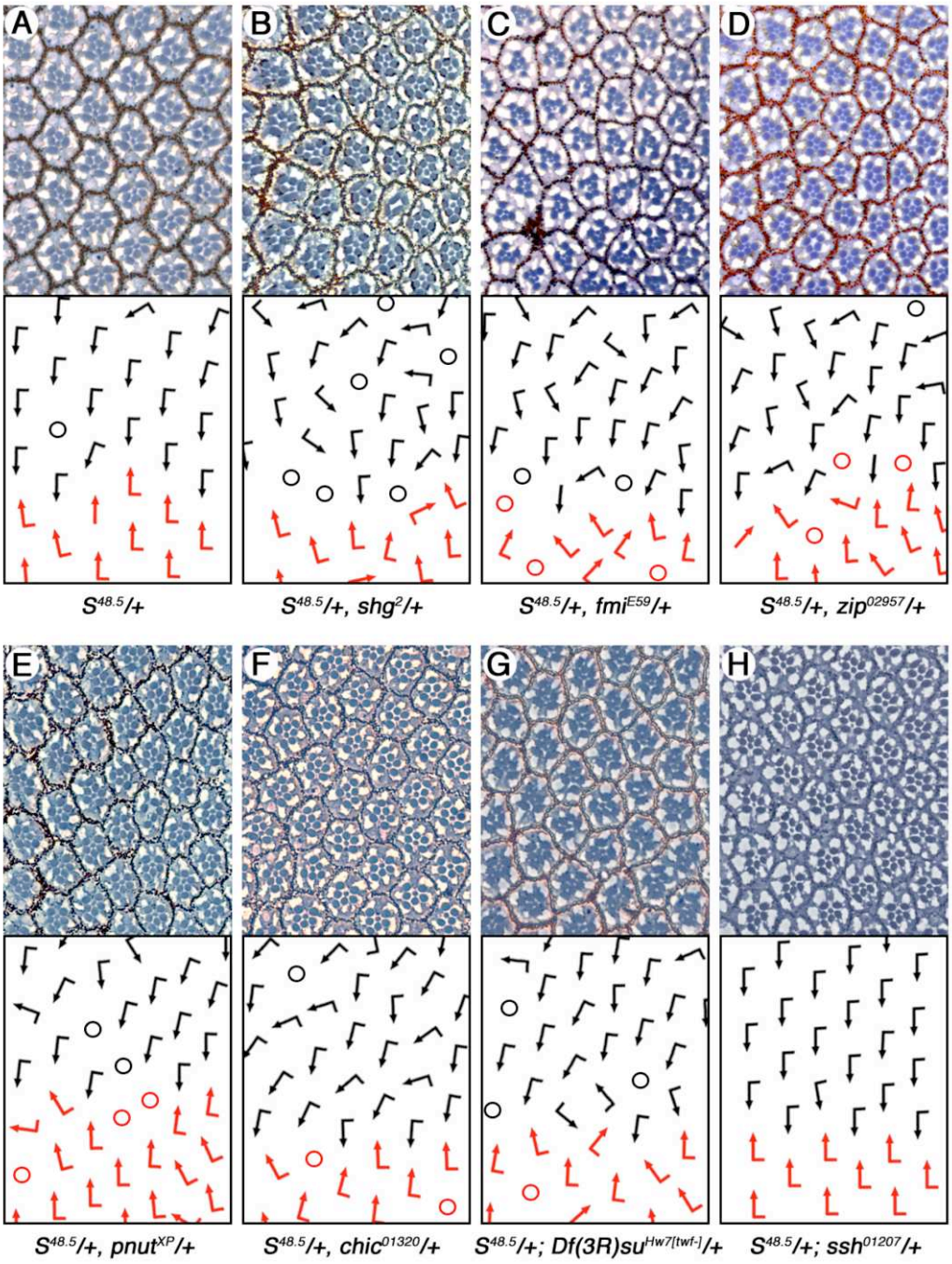

Figure 31. Rotation defects in $S^{48.5}$ eyes are modified by loss of one gene dosage of cadherin family members, non muscle Myosin II and through genes involved in actin polymerisation/depolymerisation

(A-H) Tangential section of adult eyes around the equatorial region, with corresponding schematic representation below each panel. Dorsal ommatidia are represented by black arrows and ventral ommatidia by red arrows. Flagged arrows represent ommatidia with a full complement of photoreceptors, whereas ommatidia with extra photoreceptors are indicated by straight arrows. Loss of photoreceptors are indicted by circles. Genotypes are indicated below each panel. Note that DE-cadherin/*shg* **(B)**, the atypical cadherin *fmi* **(C)**, non-muscle myosinII/*zipper* **(D),** as well as factors required for actin polymerization/depolymerisation like the septin *pnut* **(E)**, profilin/*chic* **(F)** and a Df uncovering *twf* **(G)** enhance the rotation defects of $S^{48.5}$/+, whereas the profilin-phosphatase *ssh* **(H)** is a strong suppressor.

The atypical cadherin Flamingo is mislocalised in *aos^{rlt}* eye imaginal discs

Since members of the cadherin family were among the strongest enhancers of rotation defects in *S$^{48.5}$/+* eyes, I considered if the sub-cellular localisation of cadherins might be critical for ommatidial rotation and dependent on Egfr signalling. Strong loss-of-function alleles of Egfr and its signalling components also affect other cellular processes beside ommatidial rotation (e.g. cell proliferation, cell fate determination and cell survival, Xu and Rubin, 1993; Freeman, 1996; Dominguez et al., 1998; Baker and Yu, 2001; Baonza et al., 2001) and therefore make such an analysis hard to interpret. I therefore chose the rotation-specific *aos^{rlt}* allele to study Egfr dependent effects on DE-cadherin and Fmi localisation. I found that the atypical cadherin Fmi was mislocalised in *aos^{rlt}* eye-imaginal discs (Fig. 32 and 33B, B', D), whereas the overall expression and localisation of DE-cadherin, armadillo/β-catenin and F-actin seemed largely unaffected. (Fig. 32 and 33B, B'' and D and not shown). In a wild-type eye disc, Fmi is initially present at the apical membranes of all cells within the morphogenetic furrow and subsequently becomes enriched in the R3/R4 precursor pair at column 4 (Fig. 32B). In and posterior to column 6, Fmi becomes enriched at the membrane of R4 and is largely depleted from R3 membranes not touching R4, forming a horseshoe-like R4-specific pattern (Fig. 32C-E and 33C). In *aos^{rlt}* discs, Fmi restriction to the R4 precursor is generally delayed and often not established even in columns 8-12, where high levels of Fmi are still seen around the apical membranes of R3 and R4 (Fig. 32I, J and 33D). Although the delayed restriction of Fmi to R4 is the most prominent phenotype in *aos^{rlt}* discs, Fmi localisation also appears different between neighboring clusters within the same column (Fig. 33B, B'). Furthermore, Fmi is occasionally enriched in other cells (Fig. 32G, H). Since Fmi is a homophillic cell-adhesion molecule (Usui et al., 1999), its increased abundance on R3 and other cell membranes could have a direct effect on Fmi localisation in neighboring cells and thus on the adhesive properties of the precluster. In this context, it is important to note that Fmi is a core planar polarity gene (Usui et al., 1999) and known to be required for the R3/R4 cell-fate decision (Das et al., 2002), the delay of Fmi restriction to R4 has no significant effect on the R3/R4 cell-fate decision. Even though Fmi interacts with Fz and Notch in this context (Das et al., 2002), the R4 specific *mδ0.5-lacZ* marker appears largely normal in *aos^{rlt}* eye discs (Fig. 18B, B'). Furthermore, sections through adult *aos^{rlt}* eyes show a very small fraction of ommatidia that appear to be symmetrical (1.6 ± 1.5%) or have inverted chirality (0.5 ± 0.5%, Fig. 12E). Thus, it appears that the delay in Fmi localisation and its enrichment in additional cells specifically affect ommatidial rotation. Differences in Fmi localisation most likely results in different adhesive properties of individual ommatidial clusters which could explain the broad range of rotation angles in *aos^{rlt}* eye and other Egfr pathway mutants. In summary,

these data and the genetic interactions presented above suggest that Egfr signalling modifies the cell adhesive properties of ommatidial clusters during ommatidial rotation.

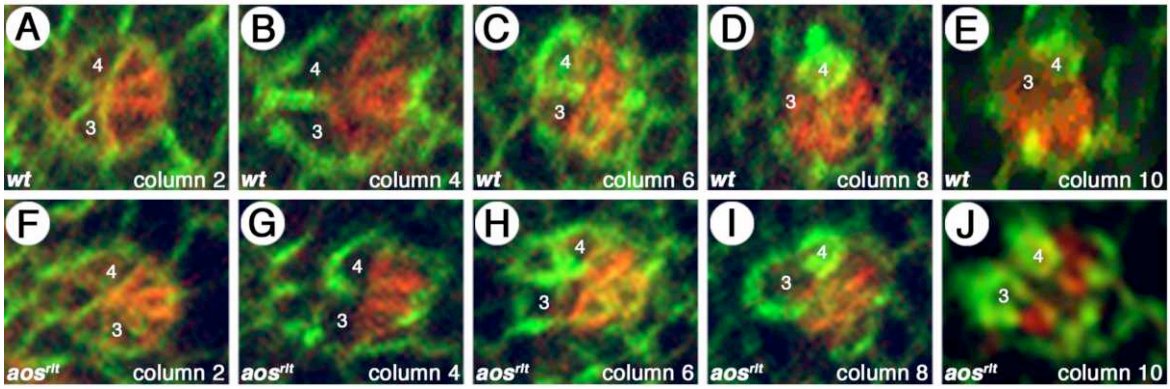

Figure 32. The subcellular localisation of the atypical cadherin Flamingo is altered in *aos^{rlt}* eye imaginal discs

(A-J) Confocal images of developing ommatidial clusters in a third instar eye imaginal discs stained with an antibody against Flamingo (green) and DE-cadherin (red). The morphogenetic furrow is on the left edge of each panel. The developmental stage of each ommatidial cluster is indicated in the lower right corner of each panel. The position of the R3/R4 photoreceptor pair is indicated with white numbers. **(A)** In wt discs, Flamingo is initially uniformly distributed around the membranes of all cells. **(B)** By column 4, Fmi becomes enriched in both cells of the R3/R4 pair. **(C)** Starting at column 6, Fmi is depleted in R3 and enriched in R4. **(D)** By column 8, Fmi is strongly enriched in R4 and almost completely absent from R3 membranes. **(F-J)** In *aos^{rlt}*, Fmi localisation is altered. **(F)** In very early clusters, Fmi distribution is similar to its localisation in wt discs. **(G)** However, by column 4, Fmi localisation is altered in *aos^{rlt}* discs. At this stage, four cells (the R3/R4 pair and two additional cells anterior to the R3/R4 pair) typically show strong Fmi enrichment. **(H)** By column 6, Fmi localisation can occasionally be observed in an additional cell between the R3/R4 pair and usually is not depleted from R3 membranes, in contrast to wt discs. **(I, J)** In most ommatidial clusters of *aos^{rlt}* discs, Fmi remains strongly enriched in both cells of the R3/R4 pair beyond column 12. Panel J shows an example from column 10, compare with the equivalent stage in *wt* discs in panel E. In all panels anterior is to the left and dorsal is up.

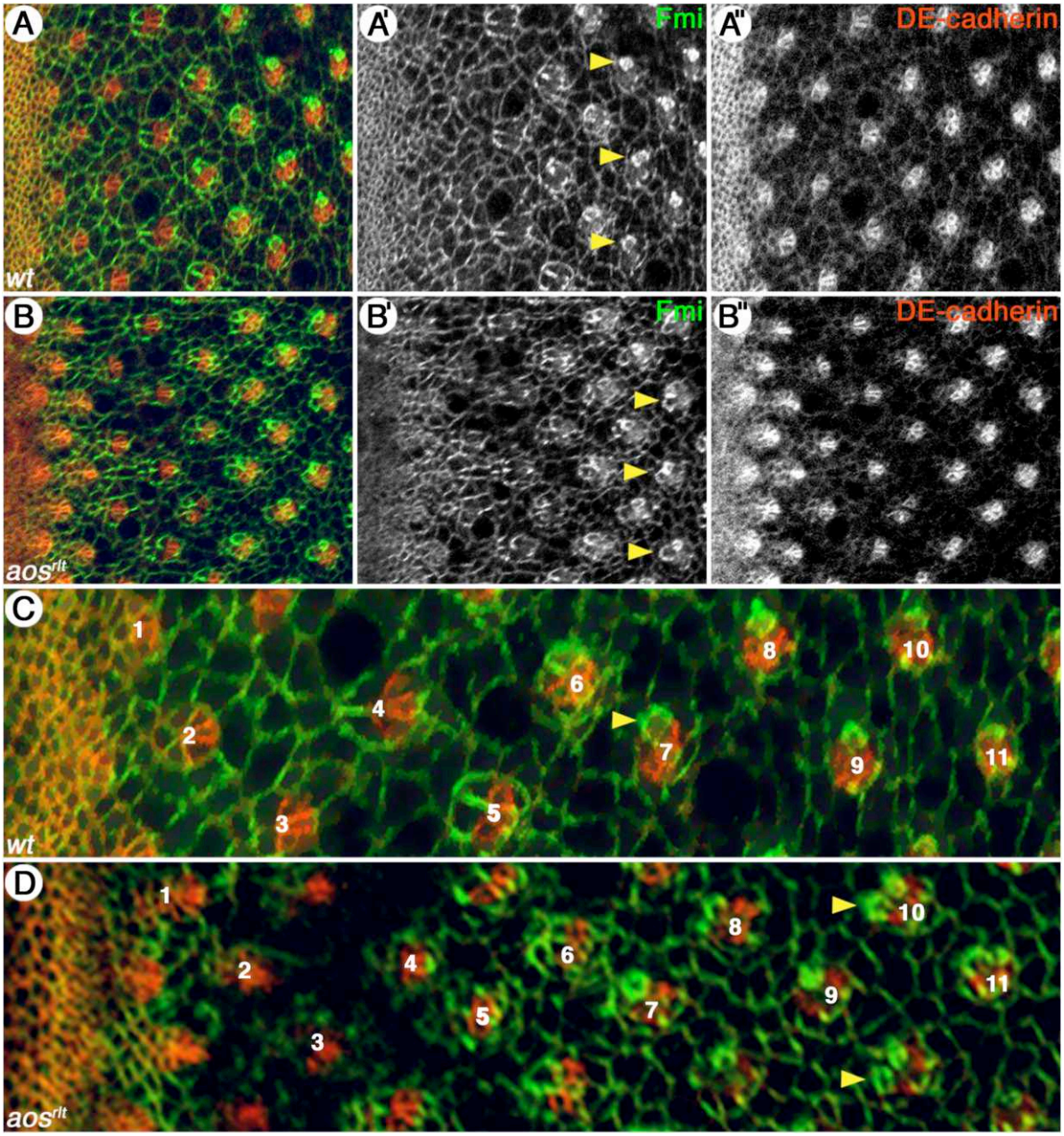

Figure 33. Flamingo restriction to R4 is delayed in *aos*^{rlt} eye imaginal discs

(A-D) Confocal images of third instar eye imaginal discs stained with an antibody against Fmi (green and single channels) and DE-cadherin (red and single channnels). The morphogenetic furrow is on the left edge of each panel. The respective genotypes are indicated in the lower left corner. Developmental stages of ommatidial clusters are indicated by white numbers indicating respective columns behind the morphogenetic furrow. **(A, A' and C)** In wt discs, Fmi is enriched in both cells of the R3/R4 pair between column four and five and is subsequently depleted in R3 and strongly enriched only in R4 from column six or seven on (yellow arrowheads in A' and C). **(B, B' and D)** In *aos*^{rlt} discs Fmi localisation is altered. In most ommatidial clusters Fmi remains strongly enriched in both cells of the R3/R4 pair beyond column 12 (yellow arrowheads in B' and D). (**A'' and B'')** The sub-cellular localisation of DE-cadherin appears largely normal in *aos*^{rlt} discs. Anterior is left and dorsal is up in all panels.

Ommatidial rotation defects in *aos*^{rlt} eyes are suppressed by mutations in *flamingo*

As shown above, several lines of evidence point towards a key role for the atypical cadherin Fmi in ommatidial rotation: alleles of *fmi* lead to a strong enhancement of the mild *Star*$^{48.5}$*/+* rotation phenotype and Fmi itself is mislocalised in *aos*^{rlt} eye imaginal discs. These findings lead to the hypothesis that improper Fmi localisation has a direct effect on the adhesive properties of the rotating preclusters. I reasoned that if loss of *aos* function results in ectopic Fmi localisation to membranes from which it is normally excluded, loss of one copy of *fmi* should rescue the rotation defects of the *aos*^{rlt} allele. To test this assumption, I created a *fmi*^{E45}; *aos*^{rlt} double mutant and analysed eyes heterozygous for *fmi*^{E45} in an homozygous *aos*^{rlt} background. I found that rotation defects in *aos*^{rlt} eyes were substantially suppressed by loss of one copy of *fmi* (Fig. 34). To quantify these results without the need of exactly determining the rotation angle of every single ommatidium, I developed a less time consuming method that allows discrimination of under-rotated, over-rotated and correctly oriented ommatidia. For this analysis, rotation angles of 90° ± 25° were scored as correctly oriented, whereas rotation angles of < 65° were scored as under-rotated and rotation angles of > 115° as over-rotated. According to these parameters, 47.4 ± 6.6% of ommatidia were correctly oriented in *aos*^{rlt} eyes, vs. 73.4 ± 8.7% in *fmi*^{E45}*/+*; *aos*^{rlt}*/aos*^{rlt} (Fig. 34C). This result clearly demonstrates that loss of one copy of *fmi* substantially rescues the *aos*^{rlt} rotation phenotype and strongly suggests that *fmi* is at least in part responsible for Egfr dependent ommatidial rotation defects. The fact that *fmi* does not completely rescue the rotation defects in *aos*^{rlt} eyes is not surprising, as there is an obvious requirement for other factors (like the Ras/Raf/MAPK cascade and *cno*) in this process.

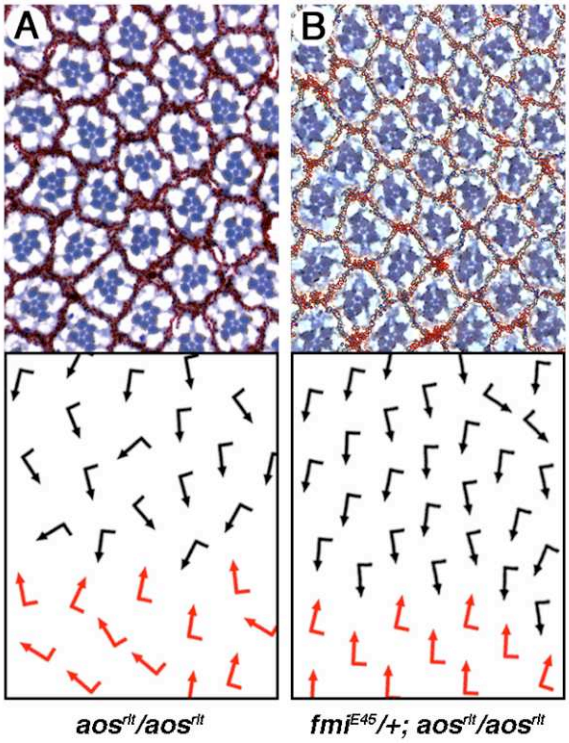

C

aos^{rlt}/*aos*^{rlt}	% ommatidia ± s.d.
under rotated	27.6 ± 8.6
over rotated	25.0 ± 5.5
correctly rotated	47.4 ± 6.8
fmi^{E45}***/+; aos***^{rlt}***/aos***^{rlt}	
under rotated	14.3 ± 7.8
over rotated	12.3 ± 4.0
correctly rotated	73.4 ± 8.7

Figure 34. Loss of one gene dosage of *flamingo* suppresses the rotation defects in *aos*^{rlt} eyes

(A, B) Tangential sections of adult eyes around the equatorial region, with corresponding schematic representation below each panel. Dorsal ommatidia are represented by black arrows and ventral ommatidia by red arrows. The respective genotypes are indicated below each panel. Note that the rotation defects in *aos*^{rlt} eyes are substantially rescued by loss of one copy of *fmi*. **(C)** Analysis of rotation angles in *aos*^{rlt}/*aos*^{rlt} and *fmi*^{E45}*/+; aos*^{rlt}/*aos*^{rlt} eyes show that *fmi* suppresses the rotation defects in *aos*^{rlt} eyes. For this analysis, ommatidia with a rotation angle of 90° ± 25° were scored as correctly oriented, whereas rotation angles of < 65° were scored as under-rotated and rotation angles of > 115° as over-rotated.

Designing a genetic screen to identify genes involved in ommatidial rotation

The key discovery that *rlt* is allelic to *aos* and that Egfr signalling controls rotation opened the door for a more detailed analysis of ommatidial rotation. In particular, the haploinsuficient $S^{48.5}$ allele emerged as a valuable tool for identifying components involved in ommatidial rotation. As demonstrated above, loss of one gene copy of *S* results in a mild rough eye phenotype and tangential sections of adult eyes reveal a mild loss of photoreceptors and 9.6 ± 1.4% misrotated ommatidia (Fig. 31A and Table 3). As demonstrated previously, the mild $S^{48.5}$/+ rotation phenotype is dosage sensitive and enhanced by mutations in components of the Egfr pathway and several other genes implicated in ommatidial rotation. Consistently, several enhancers of *S* were able to suppress the rotation defects of aos^{rlt}, providing further evidence for their requirement in the rotation process. *S* therefore appears to be an ideal tool for an F_1 loss-of-function modifier screen. However, the analysis of *S* modifiers performed so far relies on adult eye sections, a precise but time consuming method. To screen through a large number of flies more efficiently, I adapted an elegant visualisation technique developed by Frank Pichaud (Pichaud and Desplan, 2001). This approach allows the analysis of ommatidial rotation and planar cell polarity in the living fly, using a specially designed water immersion lens on a Zeiss Axioscope2 microscope (Fig. 35A, B). To assay planar polarity and ommatidial rotation in genetic modifiers of *S*, I recombined a *rhodopsin1-eGFP (rh1-eGFP)* transgene (Pichaud and Desplan, 2001) onto the $S^{48.5}$ chromosome, which introduces eGFP into the outer photoreceptors R1-R6. After neutralization of the cornea, which is achieved by immersing flies in water, the outer photoreceptors of up to 40 ommatidia can be visualised under UV-illumination using a 40x Zeiss water immersion lens (Fig. 35D). Although the quality of the obtained images is not as good as plastic sections and allows the evaluation of only 30 to 40 ommatidia per eye (compared to up to 200 per eye in plastic sections), it is far less time consuming, and still permits the characterisation of a given phenotype in sufficient detail.

To ensure that ommatidial rotation defects are detected unambiguously using this visualisation approach, I recombined the *rh1-eGFP* transgene onto the aos^{rlt} chromosome and analysed the eye phenotype of homozygous *rh1-eGFP;* aos^{rlt} flies using the new microscopic setup. The *rh1-eGFP;* aos^{rlt} flies displayed clearly visible defects in ommatidial rotation (Fig. 36A). To further test the capacity of this technique, I initiated a pilot-screen using known modifiers of $S^{48.5}$ as well as candidate genes suspected to have a role in ommatidial rotation. For the pilot screen, known modifiers of $S^{48.5}$ as well as candidate genes were crossed to the $S^{48.5}$, *rh1eGFP/SM5a:TM6b* stock and subsequently analysed for rotation defects.

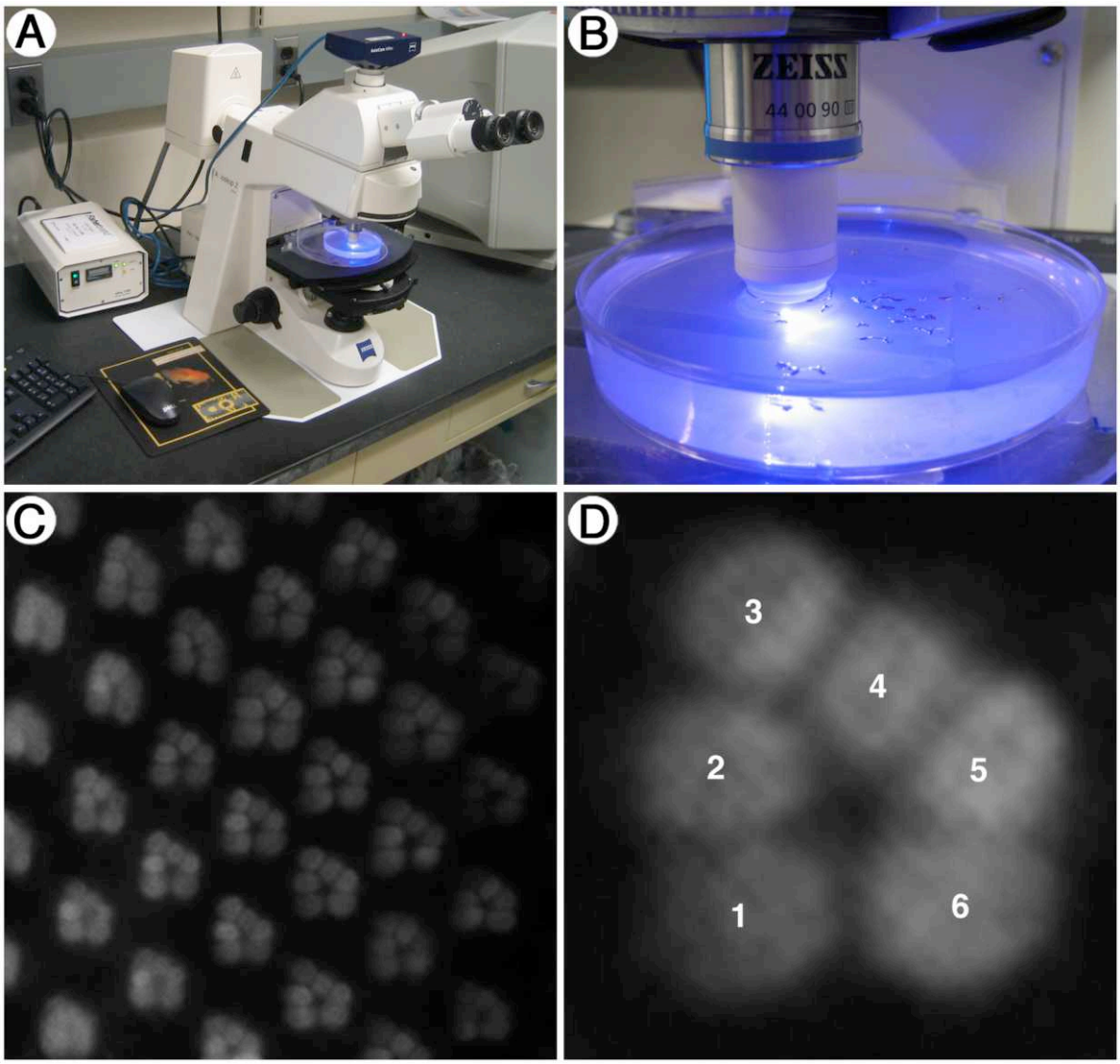

Figure 35. Microscope setup used to visualise *rh1-eGFP* expression in the $S^{48.5}$ modifier screen, designed to identify genes involved in ommatidial rotation

(A) Microscopic setup. To visualise *rh1-eGFP* expression in living flies, a Zeiss axioskop2 microscope, equipped with a Zeiss 40x water immersion lens (**B)** was used. Flies were CO_2 anesthetized, fixed to the surface of a 2% agarose gel, covered with water and subsequently analysed under UV-illumination. **(C)** Example of *rh1-eGFP* expression in a dorsal region of the eye of otherwise wild type flies. Note that the outer photoreceptors R1 – R6 are clearly visible in most ommatidia captured and that orientation and chirality of ommatidia can be visualised using this method. **(D)** Enlargement of a single *rh1-eGFP* expressing ommatidium. The photoreceptors R1 – R6 are indicated by white numbers.

Approximately ten flies were analysed per genotype. A summary of the results of this 'pilot-screen' is shown in Table 4. Interestingly, of the known planar polarity genes only *fmi* enhanced the rotation defects in $S^{48.5}$ eyes significantly, whereas the others had weak or no effects (Fig. 36C, D and Table 4). This suggests, that Egfr signalling mainly impinges upon the cell adhesion properties of the core planar polarity genes, mediated by Fmi.

As a positive control for genes that should strongly modify the $S^{48.5}$, *rh1-eGFP*/+ rotation phenotype, I tested several core components of the Egfr pathway. Conspicuously, spi^{1}, $Egfr^{top1}$ and pnt^{07825} strongly enhanced the rotation defects in $S^{48.5}$ *rh1-eGFP*/+ eyes (Table 4), whereas a strong allele of the Ras inhibitor *sty* led to an almost complete suppression (Table 4). To further investigate if moderate or mild enhancers could also be identified using this method, I tested alleles of the genes encoding non-muscle myosin light and heavy chain as well as myosin VIIa. Consistent with results obtained from adult plastic sections, *zip* and *sqh* alleles resulted in a weak to moderate enhancement of the $S^{48.5}$, *rh1-eGFP*/+ rotation defects, whereas ck^{13} had no effect (Table 4). However, it appears that a very mild enhancement or small differences between alleles might not be resolvable with this technique as satisfyingly as with tangential plastic sections of adult eyes. In addition, I also tested several alleles of the adenylyl cyclase-associated protein *capt*, which was previously identified as an enhancer of $S^{48.5}$ (see Table 3). Using the *rh1-eGFP* visualisation technique, I was able to identify the $capt^{06955}$ allele as a clear enhancer. However, the other tested alleles $capt^{E593}$, $capt^{E636}$ and $capt^{01267}$ failed to enhance the rotation defects in $S^{48.5}$, *rh1-eGFP*/+ eyes, suggesting that the enhancement of the $capt^{06955}$ allele most likely results from a second mutation on that chromosome (Table 4). A further analysis of *capt* mutant clones in the eye will reveal if this gene is indeed required for ommatidial rotation. To further complete this analysis, I also tested a null allele of *Notch (N)* and alleles of the *Drosophila* PDGF/VEGF receptor (Pvr). While I was unable to detect an interaction between *N* and $S^{48.5}$, *rh1-eGFP*/+, I found that both tested alleles of Pvr strongly enhanced the $S^{48.5}$, *rh1-eGFP*/+ eye phenotype (Fig. 36E and Table 4). Pvr has recently been reported to be partially redundant with Egfr during border cell migration (Duchek et al., 2001), suggesting that a similar relationship of Egfr and Pvr might exist in the context of ommatidial rotation. To investigate the $S^{48.5}$/*pvr* interaction in more detail, I analysed tangential plastic sections of adult $S^{48.5}$/+, pvr^{5363}/+ and $S^{48.5}$/+, pvr^{lW}/+ eyes. As expected from the *rh1-eGFP* analysis, I found that the mild rotation defects in $S^{48.5}$ eyes (9.6 ± 1.4%) were enhanced to 54.5 ± 5.8% (pvr^{5363}) or 30.5 ± 6.2% (pvr^{lW}), respectively (Fig. 37 and Table 4). While analyzing these sections, I noticed that the majority of the misrotated ommatidia were over-rotated, whereas only a small fraction of ommatidia were under-rotated. A quantification of this phenotype (using the same quantification approach as for the evaluation of rotation angles of the

fmi^{E45}*/+; aos*^{rlt}*/aos*^{rlt} interaction Fig. 34C) indeed showed that 83.8 ± 5.8% of misrotated ommatidia in *S*$^{48.5}$*/+, pvr*^{5363}*/+* eyes were over-rotated, whereas only 16.2 ± 5.8% were under-rotated. Similarly, in *S*$^{48.5}$*/+, pvr*$^{IW\ 5}$*/+* eyes 79.0 ± 6.7% of misrotated ommatidia were over-rotated compared to only 21.0 ± 6.7% of under-rotated ommatidia. Although such a detailed analysis of rotation angles has not yet been applied to all *S*$^{48.5}$*/+* interactions, the high percentage of over-rotated ommatidia is striking. At this point, it is unclear what this result means. One possible explanation could be that Pvr functions to prevent ommatidia from over-rotating.

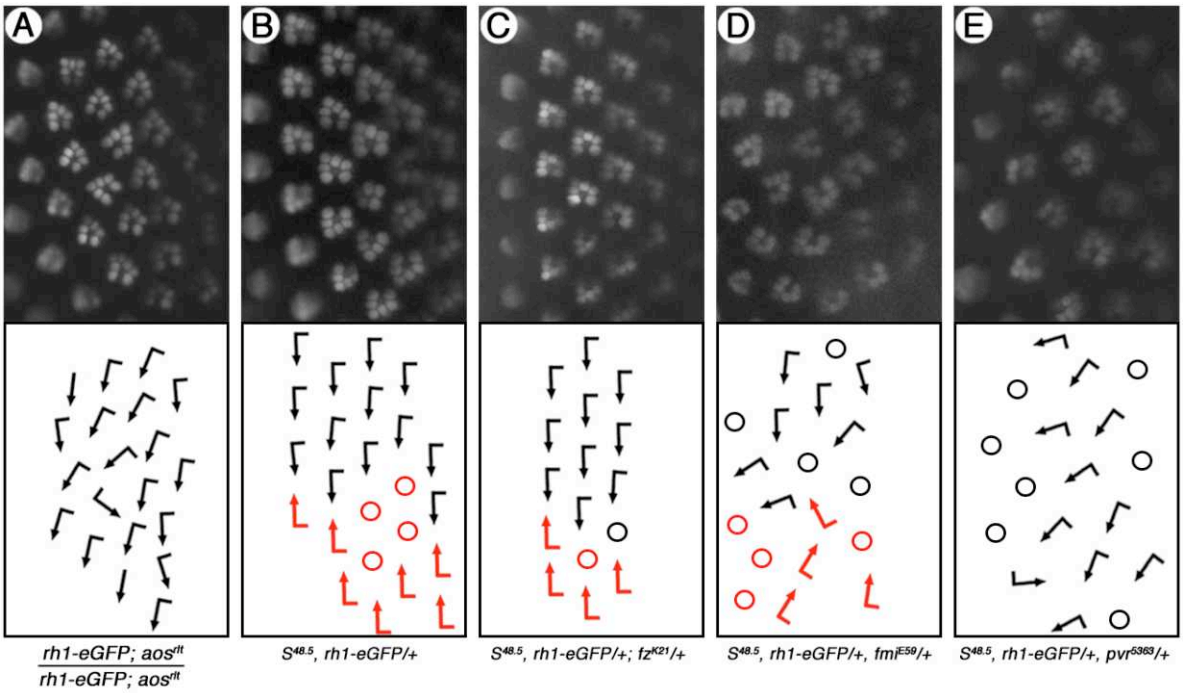

Figure 36. Examples of *S*$^{48.5}$*/+* interactions using the *rh1-eGFP* visualisation approach

(A-E) Adult *Drosophila* eyes expressing *rh1-eGFP*, examined with a 40x water immersion lens on living flies with schematic representations of ommatidial orientation below each panel. **(A)** A homozygous *rh1-eGFP; aos*^{rlt} eye displaying clearly visible rotation defects. **(B)** *S*$^{48.5}$*, rh1-eGFP/+* eyes show only very few rotation defects and some loss of photoreceptors. **(C)** *S*$^{48.5}$*, rh1-eGFP/fz*^{K21}. Loss of one copy of *fz* does not enhance *S*$^{48.5}$. In contrast loss of one copy of the the atypical cadherin Fmi **(D)** as well as loss of one copy of *Drosophila* PDGF/VEGF receptor orthologue **(E)** enhance the rotation defects in *S*$^{48.5}$*/+* eyes dramatically.

Table 4.

$S^{48.5}$, *rh1-eGFP /+* for all genes below	enhancement	moleculare function of gene
canton-S	-	wild type control (baseline)
oregon-R	-	wild type control
Classical planar cell polarity genes :		
fz^{1}	-	Sevenpass transmembrane receptor
fz^{K21}	-	Sevenpass transmembrane receptor
fz^{R54}	-	Sevenpass transmembrane receptor
fmi^{E45}	++(+)	Atypical cadherin
fmi^{E59}	+++	Atypical cadherin
dgo^{308}	-	Cytoplasmic ankyrin repeats containing protein
dgo^{269}	-	Cytoplasmic ankyrin repeats containing protein
$sple^{1}$	-	Cytoplasmic PET/LIM domain containing protein
$sple^{13}$	+	Cytoplasmic PET/LIM domain containing protein
$stbm^{6}$	-	Four transmembrane protein with C-terminal PDZ-binding motive
$stbm^{153}$	-	Four transmembrane protein with C-terminal PDZ-binding motive
Egfr pathway components:		
spi^{1}	++	TGF-α homologue, main activating ligand of EGFR in the eye
top^{1}	++	Epidermal growth factor receptor
pnt^{07825}	+++	ETS-domain transcription factor
sty^{D5}	suppression	Ras inhibitor
Motor proteins:		
zip^{1}	+	Non muscle Myosin II heavy chain
zip^{02957}	+(+)	Non muscle Myosin II heavy chain
sqh^{PL91}	+	Non muscle Myosin II light chain
ck^{13}	-	Myosin VIIa
Actin polymerising/depolymerising factors and components of the actin cytoskeleton:		
$capt^{06955}$	++(+)	Adenylyl cyclase-associated protein with actin & microtubuli binding activity, involved in actin filament polymerization and or depolymerisation
$capt^{E593}$	(+)	
$capt^{E636}$	(+)	
$capt^{01267}$	(+)	
Other candidate genes:		
pvr^{5363}	++(+)	PDGF/VEGF receptor orthologue
pvr^{IW}	++	PDGF/VEGF receptor orthologue
N^{264-39}	-	Notch receptor

Table 4. Summary of genetic interactions identified during a pilot screen for modifiers of $S^{48.5}$ using the *rh1-eGFP* visualisation approach

Modifiers were characterised according to their strength as +++ (= strong interaction), ++ (= medium interaction), + (weak interaction), - (= no interaction) or as suppressors. Parenthesis around symbols indicate a 'weak symbol'. Several known as well as new modifiers of $S^{48.5}$ were identified using the *rh1-eGFP* visualisation approach. Note that *fmi* is the only core planar polarity gene to enhance $S^{48.5}$, and that the *Drosophila* PDGF/VEGF receptor orthologue is a strong enhancer.

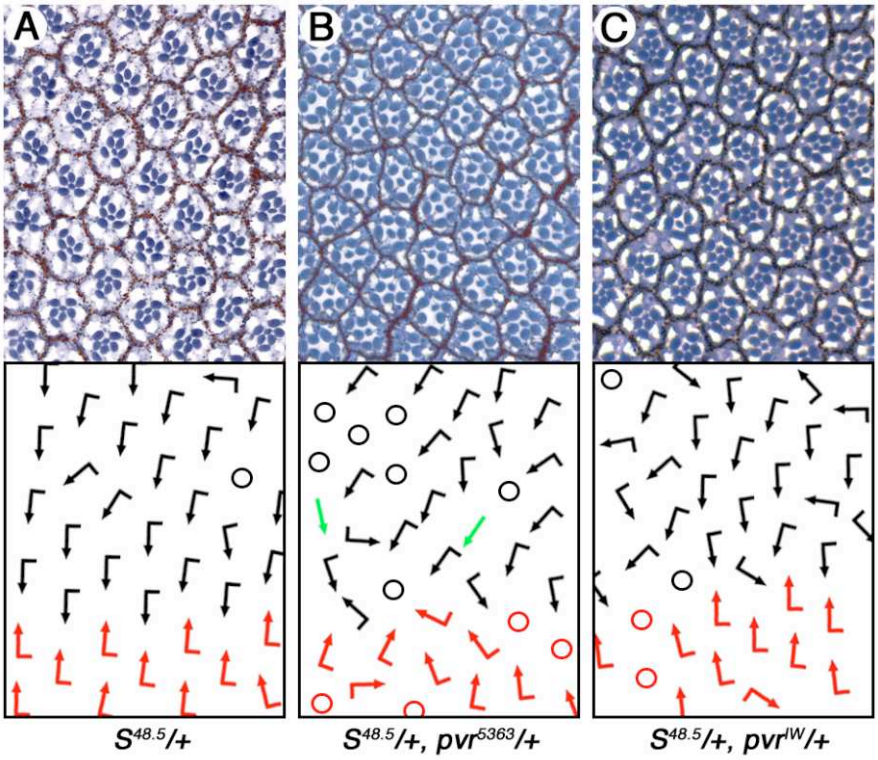

Figure 37. Loss of one copy of the *Drosophila* PDGF/VEGF receptor orthologue strongly enhances the rotation defects in $S^{48.5}$/+ eyes

(A-C) Tangential section of adult eyes around the equatorial region, with corresponding schematic representation below each panel. Dorsal ommatidia are represented by black arrows and ventral ommatidia by red arrows. Symmetrical ommatidia are indicated by green arrows and ommatidia that do not carry a full complement of photoreceptors are indicate by circles. The respective genotypes are indicated below each panel.

In summary, the data presented above show that the *rh1-eGFP* visualisation approach allows the study of ommatidial rotation in living flies. This method provides the basis for a $S^{48.5}$ modifier screen intended to identify new genes involved in ommatidial rotation. In a pilot screen, several known, as well as new, enhancers of $S^{48.5}$ could be identified. In the future, this approach will be used to screen for $S^{48.5}$ modifiers from a wide selection of well characterised mutations or deficiencies that can be obtained from *Drosophila* stock centers (http://flystocks.bio. indiana.edu/). A further loss of function analysis of these modifiers will reveal if the respective genes are in fact involved in ommatidial rotation or in other aspects of development.

III
Discussion

The key findings of this thesis, that *rlt* is an allele of *aos* and that Egfr signalling is essential for correct ommatidial rotation, have also been described by two other groups. Their work was published in *Current Biology* (Strutt and Strutt, 2003) and back to back with my work in *Development* (Brown and Freeman, 2003; Gaengel and Mlodzik, 2003). Moreover, a short review summarizing and comparing the most important findings of these papers was published shortly after in *Current Biology* as a 'Dispatch' (Wolff, 2003). I will therefore discuss concurring as well as differing interpretations presented in these publications. In addition, I will discuss results presented in this thesis that have not yet been published.

roulette is one of the few loci that specifically affects ommatidial rotation

The major aim of this thesis is to characterize the *rlt* locus and to assign a pathway that controls ommatidial rotation. The adult *rlt* eye phenotype was originally described as "strikingly abnormal in photoreceptor orientation". Most ommatidia were found to have a normal complement of photoreceptor cells in proper trapezoidal configuration, however, ommatidial rotation angles showed a broad distribution. Choi and Benzer found that 47% of the ommatidia were rotated more than 90° and therefore concluded that "*rlt* was unable to arrest rotation". It was thus proposed that the wt-function of *rlt* was to stop the rotation process once the ommatidia reached 90° (Choi and Benzer, 1994).

In a re-examination of the adult *rlt* eye phenotype I confirmed that the majority of ommatidia did in fact contain the wt complement of photoreceptor cells, as only 6.1 ± 4.1% of ommatidia displayed extra photoreceptors (Fig. 12E). In addition, a very small fraction of ommatidia appeared symmetrical (1.6 ± 1.5%) or had inverted chirality (0.5 ± 0.5%), their contribution to the overall phenotype was, however, negligible (Fig. 12E). An evaluation of ommatidial rotation angles revealed that over- and under-rotated ommatidia were present at about the same percentage (40.7% over-rotated vs. 38.5% under-rotated ommatidia). Choi and Benzer came to similar conclusions [compare Figure 5C in (Choi and Benzer, 1994) with Figure 12G in this thesis] but my data suggests that they tended to over-emphasize the importance of the over-rotated ommatidia in their discussion.

Importantly, in *rlt* mutants rotation angles are not simply randomized but instead display a Gaussian distribution. The peak of this distribution is comprised of ommatidia that have rotated between 80º and 100º, while the slopes are formed by under- and over-rotated ommatidia with decreasing percentages as rotation angles become more extreme (Fig. 5C in Choi and Benzer and Fig. 12G in this thesis). Rather than being required to "stop" rotation, my results suggest that *rlt* is required for an accurate 90° rotation, and that in *rlt* mutants the "precision" is lost.

roulette is a rotation-specific allele of *argos*

Originally described in 1994 as a spontaneous mutation on the 3rd chromosome, the molecular nature of the *rlt* allele remained a mystery for more than seven years. New genetic and molecular evidence provided in this thesis and in (Brown and Freeman, 2003; Gaengel and Mlodzik, 2003; Strutt and Strutt, 2003) demonstrates that *rlt* is a rotation specific allele of *aos*. The *rlt* locus fails to complement *aos* alleles and the homozygous *rlt* phenotype can be rescued by a *sev-aos* transgene (Brown and Freeman, 2003; Gaengel and Mlodzik, 2003; Strutt and Strutt, 2003 and Fig. 14). Genetically, *rlt* behaves as a hypomorphic allele—the homozygous *rlt* phenotype is less severe than *rlt* in trans to *aos* null alleles or deficiencies for *aos* (Gaengel and Mlodzik, 2003 and Fig. 14). In addition, none of the other known developmental defects of strong *aos* alleles are evident in *rlt*, implying that *rlt* is an eye specific, regulatory allele. Sequence analysis of the aos gene in *rlt* mutants did not reveal any amino acid changes (Strutt and Strutt, 2003), but an analysis of the non-coding region revealed the insertion of a truncated P-element in the 5' untranslated region (Gaengel and Mlodzik, 2003 and Fig. 15 and 16). The *rlt* P-element insertion maps to the proposed transcriptional start side of the *aos* gene and is therefore likely to create a regulatory mutant. Taken together these data provide strong evidence that the *rlt* allele is a weak hypomorphic loss of function allele of *aos*, which primarily affects ommatidial rotation.

argos mutant eyes show defects in ommatidial rotation

Several lines of evidence argue for a general function of *aos* in controlling ommatidial rotation. Brown and Freeman examined clones of the hypomorphic aos^{w11} allele and found that, although many ommatidia had extra photoreceptors, a significant proportion had the correct number and many of these were misrotated (Brown and Freeman, 2003). Strutt and Strutt examined heteroallelic combinations of *aos* and found, that in $aos^{\Delta 7}/aos^{5F4}$ 45% of ommatidia had extra photoreceptors and that up to 50% of the ommatidia with a wt complement of photoreceptors where misrotated, while only 5% appeared achiral and less than 15% had wrong chirality. The authors therefore concluded, that "in addition to the photoreceptor recruitment phenotype, *aos* mutations can be characterised as particularly affecting ommatidial rotation, but not R3/R4 fate" (Strutt and Strutt, 2003). In conclusion, these results clearly show, that *aos* plays a key role in ommatidial rotation.

Signalling via the Egf receptor controls ommatidial rotation during *Drosophila* eye development

Aos has long been known as an antagonist of Egfr signalling (Schweitzer et al., 1995a). The characterisation of *rlt* as a rotation specific allele of *aos* therefore strongly suggested a direct role for Egfr in ommatidial rotation. The analysis of several mutant combinations of Egfr itself, as well as loss and gain-of-function studies of various established components of the Egfr signalling pathway confirmed this assumption (Brown and Freeman, 2003; Gaengel and Mlodzik, 2003; Strutt and Strutt, 2003; Wolff, 2003).

Evidence for a direct requirement of the Egf receptor in ommatidial rotation

The analysis of Egfr in the context of ommatidial rotation is complicated by its earlier roles in eye development (Xu and Rubin, 1993; Freeman, 1996; Dominguez et al., 1998; Baker and Yu, 2001; Baonza et al., 2001). Egfr null-mutant clones are not informative in the context of ommatidial rotation, since Egfr function is required for the differentiation of all cell types except R8 (Freeman, 1996; Dominguez et al., 1998; Baker and Yu, 2001). However, several hypomorphic Egfr alleles have been described (Clifford and Schupbach, 1989). An analysis of different mutant combinations of these alleles revealed that several ommatidia were in fact misrotated (Gaengel and Mlodzik, 2003; Strutt and Strutt, 2003) and this thesis Figure 21A and B). Similar to aos^{rlt} eyes, over- and under-rotated omatidia were found. Importantly, the alleles used were relatively mild and thus photoreceptor differentiation was largely unaffected. Often ommatidia were found to be misrotated without showing any other obvious defects and without adjacent ommatidia being defective, indicating that the observed rotation defects were not caused by incorrect spacing of cells or compromised ommatidial architecture. It is therefore likely that the rotation defects seen in Egfr hypomorphs are ‘primary rotation defects’, meaning that Egfr affects rotation independently of its role in photoreceptor induction.

Further evidence for a direct requirement of Egfr during ommatidial rotation came from experiments in which a dominant-negative form of the receptor was expressed under control of *Heat shock-Gal4* (Brown and Freeman, 2003). If only mildly expressed, the dominant negative receptor construct caused severe rotation defects, as both under- and over-rotated ommatidia could be observed. Similar to the results obtained from the hypomorphic alleles analysed, the misrotated ommatidia were often correctly specified (Brown and Freeman, 2003).

Importantly, the expression of a constitutively-active form of Egfr (*λ-top*, Queenan et al., 1997) under control of the *mδ0.5 Gal4* enhancer also caused rotation defects. As in the mutant and dominant-negative experiments described above, under- and over-rotated

ommatidia were observed. (Figure 21C). Given the fact that *aos*^{rlt} mutants show striking rotation defects, this result is not surprising, as loss of *aos* function also creates a situation in which Egfr signalling is hyperactive.

In summary these results clearly show, that gain and loss of Egfr function leads to ommatidial rotation defects with both over- and under-rotated ommatidia.

The role of Egfr ligands and the ligand processing machinery in ommatidial rotation

The analysis of Egfr ligands and factors required for ligand processing provided further evidence for a role of Egfr in ommatidial rotation. Brown and Freeman observed that misexpression of the Egf ligand Keren under *sevenless Gal4* control caused severe rotation defects with both over- and under-rotated ommatidia (Brown and Freeman, 2003). Although hyperactivation of Egfr signalling normally leads to an over-recruitment of cells in the eye, photoreceptor recruitment was not affected when Keren was expressed at these levels. The authors therefore concluded that Keren serves as a ligand for Egfr in the context of ommatidial rotation, and that "rotation is more sensitive than photoreceptor recruitment to perturbation of Egfr signalling". Further studies showed that only rotation was affected, as the chirality of the ommatidia remained unaffected (if Keren was overexpressed under these conditions, Brown and Freeman, 2003). If Keren actually functions as the main Egfr ligand in the context of ommatidial rotation, or if it acts redundantly with other Egfr ligands, is currently unclear as no mutant alleles of Keren have yet been described. In addition Brown and Freeman investigated the eye phenotype of a hypomorphic *spi* allele (*sp*^{iscp1}) and found that many ommatidia were under-recruited, suggesting that Egfr signalling was effectively compromised. Despite this, they observed only a few ommatidia that were misrotated and therefore concluded that Spi is either not essential for ommatidial rotation or acts redundantly with another ligand (Brown and Freeman, 2003).

Strong support for the assumption that at least one Egfr ligand is required for ommatidial rotation comes from the analysis of *S* and *Rho* mutants. S and Rho proteins are the key components of the Egfr ligand processing machinery and are required for the efficient processing of Spi, Keren and Grk (reviewed in Klambt, 2002). However, since Grk expression is limited to the female germline, Spi and Keren are the only two ligands that are processed by S and Rho in the eye (Wasserman et al., 2000; Brown and Freeman, 2003; Shilo, 2003). Rho-3, encoded by the *roughoid* (*ru*) gene, has been shown to be the most critical Rhomboid for eye development (Wasserman et al., 2000). Hypomorphic *ru*^{1} mutations are homozygous viable and display severe rotation defects with both under- and over-rotated ommatidia (Brown and Freeman, 2003). In addition, heterozygosity for *S* was found to reduce Egfr signalling levels to a degree where photoreceptor recruitment and

ommatidial rotation are affected (Brown and Freeman, 2003; Gaengel and Mlodzik, 2003). Strikingly, the mild rotation defects in *S/+* eyes are strongly enhanced if one copy of *Spi* is removed, suggesting that Spi is at least one of the ligands responsible for the Egfr mediated control of ommatidial rotation (Brown and Freeman, 2003; Gaengel and Mlodzik, 2003 and Table 2, Fig. 22A, B in this thesis). Taken together, these results show that the ligand processing machinery and at least one Egfr ligand (Spi or Keren) are critical for the Egfr dependent regulation of ommatidial rotation.

Other Egfr signalling components required for ommatidial rotation

Several experiments have demonstrated that the conserved Ras/Raf/MAPK/Pnt signalling cassette plays a key role in the control of ommatidial rotation downstream of Egfr. This is not surprising, since it is a paradigm that "all known cases of Egfr signalling are transmitted through the Ras/Raf/MAPK pathway and through a transcriptional output" (Matthew Freeman).

Ras

Evidence for a requirement of Ras in ommatidial rotation came in part from experiments in which constitutively active Ras^{V12} was misexpressed in only a subset of photoreceptors (under *mδ0.5-Gal4* control), which caused severe rotation abnormalities (Gaengel and Mlodzik, 2003 and Fig 24). In this context it is important to note that expression of the proapoptotic gene *reaper* under control of *mδ0.5-Gal4*, which causes the loss of R4 photoreceptors, does not result in severely misrotated ommatidia (Fig. 38). This indicates that the rotation defects created by overexpression of constitutively active Ras^{V12} under *mδ0.5-Gal4* control are not simply caused by a gain or loss of photoreceptors or abnormal packaging, but rather by the effects of Ras on ommatidial rotation directly.

Support for the idea that Ras is required for ommatidial rotation came from studies on a dominant gain-of-function Ras allele (*$Ras85D^{2F4}$*, Strutt and Strutt, 2003). In heterozygous *$Ras85D^{2F4}$* eyes, 1%-5% of ommatidia are misrotated and in homozygous *$Ras85D^{2F4}$* flies the rotation defects are increased up to 20%. In addition, I was able to show that alleles of *ras* are strong suppressors of the homozygous *aos^{rlt}* phenotype (Gaengel and Mlodzik, 2003 and Fig. 23C). This is exactly what one would predict if Ras mediates Egfr signalling in the context of ommatidial rotation. The reasoning for this conclusion is as follows: In an *aos^{rlt}* mutant background, Spi inhibition is compromised and Egfr signalling is therefore hyperactive. If Egfr really signals through Ras in the context of ommatidial rotation, reducing Ras protein levels by means of loss-of-function alleles would be predicted to attenuate the hyperactivated signalling levels and therefore rescue the rotation

phenotype in *aos*^{rlt} eyes. Furthermore, removal of one copy of *ras* dominantly enhanced the rotation defects in *S/+* eyes dramatically (Gaengel and Mlodzik, 2003 and Table 2, Fig. 22D). Srutt and Strutt also provided evidence for a potential role of Ras64B in ommatidial rotation. Ras64B is a second Ras homologue (also called Ras2) for which no mutants have yet been identified (Harrison et al., 1995). Overexpression of a constitutively active Ras64B^{V14} under control of the *actin* promotor caused severe rotation defects. Ras64B is thought to act as a negative regulator in the Egfr signalling pathway, which is supported by the finding that the rotation defects in *actin-Ras64B*^{V14} eyes are suppressed by removal of one copy of *aos*, *sty* or by the gain of function *Ras85D*^{2F4} allele (Strutt and Strutt, 2003).

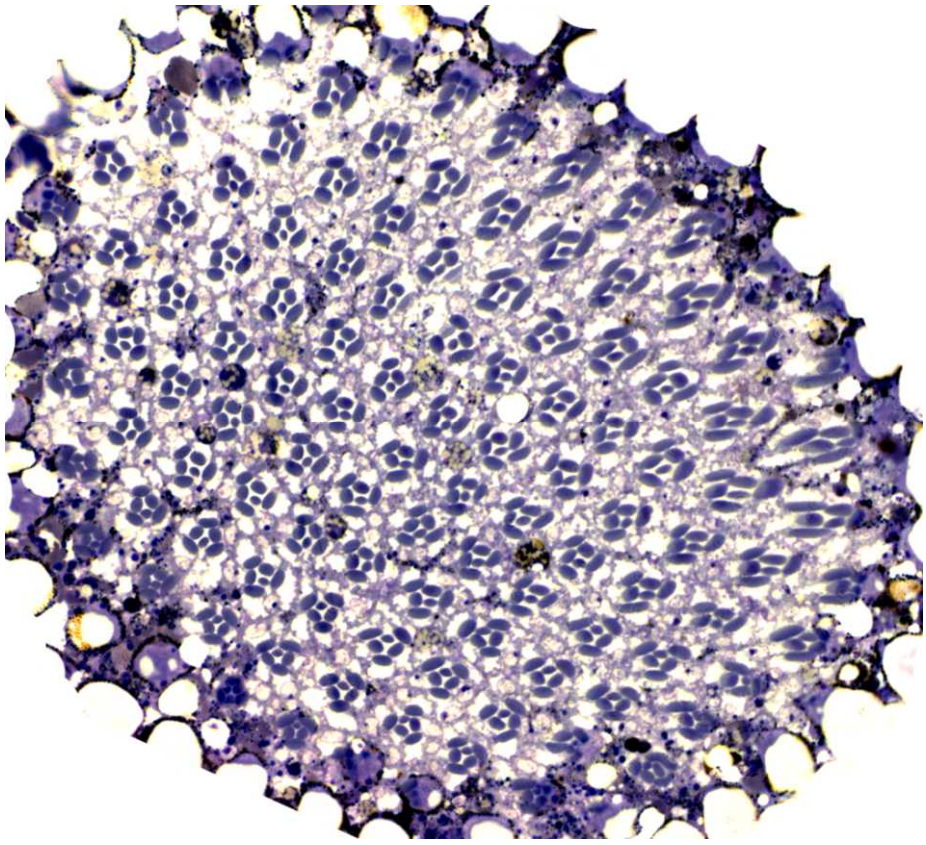

Fig. 38 Ablation of the R4 photoreceptor cell does not cause severe rotation defects

Tangential section through an eye in which the proapoptotic gene *reaper* was expressed under contol of *mδ0.5-Gal4*. Note that almost all ommatidia display a triangular shape due to the loss of the R4 photoreceptor cell, but that ommatidial rotation is largely normal. In order to preserve the overall impression of this ablation experiment, and to show that ommatidia in the dorsal and in the ventral half of the eye have rotated correctly, the image was not cropped and a whole eye section is shown. Anterior is left and dorsal is up.

Raf/MAPK.

So far no one has actually demonstrated a direct requirement of either Raf or Rl acting downstream of Egfr in ommatidial rotation. In fact, removal of one copy of Raf or Rl was not sufficient to suppress the rotation defects in homozygous *aos*^{rlt} eyes (Fig. 23D and not

shown). However, there is strong reason to believe that Raf and Rl do in fact mediate Egfr signalling in the context of ommatidial rotation. First, Raf and Rl are 'dogmatically believed' to transduce all known cases of Egfr signalling in *Drosophila* (Casci and Freeman, 1999; Brown and Freeman, 2003). Second, the fact that Raf and Rl alleles fail to suppress the homozygous aos^{rlt} eye phenotype could be explained with the argument that these kinases are not rate limiting in this process. Third, the fact that the transcription factor Pnt is required for ommatidial rotation (as discussed below) strongly argues for a requirement of Rl in this context, as Pnt is known to be directly activated by Rl.

Pointed

An obvious candidate for a transcription factor that mediates the Egfr dependent control of ommatidial rotation is Pnt. Pnt is involved in most aspects of Egfr signalling (Klambt, 1993; Brunner et al., 1994a; O'Neill et al., 1994) and has been shown to directly upregulate *aos* expression in the embryo (Golembo et al., 1996). Thus, it was very likely that Pnt also transduces Egfr signalling in the context of ommatidial rotation. In support of this hypothesis, alleles of *pnt* where found to strongly enhance the rotation defects in $S^{48.5}/+$ eyes (Table 2 and Fig. 22E). In addition, Brown and Freeman examined hypomorphic alleles of Pnt (pnt^{1277}/pnt^{88}) and found that the majority of ommatidia showed an under-recruitment of photoreceptors, but that rotation defects where frequent in those ommatidia that where correctly specified (Brown and Freeman, 2003). Moreover, I was able to show that alleles of *pnt* are among the best suppressors of the homozygous aos^{rlt} phenotype, which strongly suggests that Egfr signals through Pnt in the context of ommatidial rotation (Gaengel and Mlodzik, 2003 and Fig. 23E).

Sprouty

In addition to the Egfr signalling components described above, I found the Sty^{D5} allele to be a potent suppressor of the rotation defects observed in $S^{48.5}/+$ eyes (Table 2 and Fig. 22F). This observation is consistent with the idea that Sty acts as a negative regulator of Ras signalling. Further support for an involvement of Sty in ommatidial rotation came from the analysis of Sty mutant imaginal discs that were reported to show rotation defects (Strutt and Strutt, 2003).

In summary, these results demonstrate that Egfr mediates its effects on ommatidial rotation at least in part through the canonical Ras/Raf/MAPK/Pnt signalling cascade.

At which stage of eye development does Egfr signalling affect ommatidial rotation?

Although all three groups find that altering Egfr signalling, either positively or negatively, results in ommatidial rotation defects, different opinions exist as to when these rotation defects occur. To determine if Egfr dependent ommatidial rotation defects occur during the actual rotation process or at a later stage, third instar eye imaginal discs of several genetic backgrounds were analysed for their effects on ommatidial rotation. Brown and Freeman examined the effects of overexpressed Keren on ommatidial rotation in third instar eye imaginal discs. Surprisingly, the authors found that initial rotation was essentially unaffected as the vast majority of ommatidia reach 45° and at the back of the disc have turned to 90°. Although 4.9% of ommatidia where found to be misrotated, this is not significantly different from wild type discs in which 5.1% of ommatidia were found to be misrotated. In contrast, adult eyes of the same genotype show that 28% of ommatidia have rotated less than 90°, 6.2% have rotated less than 45° and 65% that have rotated more than 90°. Brown and Freeman therefore conclude that the rotation defects caused by the overexpression of Keren arise at a stage later in development than the third instar disc. A further investigation of pupal eye discs revealed that at 6 hours post-pupariation, no rotation defects are apparent, as *sevGal4>UAS*-Keren discs were indistinguishable from the wild type control. At this stage of development ommatidia in several columns have already reached 90°. Thus, if Egfr signalling served as a stop signal, rotation defects should be visible at this stage. The absence of rotation defects in these discs lead Brown and Freeman to conclude, that Egfr signalling does not control the stop of rotation and that Egfr dependent rotation defects must occur at later stages in development. However, at 30 hours post-pupariation, rotation defects were clearly visible indicating that rotation becomes disrupted between 6 and 30 hours post-pupariation (Brown and Freeman, 2003). In addition, Brown and Freeman used a dominant-negative form of Egfr under control of the *heat shock Gal4* driver to disrupt Egfr signalling at specific times of development. In the adult eye, these heatshocks create bands of ommatidia that show rotation defects. Depending on when these heatshocks were given, the band of misrotated ommatidia was shifted. Consistent with the posterior to anterior progression of eye development, the older the flies were at the time of heatshock, the more anterior the band of misrotation. The different positions of these bands of misrotated ommatidia were then used to deduce the time when Egfr signalling was reduced. From these experiments Brown and Freeman concluded that Egfr is required during the second 45° rotation step, as the sensitivity to loss of Egfr corresponds to approximately columns 10-15 posterior to the morphogenetic furrow. Consistent with this observation, the authors found that rotation defects occur immediately posterior to

recruitment defects which corresponds to a period during the second 45° rotation step (Brown and Freeman, 2003). It is important to realize that Brown and Freeman clearly state that Egfr signalling is required during the second 45° of rotation, whereas they find that Egfr dependent rotation defects become apparent only much later. However, their conclusions derive from two different sets of experiments. Whereas a dominant-negative Egfr construct (creating a loss-of-function situation) was used to determine the time frame in which Egfr signalling is critical for ommatidial rotation, a *UAS-Keren* construct (creating a gain-of-function situation) was used to deduce when rotation defects first become visible. It therefore cannot be concluded with confidence that gain and loss of Egfr function affects rotation at exactly the same time, nor has it been determined when rotation defects in loss-of-Egfr function situations first become visible.

In contrast to Brown and Freeman, Strutt and Strutt find that upon alteration of Egfr signalling levels, the third instar eye imaginal disc is affected in several aspects. First, misrotated ommatidia were observed in *aos* and *sty* transheterozyous discs. Second, a partial transformation of mystery cells into photoreceptors was observed in aos^{rlt} discs. Third an abnormal localisation of Fz-GFP was noted in an aos^{rlt} mutant background. Whereas the authors only state that 'the developing ommatidial clusters are not uniformly rotated relative to each other', they investigate the partial transformation of mystery cells into photoreceptors and the abnormal localisation of Fz-GFP in aos^{rlt} mutant discs in more detail (Strutt and Strutt, 2003, discussed below).

My own data are in general agreement with Egfr signalling being required primarily during the second 45° of rotation. However, in contrast to Brown and Freeman, I found that ommatidial rotation defects are already visible in third instar eye imaginal discs mutant for *aos*. Although ommatidia rotation defects were mild in aos^{rlt} discs, I found that many ommatidia were misrotated in discs homozygous mutant for the strong hypomorph aos^{w11} (Gaengel and Mlodzik, 2003 and Fig. 19 and 20). Concerned about the finding of Brown and Freeman that rotation defects do not become apparent until pupa stages, I repeated the analysis of aos^{w11} discs and came to the same conclusion, namely that ommatidial rotation defects are already visible in the third instar eye imaginal disc (Fig. 39). However, given the severe adult rotation phenotype, it remains puzzling why aos^{rlt} discs show only a mild phenotype in the disc. Thus, in conclusion, there is a general agreement that Egfr signalling affects the second 45° of rotation, however different interpretations exist as to when these rotation defects become visible.

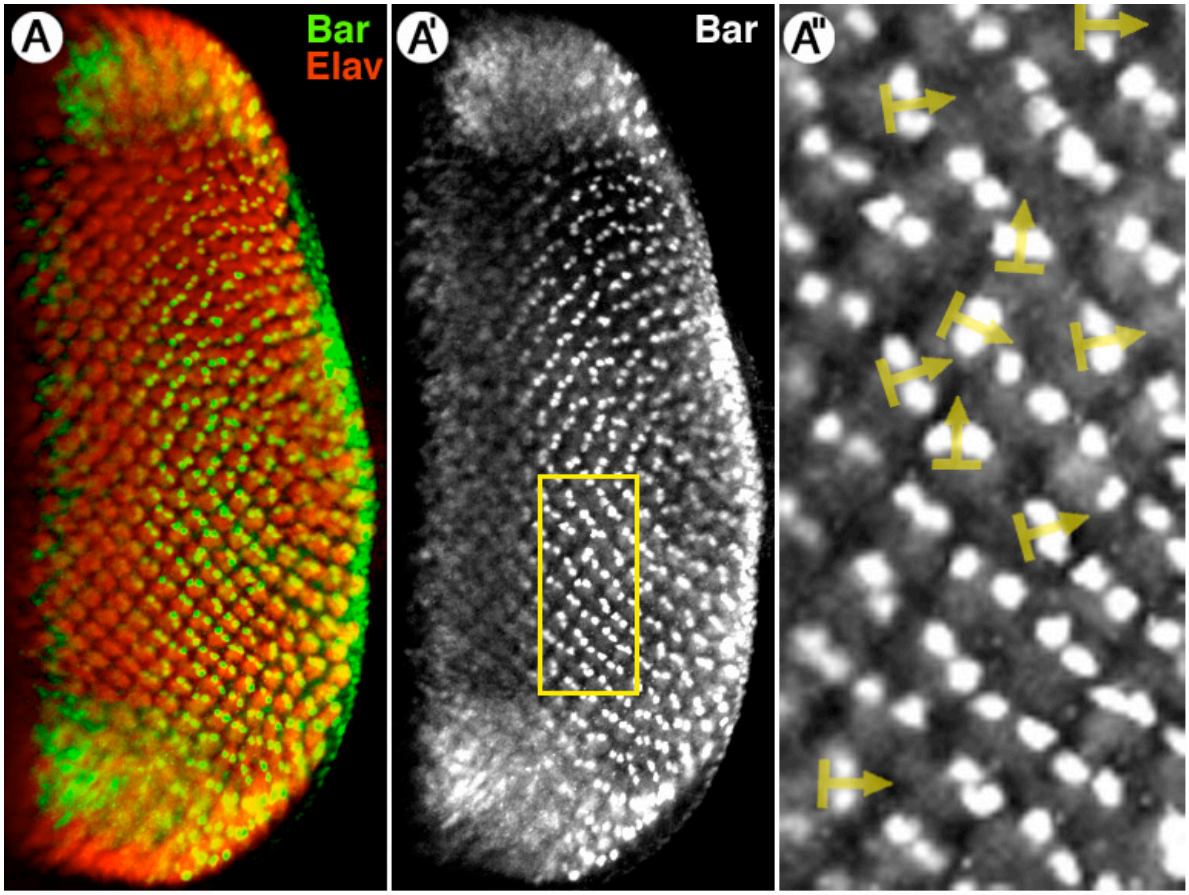

Figure 39. Ommatidial rotation defects in *aos*^{W11} are already apparent in the third instar eye imaginal disc
(A-A'') Confocal images of *aos*^{W11} third instar eye imaginal discs stained for Elav (red) and Bar (green and white in A'-A''). **(A'')** shows an enlargement of the boxed area in A'. Ommatidia that are strongy misrotated compared to their neighbours or developmental stage are indicated by transparent yellow arrows. (Compare to the wild type Bar staining in Fig. 17C-C''). Anterior is to the left and dorsal is up in all panels.

Planar cell polarity genes and Egfr dependent ommatidial rotation

The observation that Egfr signalling controls ommatidial rotation combined with the fact that the direction of rotation is initially determined by the core planar polarity genes raises the question if these pathways are interconnected. Several lines of evidence suggest that they are in fact interconnected. A strong argument for a link between these pathways is that *aos*, *sty* and a gain-of-function *ras* allele were isolated as enhancers of the *fz*^{19}/*fz*^{20} polarity phenotype in a screen for new regulators of ommatidial polarity (Strutt and Strutt, 2003).

In addition it was found that two core planar polarity factors, Fz and Fmi, were mislocalised in *aos*^{rlt} eye imaginal discs (Gaengel and Mlodzik, 2003; Strutt and Strutt, 2003). However, different theories exist as to how exactly the localisation pattern of these genes is altered in *aos*^{rlt} mutants.

Strutt and Strutt observed that in the wild type Fz-GFP is enriched by column 4 at the apical membranes of R3 and R4 except where they contact R2/R5, and at the posterior

side of R8. By column 6, Fz-GFP in the R3 cell is localised specifically at the R3/R4 boundary, whereas in the R4 cell, it is excluded from the R3/R4 boundary and the boundary with R5, but remains enriched on other apical membranes (Strutt and Strutt, 2003). In *aos*^{rlt} mutants Fz-GFP was found to be localised by column 4 at the apical membranes of R3/R4. However, Fz-GFP was in addition found to be enriched in a variable number of additional cells, which the authors believed to be transformed mystery cells. By column 6, Fz-GFP was still apically localised in these additional cells in most ommatidial clusters (rather than specifically in the R3/R4 pair). Fmi was found to be mislocalised in a very similar pattern to Fz-GFP in *aos*^{rlt} eyes discs. Strutt and Strutt therefore concluded that "at the time when ommatidia begin to rotate, Fz-GFP distribution is abnormal and is asymmetrically distributed in multiple cells that are partially transformed to the R3/R4 fate". The authors further suggest that, "as Fz is required in R3/R4 for correct ommatidial chirality and rotation, the presence of extra cells containing localised Fz-GFP could be providing the ommatidium with conflicting cues that disrupt normal rotation".

Like Strutt and Strutt, I find that in *aos*^{rlt} eye discs by column 4, Fmi is enriched at the apical membranes of R3/R4 and to a variable number of additional cells (most likely mystery cells, Fig. 32G). In some ommatidial clusters these additional cells are still present by column 6 (Fig. 32H). However, this phenotype appeared far less striking to me than the observation that restriction of Fmi to the R4 cells was dramatically delayed. In the wild type control, Fmi is depleted from R3 membranes by column 7, whereas in *aos*^{rlt} Fmi remains strongly enriched in both cells of the R3/R4 pair, often beyond column 12 (Fig. 32I, J and Fig. 33 D). Interestingly, the delayed Fmi restriction to R4 does ultimately not cause chirality defects, as almost no defects are visible with the *mδ0.5-lacZ* marker (highlighting R4 identity, see Fig. 18) or in adult eye sections (Fig. 12E and Gaengel and Mlodzik, 2003). Thus, the delay in Flamingo restriction to R4 and its enrichment in additional cells specifically affects ommatidial rotation. Since Fmi is a homophillic cell-adhesion molecule (Usui et al., 1999), its increased abundance on R3 and other cell membranes is likely to have a direct effect on Fmi localisation in neighboring cells and thus on the adhesive properties of the preclusters, which could explain the broad range of rotation angles in *aos*^{rlt} eye and other Egfr pathway mutants. In support of this hypothesis, loss of one copy of Fmi was found to substantially suppress the rotation defects in homozygous *aos*^{rlt} eye (Fig. 34). However, how Egfr signalling affects Fmi and Fz localisation is currently unclear.

In summary, it can be concluded that in the context of ommatidial rotation, a link between Egfr signalling and the core planar polarity genes exists and that Egfr regulates ommatidial rotation at least in part via modulation of cell adhesive properties mediated through Fmi.

Additional factors involved in ommatidial rotation

In the context of ommatidial rotation it is highly likely that Egfr not only signals via the canonical Ras/Raf/MAPK cascade to trigger transcriptional responses, but might also affect cell affinity or cytoskeletal rearrangements more directly. One example of a homophillic cell adhesion molecule involved in ommatidial rotation is the atypical cadherin Fmi. As discussed above, Fmi localisation is drastically altered if Egfr signalling is perturbed. However, it is unknown if the effects of Egfr on Fmi involve the Ras/Raf/MAPK cascade and transcriptional responses or if Egfr signalling affects Fmi localisation more directly.

So far, all known examples of Egfr signalling in *Drosophila* utilise the small GTPase Ras and in the vast majority of cases Ras transduces its signal via Raf (Casci and Freeman, 1999). However, in other contexts Ras has been found to affect cell growth and/or cytoskeletal rearrangements via its effectors Phospho-inositol-3-Kinase (PI3K, Rodriguez-Viciana et al., 1996; Prober and Edgar, 2002), Rgl/Ral (Mirey et al., 2003) and Canoe/AF6 (Matsuo et al., 1997). In fact, overexpression of Ras-effector loop mutations that selectively stimulate only certain Ras effectors suggest that Ras utilises additional effectors besides Raf in the context of ommatidial rotation (Fig. 24).

A role for PI3K in ommatidial rotation?

Although the overexpression of Ras^{V12G37} (which fails to induce Raf/MAPK signalling but is known to activate PI3K specific responses in eye and wing imaginal discs, Prober and Edgar, 2002), causes ommatidial rotation defects (Fig. 24C, D), clones of null alleles of PI3K have previously been reported to affect growth but not ommatidial rotation (Leevers et al., 1996). In addition, the overexpression of Dp^{110A} (the catalytic subunit of PI3K) under *mδ−0.5-Gal4* control failed to create convincing rotation defects and the role of PI3K in ommatidial rotation was therefore not investigated further. However, a recent article suggests that PI3K might in fact regulate ommatidial rotation (Bateman and McNeill, 2004). In this paper, the authors provide evidence that the temporal control of differentiation is regulated via the Insulin/Tor pathway (of which PI3K is a key component), and that in adult eye sections of clones of PI3K or its negative regulator PTEN (Phosphatase and Tensin homologue) many ommatidia are misrotated. The authors further find that mutations in tuberous sclerosis complex 1 (Tsc1), a negative regulator of the target of rapamycin (TOR) pathway, caused severe ommatidial rotation defects in the adult eye. An analysis of Tsc1 and PTEN mutant clones in the developing eye imaginal disc revealed that loss of either Tsc1 or PTEN caused precocious differentiation, while clones of the positive regulator PI3K caused delays in differentiation. Importantly the authors find that cell fates are unchanged in

either Tsc1, PTEN or PI3K mutant backgrounds and that the effects on ommatidial rotation are caused by the loss of developmental timing control.

In conclusion, it thus appears as if PI3K, PTEN and Tsc1 are required to control the timing of ommatidial rotation, rather than the rotation process itself.

A preliminary analysis of the Ral eye phenotype

In mammalian cell culture, Ras has been known for many years to bind to and activate a number of Ral guanine nucleotide exchange factors (RalGEFs, reviewed in Wolthuis and Bos, 1999), which in turn activate the Ral GTPase (Feig et al., 1996). In tissue culture systems Ras^{V12G37} retains the ability to activate RalGEFs and therefore Ral specific responses (Rodriguez-Viciana et al., 1997). The observation that overexpressed Ras^{V12G37} caused ommatidial rotation defects (Fig. 24C, E) therefore suggested a possible role for RalGEFs/Ral as an effector of Ras in the process of ommatidial rotation. However, the exact relationship of Ras and Ral in *Drosophila* is not well understood and a recent report suggested that Ral functions downstream of the RapGTPase, rather than downstream of Ras (Mirey et al., 2003). Nevertheless, since Ral has previously been implicated in cytoskeletal rearrangements in *Drosophila* (Sawamoto et al., 1999a; Sawamoto et al., 1999b), I examined its role in ommatidial rotation more closely. Strikingly, the expression of an activated form of the human Ral orthologue Ral^{G23V} under control of the GMR promotor caused severe rotation defects (Sawamoto et al., 1999b; Gaengel and Mlodzik, 2003) and Fig. 29A). In addition, clones of ral^{PG89} *or* ral^{PL56} generated in the eye cause a roughened eye structure and tangential sections revealed a mild loss of photoreceptors as well as problems with photoreceptor morphogenesis and occasional rotation defects (Fig. 29B-G). However, the analysis of the adult *ral* eye phenotype remains preliminary as all three available *ral* alleles are P[w^+] marked and therefore do not allow the identification of mutant tissue in adult eye sections unambiguously (since heterozygous and homozygous mutant tissue will be w^+ marked and therefore cannot be distinguished). A detailed analysis of the adult eye phenotype can therefore not be completed until suitable alleles (in a w^- background) are generated.

Clones of *ral* induced in the developing eye imaginal discs can be marked unambiguously using an *armadillo-lacZ FRT* chromosome. A preliminary analysis of ral^{PG89} clones in the eye disc indicates that loss of Ral function does not impair photoreceptor development in general, as the neuronal marker Elav appears largely normal (Fig. 30A). However, some ommatidia show Bar expression in only one cell of the R1/R6 pair, indicating either an incorrectly specified cell or cell loss. In addition, a number of photoreceptors also appear misrotated (Fig. 30A-A').

Taken together, my preliminary results suggest that *ral* might be required for photoreceptor cell fate specification and/or survival. In addition, *ral* function is most likely needed for proper rhabdomere morphogenesis and might also have an impact on ommatidial rotation. However, my analysis of ral function is preliminary and further experiments are required to clarify the adult eye phenotype and the potential involvement of ral in ommatidial rotation.

A role for Canoe in ommatidial rotation

AF-6, the human orthologue of *Drosophila* Cno was first described as a fusion partner of ALL-1 in a chimeric protein associated with acute myeloid leukemias (Prasad et al., 1993). In mice, the *cno* orthologue AF6 is critical in tight junctions and its absense has been reported to disrupt epithelial cell-cell junctions and cell polarity leading to embryonic lethality by 10.5 days *post coitum* (Zhadanov et al., 1999). In *Drosophila*, Cno was first identified as a mutation precluding the morphogenetic movements during embryonic dorsal closure (Jürgens, 1984; Takahashi et al., 1998). Cno is a critical component of junctional integrity in *Drosophila* and has been shown to localise to adherens junctions in the *Drosophila* eye (Matsuo et al., 1999 and Fig. 27, 28). For many years Cno has been known as a binding partner of Ras (Van Aelst et al., 1994; Kuriyama et al., 1996; Linnemann et al., 1999), and an analysis of Cno function during eye development revealed that Cno regulates cone cell formation in a Ras dependent manner (Matsuo et al., 1997). Furthermore Cno interacts genetically with Notch and Sca during eye and wing development (Miyamoto et al., 1995). It is particularly interesting that loss of one copy of cno stongly enhances the *sca1* eye phenotype. Even though the biochemical function of Sca remains obscure, it has been implicated as a Notch ligand in several contexts (Powell et al., 2001) and was recently reported to control ommatidial rotation by antagonizing nemo activity (Chou and Chien, 2002). Thus, the link between Cno and Sca/Notch is intriguing. In addition, Cno has been reported to associate with the actin cytoskeletal regulator profilin (Boettner et al., 2000) and to bind actin directly (Mandai et al., 1997). Furthermore, the Cno protein shows similarities to kinesin and myosin domains and might act as a motor protein in certain contexts (Ponting, 1995). Thus, Cno appears to be compelling candidate to regulate ommatidial rotation.

Three lines of evidence suggest that Cno is in fact involved in the regulation of ommatidial rotation. First, strong alleles of *cno* enhance the rotation defects of $S^{48.5}/+$ eyes (Gaengel and Mlodzik, 2003 and Fig. 25A, B and Table 3). Second, overexpression of *cno* under control of the *mδ0.5-Gal4* driver causes severe rotation abnormalities (Fig. 25C).

Third, transheterozygous mutant combinations of *cno^{mis1}/cno^{2}* display rotation defects (Gaengel and Mlodzik, 2003 and Fig. 25D).

Although these results strongly suggest that Cno plays an important role in ommatidial rotation, it has not been established that Cno functions strictly downstream of Ras in this context. Interestingly, Rap1, another Ras-like small GTPase, is also known to bind Cno (Boettner et al., 2000) and a recent report showed that Cno binds to and acts as an effector of Rap1 in the context of dorsal closure (Boettner et al., 2003). In addition, the Cno orthologue AF-6 was recently reported to control integrin-mediated cell adhesion by regulating Rap1 activity in 293T cells (Su et al., 2003). The link between Cno and integrin-mediated cell adhesion is compelling, since results from our group indicate that ommatidial rotation is controlled by integrin-mediated cell adhesion (Maria Thuveson and Marek Mlodzik, in preparation).

Taken together, these data suggest that Cno serves to integrate signals from different pathways and relays these signals to generate cytoskeletal rearrangements.

Ommatidial rotation and cadherin based cell adhesion

Cellular adhesion is likely to be required for several aspects of ommatidial rotation. One obvious requirement is that cells within the ommatidium adhere to one another more strongly than to surrounding non-ommatidial cells in order to allow the cluster to rotate as a unit. In addition, it seems essential that cell-cell and cell-matrix adhesion between ommatidial cells and surrounding cells or the extracellular matrix become modified while ommatidia rotate. One example of a homophillic cell adhesion molecule crucial during the rotation process is the atypical cadherin Fmi (discussed above). Moreover, results from two groups suggest that DE-cadherin *(shg,* Tepass et al., 1996) plays an important role during this cell motility process, as alleles of *shg* are strong enhancers of the *S$^{48.5}$/+* rotation phenotype (Brown and Freeman, 2003; Gaengel and Mlodzik, 2003 and Table 3, Fig. 31). In addition, results from our group confirm that DE-cadherin is in fact required for normal ommatidial rotation (Ivana Mirkovic and Marek Mlodzik, in preparation).

In this context it is intriguing to note that during the time when planar polarity is established, DE-cadherin and Fmi are localised in complementary pattern in wild type third instar eye imaginal discs (Fig. 40). The complementary localisation of these proteins suggests that they are required for different aspects of adhesion during ommatidial rotation. Interestingly, Egfr signalling has previously been reported to affect DE-cadherin mediated adhesion during the development of the early larval visual system (Dumstrei et al., 2002), thus a more general effect of Egfr signalling on DE-cadherin mediated adhesion might exist in other developmental contexts.

In summary, these results suggest that Egfr mediated regulation of cellular adhesion is critical for normal ommatidial rotation to occur, and that at least two cadherin family members (Fmi and DE-cadherin) are involved in this process.

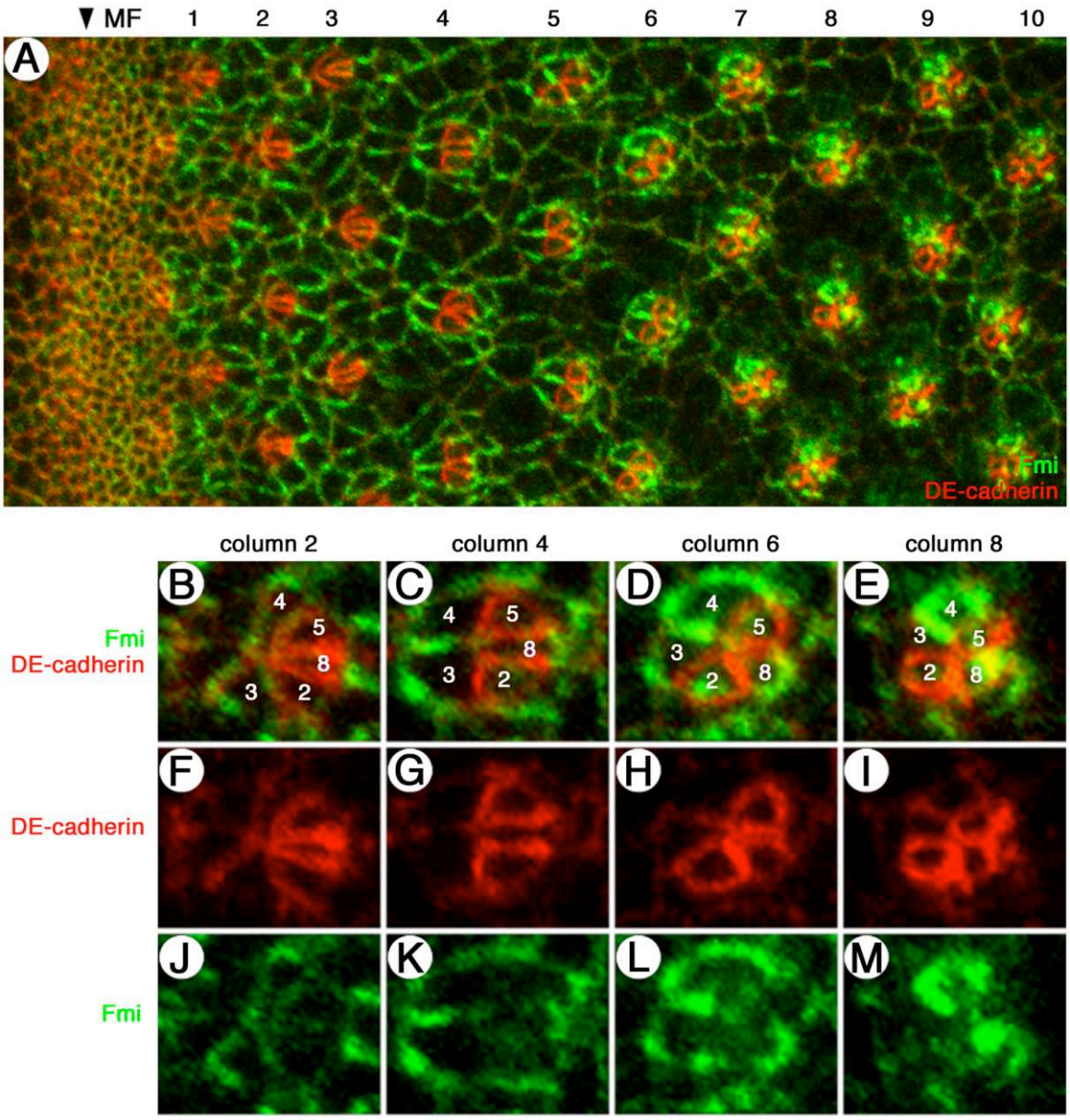

Fig. 40 DE-cadherin and Fmi are localised in complementary patterns during planar polarity establishment in the third instar eye imaginal disc

(A-M) Confocal images of developing ommatidial clusters in a third instar eye imaginal discs stained with an antibody against Fmi (green) and DE-cadherin (red). The morphogenetic furrow is to the left in each panel. Respective columns are indicated above the images. The position of relevant photoreceptors are indicated with white numbers. **(B, J)** In wt discs, Flamingo is initially uniformly distributed around the membranes of all cells. **(C, K)** By column 4, Fmi becomes enriched in both cells of the R3/R4 pair. **(D, L)** Starting at column 6, Fmi is depleted from R3 membranes and enriched at R4 and R8 membranes. **(E, M)** By column 8, Fmi is strongly enriched at R4 and R8 membranes and almost completely depleted from R3 membranes. **(A-I)** DE-cadherin, initially uniformly distributed around the membranes of all cells, is strongly enriched at R2/R5 membranes from column 2 on and persists until ommatidial rotation is completed.

A potential function for motor proteins and components of the actin cytoskeleton in ommatidial rotation

Although not yet fully understood, it seems that ommatidial rotation utilises at least some of the components used in other contexts of cellular motility. A number of factors previously implicated in cell motility were isolated as dominant enhancers of the mild $S^{48.5}/+$ rotation phenotype (Gaengel and Mlodzik, 2003 and Table 3 and Fig. 31) and are therefore likely to play a role in Egfr mediated ommatidial rotation.

Two motor proteins, non-muscle Myosin II light chain (*sqh*, Karess et al., 1991; Jordan and Karess, 1997) and non-muscle Myosin II heavy chain (*zip*, Young et al., 1993; Edwards and Kiehart, 1996), were found to specifically enhance the rotation defects in $S^{48.5}/+$ eyes (Table 3 and Fig. 31D). Non-muscle Myosin II heavy chain is well studied and known to be required for a number of morphogenetic processes in *Drosophila* including border cell migration, dorsal closure, head involution and ommatidial organization (summarized in Edwards and Kiehart, 1996). Intriguingly, *sqh* and *zip* have previously been shown to control wing hair polarity downstream of *Drok*, a gene implicated in ommatidial rotation (Winter et al., 2001). Surprisingly, alleles of *Drok* failed to enhance the $S^{48.5}/+$ rotation phenotype (Table 3) suggesting that *sqh* and *zipper* might be regulated via alternative mechanisms in this context.

In addition, several components involved in actin polymerization/depolymerisation were isolated as modifiers of the mild $S^{48.5}/+$ rotation phenotype. Among these is *chic* encoding the *Drosophila* orthologue of Profilin (Cooley et al., 1992), known to be required for several actin-dependent processes during *Drosophila* development (Verheyen and Cooley, 1994; Hopmann and Miller, 2003). Profilin is thought to promote actin filament assembly on barbed ends. In the absence of barbed ends, it functions as an actin monomer-sequestering protein (reviewed in Paavilainen et al., 2004). Interestingly, *chic* was recently isolated as an enhancer of a weak Ras1 eggshell phenotype, indicating that a more general link between Egfr/Ras signalling and *chic* might exist (Schnorr et al., 2001). Moreover, Profilin has been found to bind to the human Cno orthologue AF-6, suggesting that during ommatidial rotation Egfr/Ras signalling might affect Profilin dependent actin dynamics via Cno (Boettner et al., 2000).

A further enhancer of the $S^{48.5}/+$ rotation defects is the *Drosophila* orthologue of Cofilin encoded by the *tsr* gene (Gunsalus et al., 1995). Cofilin binds to both monomeric and filamentous actin and primarily increases actin dynamics by depolymerising actin filaments from their pointed ends. However, under certain conditions Cofilin can increase the concentration of barbed ends and thus promote actin polymerisation (reviewed in Paavilainen et al., 2004). Elegant experiments from the Condeelis group have shown that

Egf stimulation of metastatic MTLn3 cells causes a transient increase in Cofilin at the leading edge of extending lamellipodia, resulting in actin polymerization and ultimately defining the direction of cell motility (Chan et al., 2000; Ghosh et al., 2004; Mouneimne et al., 2004). In *Drosophila*, Cofilin is essential for most actin based cell motility processes including border cell migration and oogenesis (Chen et al., 2001). Cofilin activity is know to be negatively regulated by LIM-kinase 1 dependent phosphorylation and reactivated through dephosphorylation mediated by the phosphatase Ssh (Niwa et al., 2002). Strikingly, I found that, alleles of *ssh* are among the strongest suppressors of the rotation defects in $S^{48.5}/+$ eyes (Table 3 and Fig. 31H), implying both *tsr* and *ssh* in Egfr mediated ommatidial rotation.

Another key regulator of actin-dependent cytoskeletal dynamics that enhances the rotation defects in $S^{48.5}/+$ eyes is Twf. Twf binds only to monomeric actin and does not promote actin filament depolymerisation. It is thought that Twf sequesters ADP-actin monomers in the cytoplasm and then delivers them to sites of rapid actin-filament assembly through its interactions with Capping proteins. However, Twf is the most recently discovered actin-monomer-binding protein and its role in actin polymerisation/depolymerisation is not fully understood (reviewed in Paavilainen et al., 2004). In *Drosophila,* Twf is required for several actin dependent developmental processes including bristle and eye morphogenesis. Importantly, *tsr* genetically interacts with *twf*, as removing one copy of *tsr* strongly enhances the homozygous *twf* eye phenotype (Wahlstrom et al., 2001). The hypomorphic twf^{3701} allele is homozygous viable and causes a rough eye phenotype and bristle morphogenesis defects. Tangential sections through homozygous twf^{3701} eyes display a mild photoreceptor loss and several severely misrotated ommatidia, confirming that *twf,* and thus actin-dependent cytoskeletal rearrangements, are required for ommatidial rotation (Fig. 41). While this initial loss of function analysis of an actin-monomer binding protein in the context of ommatidial rotation is intriguing, further work is needed to clarify exactly how actin dynamics relate to cell motility in this context, and how Egfr signalling impacts on the actin polymerization/depolymerisation machinery.

In summary, my results indicate that at least two motor proteins -- non-muscle Myosin II heavy and light chain – and proteins controlling actin dynamics are involved in ommatidial rotation

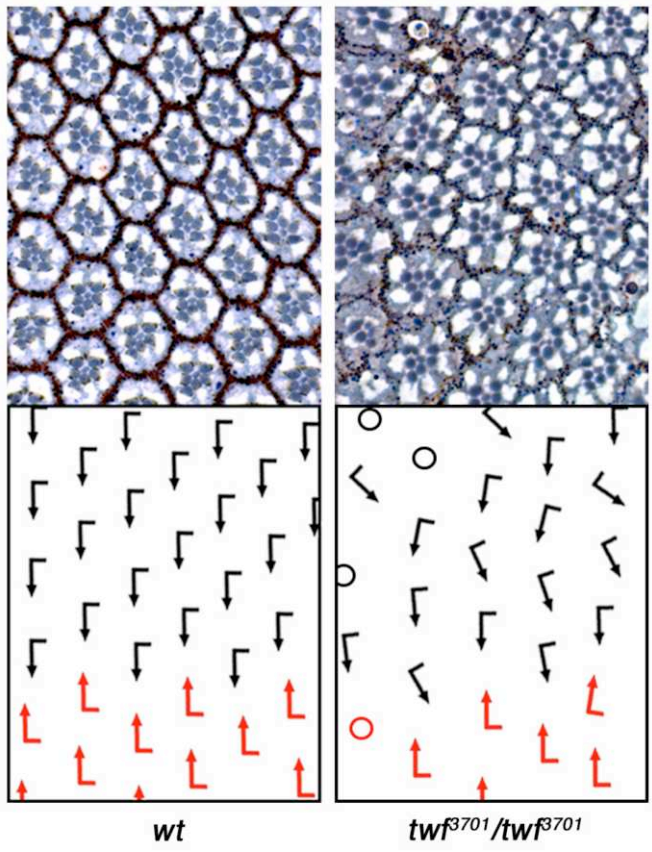

Fig. 41 Twinfilin mutants display ommatidial rotation defects

Tangential section of adult eyes around the equatorial region, with corresponding schematic representation below each panel. Dorsal ommatidia are represented by black arrows and ventral ommatidia by red arrows. Ommatidia that do not carry a full complement of photoreceptors are indicate by circles. The respective genotypes are indicated below each panel.

A pilot screen designed to discover genes involved in ommatidial rotation identifies PVR as a potential rotation gene

During this thesis, the haploinsuficient $S^{48.5}$ allele emerged as a particularly valuable tool to identify genes involved in Egfr mediated ommatidial rotation. The mild $S^{48.5}$/+ rotation phenotype is dosage sensitive and enhanced by alleles of Egfr pathway components and by several other mutations in genes implicated in ommatidial rotation. $S^{48.5}$/+ therefore creates an ideal genetic background to perform a F_1 modifier screen. While an obvious concern is that many genes might non-specifically interact with $S^{48.5}$, several of the isolated enhancers were subsequently found to suppress the rotation defects in homozygous aos^{rlt} eyes (compare Fig. 22 with Fig. 23), supporting the idea that these genes are in fact involved in ommatidial rotation.

In order to screen through a large number of mutants, I adapted an elegant visualisation technique developed by Frank Pichaud that allows the analysis of ommatidial rotation defects in living flies (Pichaud and Desplan, 2001 and Fig. 35 and 36). Using this

approach, I tested known modifiers of *S* as well as several other candidate genes in a small pilot screen. Besides known Egfr pathway components, I identified alleles of the *Drosophila* PDGF/VEGF receptor orthologue PVR (Fig. 36E) as enhancers of $S^{48.5}$/+. Interestingly, Pvr has recently been reported to be partially redundant with Egfr in controlling border cell migration in *Drosophila* (Duchek et al., 2001). Although pure speculation at this point, the idea of a similar relationship between Egfr and Pvr during ommatidial rotation appears very attractive and will be investigated in future experiments.

While my results are preliminary, they demonstrate that the *rh1-eGFP* visualisation approach can be used to identify modifiers of the $S^{48.5}$/+ rotation phenotype. This approach might be used in the future to screen a large number of well characterised mutants or deficiencies which can be obtained from *Drosophila* stock centers. Subsequent loss-of-function analysis of the isolated modifiers will reveal if these genes function in ommatidial rotation or in other aspects of Egfr signalling.

Further perspectives

Ommatidial rotation is a precisely controlled cell motility process, which is poorly understood. Prior to this thesis only a few genes have been implicated in ommatidial rotation and their inter-relationship was not established. The discovery that Egfr signalling controls ommatidial rotation assigns the first pathway to this process and opens the door for a more detailed analysis. This work establishes the first link between Egfr signalling and the planar cell polarity gene Fmi and suggests that cadherin-based adhesion, motor proteins and components regulating the actin cytoskeleton are critical for the rotation process. However, a further loss-of-function analysis of the newly implicated genes will be crucial to understand their role during the rotation process and to reveal the mechanistic aspects of rotation. Moreover, it will be necessary to find links between the genes previously known to regulate rotation and the Egfr pathway. In addition, the rotation process itself needs to be studied in more detail on a cellular level. In this context, the Cno:GFP transgene is a promising tool for a live-imaging approach, which is currently under investigation.

IV
Materials and Methods

Flystocks

If not noted otherwise, fly stocks used are as described in Flybase (http://flybase.bio.indiana.edu/) and are either part of the Mlodzik Lab stock collection (Marek.Mlodzik@mssm.edu) or were obtained from the Bloomington Stock Center (http://flystocks.bio.indiana.edu/).

Mutant fly strains:

- *rlt* and *nemo* alleles used in this study were a gift from Kwang-Wook Choi (kchoi@bcm.tmc.edu)
- aos^{W11}, $aos^{\Delta 5}$ and $aos^{\Delta 7}$ mutants were a gift from Christian Klämbt (klaembt@mail.uni-muenster.de)
- *DF(3L) std11* was provided by Andreas Jenny (Andreas.Jenny@mssm.edu)
- all other deficiencies used to map the *rlt* locus were obtained from (http://flystocks.bio.indiana.edu/)
- The Egfr hypomorphes top^{1} and top^{EC20} as well as the $S^{48.5}$ allele were a kind gift from Trudi Schupbach (gschupbach@molbio.princeton.edu)
- sty^{D5} mutants were a kind gift from Matthew Freeman (mf1@mrc-lmb.cam.ac.uk)
- alleles of Dp110A (PI3K) were obtained from Sally Leevers (sally.leevers@cancer.org.uk)
- cno^{2} and cno^{3} alleles were a gift from Ulrike Gaul (gaul@rockvax.rockefeller.edu)
- cno^{Mis1} flies were obtained from Daisuke Yamamoto (daichan@waseda.jp)
- sqh^{PL91}, ral^{PL56} and ral^{PG89} alleles (Bourbon et al., 2002) were obtained from Stephan Noselli (noselli@unice.fr)
- fz^{1}, fz^{R54} and Fz^{K21} were a gift from Paul Adler (pna@virginia.edu)
- fmi^{E45} and fmi^{E59} alleles were obtained from Tadashi Uemura (tuemura@virus.kyoto-u.ac.jp)
- dgo^{269} and dgo^{308} were a gift from Suzanne Eaton (eaton@mpi-cbg.de)
- $sple^{1}$ and $sple^{13}$ alleles were a gift from David Gubb (dgubb@cicbiogune.com)
- $stbm^{153}$ and $stbm^{6}$ were a gift from Tanya Wolff (twolff@genetics.wustl.edu)
- The twf^{EP3701} stock was a gift from Tapio Heino (tapio.heino@helsinki.fi)
- PVR^{5363} and PVR^{IW} alleles were a gift from Paul Garrity (pgarrity@mit.edu)

Marker lines:

- The *md05-lacZ* marker line was kindly provided by Sarah Bray (sjb32@mole.bio.cam.ac.uk)
- *svp-lacZ* $^{l(3)7842}$ is part of the Mlodzik Lab stock collection (Marek.Mlodzik@mssm.edu)
- *cno:GFP* lines were established during this thesis (see below for details)
- *rh1-eGFP* lines were a kind gift from Frank Pichaud (fp17@nyu.edu)

Gal4 driver lines:

- *mδ05-Gal4* (Gaengel, 2000; Gaengel and Mlodzik, 2003) (Konstantin.Gaengel@mssm.edu)
- *sev-Gal4 (K25*) was a gift from Konrad Basler (basler@molbio.unizh.ch)

UAS-lines:

- *UASRas*^{V12}, *UASRas*^{V12S35}, *UASRas*^{V12G37}, *UASRas*^{V12C40} and *UAS-cno* lines lines were a kind gift from Ulrike Gaul (gaul@rockvax.rockefeller.edu)
- *UASλ-top* lines (4.4 and 4.2) were a gift from Trudi Schupbach (gschupbach@molbio.princeton.edu)
- *UAS-Dp110A* (PI3K) stocks were a kind gift from Sally Leevers (sally.leevers@cancer.org.uk)

Direct constructs:

- *sev-aos* fly stocks were a kind gift from Matthew Freeman (mf1@mrc-lmb.cam.ac.uk)
- *GMR-V-Ral* flies were obtained from Hideyuki Okano (okano@nana.med.osaka-u.ac.jp)

FLP/FRT stocks:

- the y[1] w[1118] P{ry[+t7.2]=neoFRT}19A armadillo Lac-Z; P{ry[+7.2]=ey-FLP.N}5 stock was a gift from Jessica Treisman (treisman@saturn.med.nyu.edu)
- FRT chromosoms of ral^{PG89} or ral^{PL56} were generated by recombining these alleles on the *P{ry[+t7.2]+neoFRT}19A; ry[506]* stock, which was obtained from (http://flystocks.bio.indiana.edu/).

All crosses were performed at 25°C in Forma Scientific incubators (model# 3940), except for aos^{W11} homozygous mutant combinations, which were raised at 18°C. Flyfood was provided by a Mount Sinai shared research facility coordinated by Ursula Weber (Ursula.Weber@mssm.edu) and prepared by Zhongfang Du.

Histology

An in dept description of histological techniques used in this thesis can be found in *Drosophila* Protocols (Sullivan, 2000). The techniques used are in most cases identical, or slight variations of these protocols.

Plastic sections of adult *Drosophila* eyes

The protocol for adult eye sections used in this thesis is a variation of the method described by Tomlinson and Ready (Tomlinson and Ready, 1987). Adult *Drosophila* eye sections require a multi-step protocol. Eyes have to be dissected, fixed, embedded and finally sectioned. The following list of Materials and Solutions is thus subdivided into these single steps.

Materials and Solutions:

Dissection step:

- Binocular: Zeiss Stemi 2000 or Stemi SV11 (http://www.zeiss.com)
- Light source: Schott KL1500 or Schott-Fostec LLC (http://www.us.schott.com)
- Fly pads: EMBL manufactured
- CO_2 station (various suppliers, country dependent)
- Fly brush: #1 Pearl 308 Golden Takalon USA (http://www.pearlpaint.com)
- Disposable scalpels: Feather No. 11 (http://www.emsdiasum.com)

Fixation and embedding step:

- Durcupan® ACM resin: Sigma #D-0166 (http://www.sigmaaldrich.com)

  → The Durcapan resin is based on the formula for Araldite resin and comes as four different components: A (epoxy resin), B (hardener), C (accelerator), D (plasticiser). To prepare resin for eye embedding mix these components in the ratios indicated below in a plastic beaker using a stir bar. Aliquot the resin in 20 ml plastic vials and store at -20°C.

components	amount
A	108g
B	89g
C	5g
D	20g

- 0.5M Na_2 H PO_4
- 0.5M Na H_2 PO_4•H_20
- 0.2M Na-phosphat buffer pH 7.2

  → (for 500ml mix 136.8ml of 0.5M Na_2 H PO_4 with 63.2ml 0.5M Na H_2 PO_4•H_20 and add 300ml H_20).
- *Fix solution*: 2% glutaraldehyde solution in phosphate buffer

  → (for 40 ml mix 10ml 8% glutaraldehyde solution with 20ml 0.2M Na-phosphat buffer pH 7.2 and add 10 ml H_20. The fixation solution should be store at 4°C and should not be used if older than 4 weeks.)
- *Osmium solution*: 2% OsO_4 in phosphate buffer

  → (Mix equal amounts of 4% OsO_4 and 0.2M Na-phosphat buffer pH 7.2; prepare fresh)
- 8% glutaraldehyde solution: Fluka #49627 (http://www.fluka.com or http://www.sigmaaldrich.com)
- 4% OsO_4: Polyscience, Inc. (http://www.polysciences.com)
- Conical tubes: 15ml or 50ml Falcon tubes (#352097 or #352098) were used to prepare the *Fix solution* and the *Osmium solution* (http://www.bdbiosciences.com)
- Ethanol 200 proof: Pharmco #64-17-5
- Propylene oxide: Fisher #04332-1 (https://www1.fishersci.com)
- 20ml Plastic vials for resin aliquots: Fisher #033374 (https://www1.fishersci.com)
- 1000ml Plastic beaker: Nalgene #1201-1000 (http://www.nalgenelabware.com)
- Stir-bar: Fisher (https://www1.fishersci.com)
- 1.7 ml microcentrifuge tubes: Sorenson BioScience, Inc. #11590 (http://www.sorbio.com)
- Centrifuge: Beckman Microfuge 18 Centrifuge (http://www.beckman.com)
- Plastic transfer pipettes for resin work: Samco Scientific Corporation #225
- Pasteur pipettes: Fisher# 13-678-6B, 9 inch long (https://www1.fishersci.com)
- Embedding molds: BEEM flat embedding molds, Electron Microscopy Science #70904-12 (http://www.emsdiasum.com)
- Oven: Fisher Isotemp® 100 series model 106G (https://www1.fishersci.com)

Sectioning step:

- Trimming Block: EMBL manufactured
- Razor blades: Single edge Teflon coated, Electron Microscopy Science # 71970 (http://www.emsdiasum.com)
- Microtome: Sorvall Ultra Microtome MT5000 (http://www.sorvall.com)
- Microtome knife: Leica 'histo'-diatome diamond knife. Size 6, knife angle: 45° (http://www.emsdiasum.com/diatome)
- Microscope slides: 25x75x1mm Fischerbrand superfrost # 12-550-14 (https://www1.fishersci.com)

- Cover glass: 24x60mm Corning Lab (http://www.corning.com/Lifesciences/us-canada/en)
- *Staining solution*: dissolve 1% toluidine blue and 1% Borax in H_2O
- DPX mounting medium: Fluka #44581 (http://www.fluka.com or http://www.sigmaaldrich.com)
- Microscope: Zeiss Axioplan2 imaging (http://www.zeiss.com)
- Microscope lens: Zeiss Plan-Apochromat 63x1.40 (http://www.zeiss.com)
- Microscope lens-oil: Zeiss Immersol 518F (http://www.zeiss.com)
- Imaging software: Zeiss AxioCam software, Adobe® Photoshop® (http://www.zeiss.com); (http://www.adobe.com/products/photoshop/main.html)
- Computer: Apple Macintosh computer (http://www.apple.com)

Embedding procedure:

Flies were anaesthetized and decapitated. One eye was cut away to allow penetration of the *Fix solution* into the head structure. One-eyed heads were transferred to microcentrifuge tubes with 200µl *Fix solution* on ice and incubated from 2-40 minutes. To ensure sinking of the heads, samples were centrifuged for 1 minute at maximum speed in a table centrifuge. Directly after centrifugation, 200µl of the *Osmium solution* was added to each sample and solutions were carefully mixed. After 30 minutes – 1hour incubation on ice, the *Fix solution/Osmium solution* mix was exchanged with 200µl *Osmium solution* only and the samples were further incubated for 1-6 hours. Eyes were subsequently dehydrated in 10 minutes washing steps in the following EtOH concentrations on ice: 30%, 50%, 70%, 90%, 100% and an additional 100% step. After two additional 10 min washes with propylene oxide at room temperature, eyes were transferred into a 1:1 propylene oxide – Durcupan® resin mix and incubated over night at room temperature. The next morning, the 1:1 propylene oxide – Durcupan® resin mix was replaced with pure resin and incubated for at least 4-6 hours at room temperature. In the meantime resin was poured into embedding molds and incubated at room temperature until the resin has reached the right consistence (usually 6-8 hours). Once Resin starts to thicken, eyes were transferred with a toothpick into molds and were oriented for sectioning. Embedded eyes were baked overnight at 70°C. Approximately 1µm thick tangential sections of embedded eyes were performed, using a Sorvall Ultra Microtome with a Leica histo diatome diamond knife. Eye sections were mounted on slides and stained with *Staining solution* for 10-20 seconds. After the slides were rinsed with water and dried, eye sections were covered with DPX mounting medium and a cover glass. After hardening of the mounting medium (usually about 30 minutes) eye sections were examined using dark-field optics on a Zeiss Axioplan2 microscope. Most images were taken with a 63x lens using the Zeiss AxioCam software on an Apple Macintosh computer. Images were assembled in Adobe® Photoshop®.

Note that OsO_4, propylene oxide and unpolymerised resin should be handled with extreme care. Vinyl gloves should be worn at all times when handling one of theses

substances, as OsO_4 is a neurotoxin and Durcupan resin is carcinogenic when unpolymerised. All steps involving OsO_4 or propylene oxide should be carried out in a well-ventilated chemical fume hood. All items that become contaminated with OsO_4 should be sealed in an appropriate waste container according to institutional safety office guidelines. All items containing unpolymerised resin should be backed at 70°C over night prior to being discarded.

Antibody staining of *Drosophila* eye imaginal discs

A detailed protocol with excellent technical notes can be found in *Drosophila* Protocols (Sullivan, 2000).

Materials and Solutions:

Dissecting and fixation of *Drosohila* eye imaginal discs:

- Binocular: Zeiss Stemi 2000 or Stemi SV11 (http://www.zeiss.com)
- Light source: Schott KL1500 or Schott-Fostec LLC (http://www.us.schott.com/fiberoptics)
- Seziernapf
- Forceps: Dumont No.5, Fine Science Tools #11252-30 (http://www.finescience.com)
- 30mm petri dishes: Falcon, Fisher (https://www1.fishersci.com)
- Conical tubes: 15ml Falcon tubes, #352097 (http://www.bdbiosciences.com)
- Microcentrifuge tubes: 2ml conical tubes, Fisher #02-681-258 (https://www1.fishersci.com)
- Pasteur pipettes: Fisher# 13-678-6B, 9 inch long (https://www1.fishersci.com)
- Shaking platform: EMBL manufactured
- 8% paraformaldehyde stock solution: dissolve 80mg EM-grade paraformaldehyde Fisher #T353-500 (https://www1.fishersci.com) per milliliter of H_2O and heat to 60°C on a stir plate (in a ventilated chemical fume hood) to dissolve. Add a trace of NaOH to help dissolving the paraformaldehyde. Do not overheat. Adjust pH with 1N HCl to ~7.0. Aliquot as 7ml stocks in conical tubes and store at -20°C.
- 0.2M Na-phosphat buffer pH 7.2
  → (for 500ml mix 136.8ml of 0.5M Na_2 H PO_4 with 63.2ml 0.5M Na H_2 PO_4•$H_2$0 and add 300ml $H_2$0).
- *Fix solution*: (4% paraformaldehyde in 0.1M Na-phosphat buffer pH 7.2). Prepare *Fix-solution* fresh before dissecting. Defrost one aliquot of 8% paraformaldehyde stock solution in a 60°C water bath until completely dissolved. Mix with an equal volume of 0.2M Na-phosphat buffer pH 7.2, keep on ice.
- *Post-Fix solution*: mix equal volumes of *Fix-solution* and 1xD-PBS. Keep on ice.
- 10xD-PBS stock solution: combine all components in less than 1L of $H_2$0 and stir to dissolve. Adjust the pH to 7.2 and bring to a final volume of 1L with $H_2$0. Sterilize by autoclaving. Use as a 1x solution.

components	for 1 L
1.3M NaCl	75.97g
70mM Na_2HPO_4•H_2O	12.46g
30mM NaH_2PO_4•H_2O	4.8g

- 1xD-PBS: 130mM NaCl, 7mM Na_2HPO_4•H_2O, 3mM NaH_2PO_4•H_2O. Prepare from 10x stock solution

- 1xD-PBS-T: 1xD-PBS + 0.1% Triton X-100
- 1xD-PBS-T+BSA: 1xD-PBS + 0.1% Triton X-100 + 0.1% BSA sterile filter and store at 4°C.
- Triton X-100: Sigma #T-9284 (http://www.sigmaaldrich.com/),
- Bovine Serum Albumin (BSA): Fisher #BP1600-100 (https://www1.fishersci.com)
- Sterile filter: Millipore Stericup, Fisher #SCGPU11RE (https://www1.fishersci.com)
- Normal Goat Serum: Jackson Immuno Research Laboratories #005-000121 (http://www.jacksonimmuno.com)
- Normal Donkey Serum: Jackson Immuno Research Laboratories #017-000-121 (http://www.jacksonimmuno.com)
- Mounting media: VECTASHIELD #H-1000 Vector Laboratories (http://www.vectorlabs.com)
- Microscope slides: 25x75x1mm Fischerbrand superfrost # 12-550-14 (https://www1.fishersci.com)
- Cover glass: 24x60mm, 24x40mm or 24x24mm; Corning Lab (http://www.corning.com/Lifesciences/us-canada/en)

Primary antibodies:

- Rabbit anti-Bar 1:100 (Higashijima et al., 1992)
- Mouse anti-Boss 1:1000 (Kramer et al., 1991)
- Rat anti-DE-cadherin (DCAD2) 1:20 (Oda et al., 1994), DSHB (http://www.uiowa.edu/~dshbwww)
- Mouse anti-discs large (4F3) 1:1000 (Parnas et al., 2001), DSHB (http://www.uiowa.edu/~dshbwww)
- Rat anti-Elav (7E8A10) 1:50-1:200 (O'Neill et al., 1994), DSHB (http://www.uiowa.edu/~dshbwww)
- Mouse anti-Elav (9F8A9) 1:50-1:200 (O'Neill et al., 1994), DSHB (http://www.uiowa.edu/~dshbwww)
- Mouse anti-Flamingo (74) 1:10 (Usui et al., 1999), DSHB (http://www.uiowa.edu/~dshbwww)
- Rabbit anti-β-Galactosidase 1:2000 Cappel #55976 (http://www.rockland-inc.com)
- Rat anti-β-Galactosidase 1:500 (Jun Wu unpublished)
- Mouse anti-β-Galactosidase 1:200-1:500 Promega #Z3781 (http://www.promega.com)
- Rabbit anti-GFP 1:250 abcam #ab6556 (http://www.abcam.com)

Secondary antibodies:

- Rhodamine phalloidin 1:200 Molecular Probes #R-415 (http://probes.invitrogen.com)
- All secondary antibodies used were derived from donkey and conjugated with FITC, TRITC or CY5. All secondary antibodies used were obtained from Jackson Immuno Research Laboratories (http://www.jacksonimmuno.com)

Imaging:

- Microscope: Images were taken on a Zeiss LSM 510 Confocal microscope (http://www.zeiss.com)
- Imaging software: Zeiss LSM software Version 3.2 (http://www.zeiss.com)
- Image processing software: Adobe® Photoshop® (http://www.adobe.com/products/photoshop/main.html)

Staining procedure:

Imaginal discs were dissected from third instar larvae in eis-cold 1xD-PDS and transferred to 30mm Petri dishes containing ~4ml *Fix-solution*. Discs were fixed at room temperature for 20-40 minutes and subsequently transferred to 2ml microcentrifuge tubes filled with ~ 1.7 ml of 1xPBS-T. Discs were washed 3 times for 5-15 minutes on a shaking platform in

1xPBS-T followed by a 30 minutes wash in 1xPBS-T+BSA. The wash solution was then exchanged against the primary antibody mix (containing the desired primary antibody combinations in 1xD-PDS-T+BSA with 10% normal goat or normal donkey serum) and discs were incubation over night at 4°C or alternatively for 1-2 hours at room temperature (the over night incubation usually tend to give slightly better results). Following the incubation with the primary antibody mix, imaginal discs were washed 4-5 times for 10-30 minutes in 1xPBS-T at room temperature while gently shaking. After an additional 30 minutes wash in 1xPBS-T+BSA, discs were incubated with the secondary antibody mix (containing the desired secondary antibody combinations in 1xD-PDS-T+BSA with 2% normal goat or normal donkey serum) either over night at 4°C or for 1-2 hours at room temperature. After the incubation with the secondary antibody mix, imaginal discs were washed 3 times for 10-30 minutes in 1xPBS-T at room temperature while gently shaking, followed by a 20 minutes post-fix with *Post-fix solution*. Discs were subsequently washed two more times for 10-30 minutes in 1xPBS-T at room temperature, rinsed in 1xPBS and incubated over night in mounting media at 4°C. The next day, remaining unwanted tissue was dissected away on a slide with mounting media and discs were transferred to a new slide with mounting media and covered with a cover glass. Slides were stored at -20°C until analysed.

Molecular techniques

General molecular techniques were performed according to standard protocols (Sambrook et al., 1989) if not otherwise noted. For general cloning purposes either Roche or New England Biolabs enzymes were used according to the instructions of the manufacturer. For DNA preparation the following kits were used: QIAGEN® Plasmid Maxi Kit, QIAquick® PCR Purification Kit, QIAquick® Gel Extraction Kit, QIAprep® Spin Miniprep Kit. DNA transformations were performed in XL-1 blue or XL-2 blue electro-competent *E. coli* cells using BIO-RAD Gene Pulser® Cuvettes and a BIO-RAD Gene Pulser® II with a Pulse Controller Plus, according to the instructions of the manufacturer. Usually 5-10ng DNA was transformed into 40 µl electro-competent E.coli cells. LB medium, for general bacteria work, as well as LB-agar plates containing the desired antibiotics were provided by Zhongfang Du or John Suriano and were prepared according to standard protocols.

Materials and Solutions:

- All enzymes were provided from Roche (http://www.biochem.roche.com) or New England Biolabs (http://www.neb.com) if not otherwise mentioned.

- Chemicals were obtained from Fisher (https://www1.fishersci.com) or Sigma (http://www.sigmaaldrich.com/), if not otherwise noted.
- DNA preparation: QIAGEN® Plasmid Maxi Kit, QIAprep® Spin Miniprep Kit, QIAGEN® EndoFree™ Plasmid Maxi Kit (http://www.qiagen.com)
- DNA purification: QIAquick® PCR Purification Kit, QIAquick® Gel Extraction Kit (http://www.qiagen.com)
- TOPO TA cloning kit (http://www.invitrogen.com)
- Electrocompetent cells: XL2-Blue strain: recA1 endA1 gyrA96 thi-1 hsdR17 supE44 relA1 lac [F`proAB $lacI^q$ ZΔM15 Tn10 (Tet^r) Amy Cam^r]^a were obtained from Stratagene (http://www.stratagene.com).
- LB-medium: 1% Bacto tryptone, 0.5% Bacto yeast extract, 0.5% NaCl; autoclaved
- LB-Ampicillin medium: Ampicillin (Roche) was added to LB-medium to a final concentration of 50 μg/ml
- For transformation of *E. coli* a BIO-RAD Gene Pulser® II was used with a Pulse Controller Plus (settings: 2.5 kV; 25μF) (http://www.bio-rad.com)
- Electroporation cuvettes (0.2 cm): Fisher #FB102 (https://www1.fishersci.com)
- DNA marker: 1kb-ladder Invitrogen (http://www.invitrogen.com)
- Agarose: ultra pure agarose electrophoresis grade from Invitrogen (http://www.invitrogen.com)
- 5x TBE stock solution: 89mM Tris base, 89mM boric acid, 20mM EDTA
- Centrifuges: a Sorvall RC-3B centrifuge with a Sorvall H6000A rotor and a Sorvall RC5C centrifuge with an SS34 rotor (http://www.sorvall.com) were used for preparation of electrocompetent cells and DNA-maxipreps. In addition, a Hettich Universal 32R centrifuge (http://www.gmi-inc.com) and a Beckmann Microfuge 18 table centrifuge (http://www.beckman.com) were used.
- Sequence analysis: Sequencing was performed in the Mount Sinai School of Medicine DNA Sequencing Core Facility (http://www.mssm.edu/genetics/dnacore)

Preparation of competent *E. coli* cells

Competent cells were either provided by Micheal Burnett – a technician in the lab – or prepared as described below. Two days before preparation of electrocompetent cells XL-2 blue cells were plated on an agar plate and incubated at 37°C over night. The next day a single colony was inoculated in 10 ml LB medium and incubated over night in a rotation wheel at 37°C. The following day 1 liter LB was inoculated with 10 ml of a fresh overnight culture and grown at 37°C with vigorous shaking to an ABS_{600} of 0.5-1.0 The flask was chilled on ice for 15 to 30 minutes and bacteria were harvested at 4000 x rcf for 15 minutes at 4°C. The supernatant was removed and cells were subsequently resuspended in a total of 1 liter of ice-cold sterile water. Bacteria were sedimented as described above and the pellet was resuspended in 0.5 liter of ice-cold sterile water and sedimented again (same settings as above). The supernatant was removed and cells were then resuspended in 20 ml 10% sterile filtered ice-cold glycerol and were sedimented as described. Finally, the supernatant was removed and cells were resuspended in 2 ml of ice-cold sterile filtered, 10% glycerol (the cell concentration should be about 1-3 x 10^{10} cells/ml). Cells were frozen in liquid nitrogen in 50 μl aliquots and stored at -80°C. (Under these conditions they are

good for at least 6 months. Note: solutions and media were either autoclaved or sterile filtered. All steps were performed in a cold room at 4°C)

Preparation of genomic DNA from adult flies

Materials and Solutions:

- 1.7 ml microcentrifuge tubes: Sorenson BioScience, Inc. #11590 (http://www.sorbio.com)
- Centrifuge: Beckmann Microfuge 18 table centrifuge (http://www.beckman.com)
- Homogenisation buffer: (0.1M Tris-HCl pH 9, 0.1M EDTA, 1% SDS)
- 5M Potassium Acetate
- Homogenization pistils: Eppendorf (http://www.eppendorf.com)
- Ethanol 200 proof: Pharmco #64-17-5
- Isopropanol: Fisher #A416-4 (https://www1.fishersci.com)
- TE Buffer: from Quiagen DNA purification kits (http://www.qiagen.com)

Procedure:

10 male and 10 female flies were transferred to a microcentrifuge tube and homogenised in 200μl homogenisation buffer on ice using a suitable pistil. Homogenised flies were then incubated at 65°C for 30 minutes. After adding 45μl of 5M Potassium acetate the microcentrifuge tube were incubated on ice for 30 minutes and subsequently centrifuged at 4°C in a table centrifuge at maximum speed for 10 minutes. The supernatent was transferred into a new microcentrifuge tube and centrifuged a second time at 4°C for 5 minutes. The supernatant was again transferred into a fresh microcentrifuge tube and mixed with 100μl Isopropanol (mix well – but do not vortex – genomic DNA). After a 5 minute incubation at room temperature, samples were centrifuged at room temperature with maximum speed for 5 minutes. The precipitated DNA was washed in 1ml 70% EtOH and re-centrifuged for 2 minutes at maximum speed. As much liquid as possible was removed and samples were re-centrifuged one more time for 2 minutes at maximum speed at room temperature. The remaining liquid was removed and genomic DNA pellets were air-dried for ~ 1 minute before they were re-suspended in 100μl TE buffer. Genomic DNA can be stored for several weeks at 4°C.

Genomic-PCR analysis of homozygous *aos*^{rlt} flies

Materials:

- Taq polymerase: Roche #1435094 (http://www.roche.com)
- dNTPs: Roche (http://www.roche.com)
- 10xPCR buffer (including 15mM $MgCl_2$): Applied Biosystems/Roche #58002067-01 (http://www.roche.com)
- PCR tubes: MJ Research, INC. #MLP-4801 (http://www.mjr.com) or Roth #H560.1

• Termal Cycler: MJ Research PTC-200 (http://www.mjr.com)

• PCR primer pairs:	5'aosI	GTTGTGGCTAAGGCAGGAAT
	3'aosI	CCCTCGCTCTATCGTTGTTC
	5'aosII	CACAGACACGCACATACCG
	3'aosII	GTCAGCAGCAACAGCAGCAT
	5'aosIII	GATCCAGATCCAGATTCTCGA
	5'aosIII	GATCCAGATCCAGATTCTCGA
	3'aosIII	GCAACCAGTTGAACAGGTGT
	5'aosIV	CATCAAGAGGATAATAAAAGGC
	3'aosIV	GTCTTATCGGCAATGGTGTG
	5'aosV	CTGCCCTATGCGGAGGTG
	3'aosV	GTGTGGAATGATCCCCTGG
	5'aosVI	TAACTCGTTGTGCCAGTGCC
	3'aosVI	TTTCAAACTGCCTTCGCTATG
	5'aosVII	TCAAAGAGCAGGATGTGCCA
	3'aosVII	CAATGGGTTTTCTAGCGGGT
	5'aosVIII	TCACAAAGGAACAACCCAAAC
	3'aosVIII	TTAAAAGGGGACTTCGCAG
	5'aosIX	CAGTTGTTCTTTTTTTGGCAT
	3'aosIX	AGAAAATCCAAAAACGAACAG
	5'aosX	ATAGAGCGAGGGCAGAGTAA
	3'aosX	GAATCTCCGTGCGTGTTGTT
• control primer:	5'rp49	TCCTACCAGCTTCAAGATGAC
	3'rp49	CACGTTGTGCACCAGGAACT

Procedure:

Homozygous *aos*^{rlt} flies were screened for a potential P-element insertion via genomic PCR. PCR products of 10 overlapping primer sets (aosI – aosX), uncovering the entire *aos* open reading frame as well as upstream and downstream sequences, were compared for the genotypes *aos*^{rlt}, *Ore-R* (wild type control) and *aos*^{W11} (control with known P-element insertion). Using the PCR conditions indicated below, genomic DNA of the expected size could be amplified with all primer pairs from the *Ore-R* wild type control. In contrast, the aosI and aosII primer pairs failed to amplify the expected size of genomic DNA from *aos*^{rlt} and *aos*^{W11} homozygous mutants. These results were expected for *aos*^{W11} genomic DNA, because the P-element which is known to inserted between these primer pairs is too large to be amplified. The fact, that the same primers failed to amplify the expected size of genomic *aos*^{rlt} DNA implicated that the *aos*^{rlt} mutation might also be caused by a P-element insertion within this region. To further investigate this possibility, I repeated the genomic PCR with the 5'aosII and 3'aosI primer combination which sit close together and amplify only 120bp from wild type genomic DNA. This primer combination was chosen, since upstream and downstream primer sets were able to amplify genomic *aos*^{rlt} DNA equal in

size to the wt control and thus, a potential P-element insertion was expected in between these primers. In fact, the 5'aosII/3'aosI primer combination amplified a DNA fragment from genomic *aos*^{rlt} DNA that was approximately 1.2kb larger than the corresponding PCR product on wild type genomic DNA. The amplified PCR product from genomic *aos*^{rlt} DNA was subsequently TOPO cloned. Sequence analysis revealed that the PCR product from genomic *aos*^{rlt} DNA enclosed a truncated P-element that had inserted between these primer pairs (see Fig. 16).

PCR reaction mix for genomic PCR

H_2O	76µl
10x PCR buffer	10µl
5' primer (10µM stock)	5µl
3' primer (10µM stock)	5µl
Genomic DNA	1.5µl
dNTP's (20mM)	1.5µl
Taq polymerase	1.0µl

PCR conditions:	Cycle#	temperature	time
	1	95°C	5 minutes
	2	95°C	30 seconds
	3	58°C	30 seconds
		-0.5/Cycle	
	4	72°C	2 minutes
	5	goto 2	7 times
	6	95°C	30 seconds
	7	55°C	30 seconds
	8	72°C	2 minutes
	9	goto 6	28 times
	10	72°C	5 minutes
	11	4°C	for ever
	12	End	

Cloning of *cno:GFP*:

Materials:

- Full length *cno* cDNA (LD24616): Open Biosystems (http://www.openbiosystems.com/)
- pEGFP-N3: Invitrogen (http://www.invitrogen.com)
- pCasper-tubulin: Gift from Julius Brennecke
- pUAST vector: Mlodzik Lab plasmid stock collection
- CIP: Roche (http://www.roche.com)
- Taq polymerase: Roche #1435094 (http://www.roche.com)
- dNTPs: Roche (http://www.roche.com)
- 10xPCR buffer (including 15mM $MgCl_2$): Applied Biosystems/Roche #58002067-01 (http://www.roche.com)
- PCR tubes: MJ Research, INC. #MLP-4801 (http://www.mjr.com) or Roth #H560.1
- Termal Cycler: MJ Research PTC-200 (http://www.mjr.com)
- Primer: 5'KpnI GCATCACCACCACACGGGATCGGG
  3'ApaI CCCTGGGCCCGCGTGCACCGCGTCTATATC

Procedure:

A full-length *cno* cDNA clone (LD24616) in pOT2 was obtained from Open Biosystems (http://www.openbiosystems.com/). In order to create a C-terminal Cno:GFP fusion protein, a C-terminal part of the *cno* open reading frame was PCR amplified from LD24616 with the 5'KpnI – 3'Apa I primer set (see conditions below). The 3'ApaI primer replaced the Stop codon of the *cno* cDNA with an ApaI restriction site. The PCR fragment was gel-purified, KpnI/ApaI digested and again gel-purified. In the mean time, the eGFP containing plasmid pEGFP-N3 was KpnI/ApaI digested, gel-purified and CIP-treated. The KpnI/ApaI digested *cno* PCR fragment was then ligated with the KpnI/ApaI digested pEGFP-N3 vector. The resulting construct was prepared for the next cloning step with an EcoRI/MluI digest followed by a gel-purification. In a separate step, the full-length *cno* cDNA (LD24616) was EcoRI/MluI digested and the largest fragment of this digest was gel-purified. The EcoRI/MluI digested *cno* cDNA fragment was subsequently cloned in the EcoRI/MluI digest pEGFP-N3 vector containing the C-terminal *cno* PCR fragment, which created a full-length cno:GFP construct in pEGFP-N3. This construct was used as basis for further cloning steps and is referred to as cnoEGFP-N3. To create the tub>cno:GFP construct used for the localisation studies in this thesis, cnoEGFP-N3 was first EcoRI digested, gap-filled and subsequently NotI digested and than cloned into the pCasper-tubulin vector, which was first KpnI digested, then blunted (via Klenow) and finally NotI digested. In order to clone cno:GFP into the Gal UAS vector pUAST, cnoEGFP-N3 was EcoRI/NotI digested and the resulting cno:GFP fragment was ligated into the EcoRI/NotI digested pUAST vector. Transgenic flies were generated in a Mount Sinai shared research facility by Zhongfang Du according to standard protocols.

PCR reaction mix for the 5'KpnI – 3' ApaI primer set:

H_2O	76.5µl
10x PCR buffer	10µl
5' KpnI primer (10µM stock)	5µl
3' ApaI primer (10µM stock)	5µl
1:1000 diluted LD24616 miniprep	1µl
dNTP's (20mM)	1.5µl
Taq polymerase	1.0µl

PCR conditions:	Cycle#	temperature	time
	1	95°C	2 minutes
	2	95°C	15 seconds
	3	69°C	15 seconds
	4	72°C	3 minutes
	5	goto 2	30x times
	6	72°C	8 minutes
	7	4°C	for ever
	8	End	

Notes on the *S*$^{48.5}$*, rh1-eGFP* screen

The *rh1-eGFP* visualisation technique was performed as described in (Pichaud and Desplan, 2001).

Materials:

- Microscope: Zeiss Axioskop2 (http://www.zeiss.com)
- Lens: Zeiss ACHROPLAN 40x/0.80W water immersion lens #440090 (http://www.zeiss.com)
- Camera: Zeiss Axiocam Mrm (http://www.zeiss.com)
- Software: Zeiss Axiovision4 software (http://www.zeiss.com)
- Agarose: ultra pure agarose electrophoresis grade from Invitrogen was used in a 2% concentration (http://www.invitrogen.com)
- Petri dishes: Fisher#08-757-12, 100mm (https://www1.fishersci.com)

V
Literature

Adler, P. N. (2002). Planar signalling and morphogenesis in Drosophila. *Dev Cell* **2**, 525-35.

Adler, P. N., Vinson, C., Park, W. J., Conover, S. and Klein, L. (1990). Molecular structure of frizzled, a Drosophila tissue polarity gene. *Genetics* **126**, 401-16.

Allard, J. D., Chang, H. C., Herbst, R., McNeill, H. and Simon, M. A. (1996). The SH2-containing tyrosine phosphatase corkscrew is required during signalling by sevenless, Ras1 and Raf. *Development* **122**, 1137-46.

Baker, N. E. and Yu, S. Y. (2001). The EGF receptor defines domains of cell cycle progression and survival to regulate cell number in the developing Drosophila eye. *Cell* **104**, 699-708.

Baker, N. E. and Zitron, A. E. (1995). Drosophila eye development: Notch and Delta amplify a neurogenic pattern conferred on the morphogenetic furrow by scabrous. *Mech Dev* **49**, 173-89.

Banerjee, U., Renfranz, P. J., Pollock, J. A. and Benzer, S. (1987). Molecular characterisation and expression of sevenless, a gene involved in neuronal pattern formation in the Drosophila eye. *Cell* **49**, 281-91.

Baonza, A., Casci, T. and Freeman, M. (2001). A primary role for the epidermal growth factor receptor in ommatidial spacing in the Drosophila eye. *Curr Biol* **11**, 396-404.

Bateman, J. M. and McNeill, H. (2004). Temporal control of differentiation by the insulin receptor/tor pathway in Drosophila. *Cell* **119**, 87-96.

Becker, H. J. (1957). [Roentgen mosaic spots & defective mutations at the eye of Drosophila & the evolutive physiology of the eye.]. *Z Indukt Abstamm Vererbungsl* **88**, 333-73.

Bier, E., Jan, L. Y. and Jan, Y. N. (1990). rhomboid, a gene required for dorsoventral axis establishment and peripheral nervous system development in Drosophila melanogaster. *Genes Dev* **4**, 190-203.

Biggs, W. H., 3rd, Zavitz, K. H., Dickson, B., van der Straten, A., Brunner, D., Hafen, E. and Zipursky, S. L. (1994). The Drosophila rolled locus encodes a MAP kinase required in the sevenless signal transduction pathway. *Embo J* **13**, 1628-35.

Boettner, B., Govek, E. E., Cross, J. and Van Aelst, L. (2000). The junctional multidomain protein AF-6 is a binding partner of the Rap1A GTPase and associates with the actin cytoskeletal regulator profilin. *Proc Natl Acad Sci U S A* **97**, 9064-9.

Boettner, B., Harjes, P., Ishimaru, S., Heke, M., Fan, H. Q., Qin, Y., Van Aelst, L. and Gaul, U. (2003). The AF-6 homolog canoe acts as a Rap1 effector during dorsal closure of the Drosophila embryo. *Genetics* **165**, 159-69.

Bogdan, S. and Klambt, C. (2001). Epidermal growth factor receptor signalling. *Curr Biol* **11**, R292-5.

Borod, E. R. and Heberlein, U. (1998). Mutual regulation of decapentaplegic and hedgehog during the initiation of differentiation in the Drosophila retina. *Dev Biol* **197**, 187-97.

Bourbon, H. M., Gonzy-Treboul, G., Peronnet, F., Alin, M. F., Ardourel, C., Benassayag, C., Cribbs, D., Deutsch, J., Ferrer, P., Haenlin, M. et al. (2002). A P-insertion screen identifying novel X-linked essential genes in Drosophila. *Mech Dev* **110**, 71-83.

Boutros, M. and Mlodzik, M. (1999). Dishevelled: at the crossroads of divergent intracellular signalling pathways. *Mech Dev* **83**, 27-37.

Boutros, M., Paricio, N., Strutt, D. I. and Mlodzik, M. (1998). Dishevelled activates JNK and discriminates between JNK pathways in planar polarity and wingless signalling. *Cell* **94**, 109-18.

Brown, K. E. and Freeman, M. (2003). Egfr signalling defines a protective function for ommatidial orientation in the Drosophila eye. *Development* **130**, 5401-12.

Bruckner, K., Perez, L., Clausen, H. and Cohen, S. (2000). Glycosyltransferase activity of Fringe modulates Notch-Delta interactions. *Nature* **406**, 411-5.

Brunner, D., Ducker, K., Oellers, N., Hafen, E., Scholz, H. and Klambt, C. (1994a). The ETS domain protein pointed-P2 is a target of MAP kinase in the sevenless signal transduction pathway. *Nature* **370**, 386-9.

Brunner, D., Oellers, N., Szabad, J., Biggs, W. H., 3rd, Zipursky, S. L. and Hafen, E. (1994b). A gain-of-function mutation in Drosophila MAP kinase activates multiple receptor tyrosine kinase signalling pathways. *Cell* **76**, 875-88.

Cagan, R. L. and Ready, D. F. (1989). Notch is required for successive cell decisions in the developing Drosophila retina. *Genes Dev* **3**, 1099-112.

Carthew, R. W. and Rubin, G. M. (1990). seven in absentia, a gene required for specification of R7 cell fate in the Drosophila eye. *Cell* **63**, 561-77.

Casci, T. and Freeman, M. (1999). Control of EGF receptor signalling: lessons from fruitflies. *Cancer Metastasis Rev.* **18**, 181-201.

Casci, T., Vinos, J. and Freeman, M. (1999). Sprouty, an intracellular inhibitor of Ras signalling. *Cell* **96**, 655-65.

Cavodeassi, F., Diez Del Corral, R., Campuzano, S. and Dominguez, M. (1999). Compartments and organising boundaries in the Drosophila eye: the role of the homeodomain Iroquois proteins. *Development* **126**, 4933-42.

Chae, J., Kim, M. J., Goo, J. H., Collier, S., Gubb, D., Charlton, J., Adler, P. N. and Park, W. J. (1999). The Drosophila tissue polarity gene starry night encodes a member of the protocadherin family. *Development* **126**, 5421-5429.

Chan, A. Y., Bailly, M., Zebda, N., Segall, J. E. and Condeelis, J. S. (2000). Role of cofilin in epidermal growth factor-stimulated actin polymerization and lamellipod protrusion. *J Cell Biol* **148**, 531-42.

Chang, H. C., Solomon, N. M., Wassarman, D. A., Karim, F. D., Therrien, M., Rubin, G. M. and Wolff, T. (1995). phyllopod functions in the fate determination of a subset of photoreceptors in Drosophila. *Cell* **80**, 463-72.

Chen, J., Godt, D., Gunsalus, K., Kiss, I., Goldberg, M. and Laski, F. A. (2001). Cofilin/ADF is required for cell motility during Drosophila ovary development and oogenesis. *Nat Cell Biol* **3**, 204-9.

Cho, K. O., Chern, J., Izaddoost, S. and Choi, K. W. (2000). Novel signalling from the peripodial membrane is essential for eye disc patterning in Drosophila. *Cell* **103**, 331-42.

Cho, K. O. and Choi, K. W. (1998). Fringe is essential for mirror symmetry and morphogenesis in the Drosophila eye. *Nature* **396**, 272-6.

Choi, K.-W. and Benzer, S. (1994). Rotation of photoreceptor clusters in the developing *Drosophila* eye requires the *nemo* gene. *Cell* **78**, 125-136.

Chou, Y. H. and Chien, C. T. (2002). Scabrous controls ommatidial rotation in the Drosophila compound eye. *Dev Cell* **3**, 839-50.

Cleghon, V., Feldmann, P., Ghiglione, C., Copeland, T. D., Perrimon, N., Hughes, D. A. and Morrison, D. K. (1998). Opposing actions of CSW and RasGAP modulate the strength of Torso RTK signalling in the Drosophila terminal pathway. *Mol Cell* **2**, 719-27.

Clifford, R. J. and Schupbach, T. (1989). Coordinately and differentially mutable activities of torpedo, the Drosophila melanogaster homolog of the vertebrate EGF receptor gene. *Genetics* **123**, 771-787.

Cooley, L., Verheyen, E. and Ayers, K. (1992). chickadee encodes a profilin required for intercellular cytoplasm transport during Drosophila oogenesis. *Cell* **69**, 173-84.

Cooper, M. T. and Bray, S. J. (2000). R7 photoreceptor specification requires Notch activity. *Curr Biol* **10**, 1507-10.

Cooper, M. T. D. and Bray, S. J. (1999). Frizzled regulation of Notch signalling polarizes cell fate in the *Drosophila* eye. *Nature* **397**, 526-529.

Daga, A. and Banerjee, U. (1994). Resolving the sevenless pathway using sensitized genetic backgrounds. *Cell Mol Biol Res* **40**, 245-51.

Daga, A., Karlovich, C. A., Dumstrei, K. and Banerjee, U. (1996). Patterning of cells in the Drosophila eye by Lozenge, which shares homologous domains with AML1. *Genes Dev* **10**, 1194-205.

Das, G., Reynolds-Kenneally, J. and Mlodzik, M. (2002). The atypical cadherin Flamingo links Frizzled and Notch signalling in planar polarity establishment in the Drosophila eye. *Dev Cell* **2**, 655-66.

Diaz-Benjumea, F. J. and Hafen, E. (1994). The sevenless signalling cassette mediates Drosophila EGF receptor function during epidermal development. *Development* **120**, 569-78.

Dickson, B. (1995). Nuclear factors in sevenless signalling. *Trends Genet* **11**, 106-11.

Dickson, B., Sprenger, F., Morrison, D. and Hafen, E. (1992). Raf functions downstream of Ras1 in the Sevenless signal transduction pathway. *Nature* **360**, 600-3.

Dickson, B. J., Dominguez, M., van der Straten, A. and Hafen, E. (1995). Control of Drosophila photoreceptor cell fates by phyllopod, a novel nuclear protein acting downstream of the Raf kinase. *Cell* **80**, 453-62.

Dokucu, M. E., Zipursky, S. L. and Cagan, R. L. (1996). Atonal, rough and the resolution of proneural clusters in the developing Drosophila retina. *Development* **122**, 4139-47.

Dominguez, M. and de Celis, J. F. (1998). A dorsal/ventral boundary established by Notch controls growth and polarity in the Drosophila eye. *Nature* **396**, 276-8.

Dominguez, M. and Hafen, E. (1997). Hedgehog directly controls initiation and propagation of retinal differentiation in the Drosophila eye. *Genes Dev* **11**, 3254-64.

Dominguez, M., Wasserman, J. D. and Freeman, M. (1998). Multiple functions of the EGF receptor in Drosophila eye development. *Curr Biol* **8**, 1039-48.

Duchek, P., Somogyi, K., Jekely, G., Beccari, S. and Rorth, P. (2001). Guidance of cell migration by the Drosophila PDGF/VEGF receptor. *Cell* **107**, 17-26.

Duffy, J. B. (2002). GAL4 system in Drosophila: a fly geneticist's Swiss army knife. *Genesis* **34**, 1-15.

Dumstrei, K., Wang, F., Shy, D., Tepass, U. and Hartenstein, V. (2002). Interaction between EGFR signalling and DE-cadherin during nervous system morphogenesis. *Development* **129**, 3983-94.

Eaton, S. (1997). Planar polarity in *Drosophila* and vertebrate epithelia. *Curr. Opin. Cell Biol.* **9**, 860-866.

Edwards, K. A. and Kiehart, D. P. (1996). Drosophila nonmuscle myosin II has multiple essential roles in imaginal disc and egg chamber morphogenesis. *Development* **122**, 1499-511.

Fanto, M. and McNeill, H. (2004). Planar polarity from flies to vertebrates. *J Cell Sci* **117**, 527-33.

Fanto, M. and Mlodzik, M. (1999). Asymmetric Notch activation specifies photoreceptors R3 and R4 and planar polarity in the *Drosophila* eye. *Nature* **397**, 523-526.

Feig, L. A., Urano, T. and Cantor, S. (1996). Evidence for a Ras/Ral signalling cascade. *Trends Biochem Sci* **21**, 438-41.

Feiguin, F., Hannus, M., Mlodzik, M. and Eaton, S. (2001). The Ankyrin repeat protein Diego mediates Frizzled-dependent planar polarization. *Developmental Cell* **1**, 93-101.

Feldmann, P., Eicher, E. N., Leevers, S. J., Hafen, E. and Hughes, D. A. (1999). Control of growth and differentiation by Drosophila RasGAP, a homolog of p120 Ras-GTPase-activating protein. *Mol Cell Biol* **19**, 1928-37.

Flores, G. V., Duan, H., Yan, H., Nagaraj, R., Fu, W., Zou, Y., Noll, M. and Banerjee, U. (2000). Combinatorial signalling in the specification of unique cell fates. *Cell* **103**, 75-85.

Fortini, M. E., Simon, M. A. and Rubin, G. M. (1992). Signalling by the sevenless protein tyrosine kinase is mimicked by Ras1 activation. *Nature* **355**, 559-61.

Freeman, M. (1994a). Misexpression of the *Drosophila argos* gene, a secreted regulator of cell determination. *Development* **120**, 2297-2304.

Freeman, M. (1994b). The spitz gene is required for photoreceptor determination in the Drosophila eye where it interacts with the EGF receptor. *Mech Dev* **48**, 25-33.

Freeman, M. (1996). Reiterative use of the EGF receptor triggers differentiation of all cell types in the Drosophila eye. *Cell* **87**, 651-60.

Freeman, M., Klämbt, C., Goodman, C. S. and Rubin, G. M. (1992). The *argos* gene encodes a diffusible factor that regulates cell fate decisions in the Drosophila eye. *Cell* **69**, 963-975.

Fu, W. and Noll, M. (1997). The Pax2 homolog sparkling is required for development of cone and pigment cells in the Drosophila eye. *Genes Dev* **11**, 2066-78.

Gabay, L., Scholz, H., Golembo, M., Klaes, A., Shilo, B. Z. and Klambt, C. (1996). EGF receptor signalling induces pointed P1 transcription and inactivates Yan protein in the Drosophila embryonic ventral ectoderm. *Development* **122**, 3355-62.

Gabay, L., Seger, R. and Shilo, B. Z. (1997). In situ activation pattern of Drosophila EGF receptor pathway during development. *Science* **277**, 1103-6.

Gaengel, K. (2000). A study of genes that affect planar polarity in the *Drosophila* eye. Diploma thesis, Ruperto-Carola University of Heidelberg, Germany.

Gaengel, K. and Mlodzik, M. (2003). Egfr signalling regulates ommatidial rotation and cell motility in the Drosophila eye via MAPK/Pnt signalling and the Ras effector Canoe/AF6. *Development* **130**, 5413-23.

Garcia-Bellido, A. and Merriam, J. R. (1969). Cell lineage of the imaginal discs in Drosophila gynandromorphs. *J Exp Zool* **170**, 61-75.

Gaul, U., Mardon, G. and Rubin, G. M. (1992). A putative Ras GTPase activating protein acts as a negative regulator of signalling by the Sevenless receptor tyrosine kinase. *Cell* **68**, 1007-19.

Ghiglione, C., Carraway, K. L., 3rd, Amundadottir, L. T., Boswell, R. E., Perrimon, N. and Duffy, J. B. (1999). The transmembrane molecule kekkon 1 acts in a feedback loop to negatively regulate the activity of the Drosophila EGF receptor during oogenesis. *Cell* **96**, 847-56.

Ghosh, M., Song, X., Mouneimne, G., Sidani, M., Lawrence, D. S. and Condeelis, J. S. (2004). Cofilin promotes actin polymerization and defines the direction of cell motility. *Science* **304**, 743-6.

Golembo, M., Schweitzer, R., Freeman, M. and Shilo, B. Z. (1996). Argos transcription is induced by the Drosophila EGF receptor pathway to form an inhibitory feedback loop. *Development* **122**, 223-30.

Gomez-Skarmeta, J. L., Diez del Corral, R., de la Calle-Mustienes, E., Ferre-Marco, D. and Modolell, J. (1996). Araucan and caupolican, two members of the novel iroquois complex, encode homeoproteins that control proneural and vein-forming genes. *Cell* **85**, 95-105.

Greenwood, S. and Struhl, G. (1999). Progression of the morphogenetic furrow in the Drosophila eye: the roles of Hedgehog, Decapentaplegic and the Raf pathway. *Development* **126**, 5795-808.

Gubb, D. and Garcia-Bellido, A. (1982). A genetic analysis of the determination of cuticular polarity during development in Drosophila melanogaster. *J Embryol Exp Morphol* **68**, 37-57.

Gubb, D., Green, C., Huen, D., Coulson, D., Johnson, G., Tree, D., Collier, S. and Roote, J. (1999). The balance between isoforms of the prickle LIM domain protein is critical for planar polarity in Drosophila imaginal discs. *Genes Dev* **13**, 2315-2327.

Gunsalus, K. C., Bonaccorsi, S., Williams, E., Verni, F., Gatti, M. and Goldberg, M. L. (1995). Mutations in twinstar, a Drosophila gene encoding a cofilin/ADF homologue, result in defects in centrosome migration and cytokinesis. *J Cell Biol* **131**, 1243-59.

Hacohen, N., Kramer, S., Sutherland, D., Hiromi, Y. and Krasnow, M. A. (1998). sprouty encodes a novel antagonist of FGF signalling that patterns apical branching of the Drosophila airways. *Cell* **92**, 253-63.

Hafen, E., Basler, K., Edstroem, J. E. and Rubin, G. M. (1987). Sevenless, a cell-specific homeotic gene of Drosophila, encodes a putative transmembrane receptor with a tyrosine kinase domain. *Science* **236**, 55-63.

Harrison, S. D., Solomon, N. and Rubin, G. M. (1995). A genetic analysis of the 63E-64A genomic region of Drosophila melanogaster: identification of mutations in a replication factor C subunit. *Genetics* **139**, 1701-9.

Heberlein, U., Borod, E. R. and Chanut, F. A. (1998). Dorsoventral patterning in the Drosophila retina by wingless. *Development* **125**, 567-77.

Heberlein, U., Wolff, T. and Rubin, G. M. (1993). The TGF beta homolog dpp and the segment polarity gene hedgehog are required for propagation of a morphogenetic wave in the Drosophila retina. *Cell* **75**, 913-26.

Heitzler, P., Haenlin, M., Ramain, P., Calleja, M. and Simpson, P. (1996). A genetic analysis of pannier, a gene necessary for viability of dorsal tissues and bristle positioning in Drosophila. *Genetics* **143**, 1271-86.

Henchcliffe, C., Garcia-Alonso, L., Tang, J. and CS., G. (1993a). Genetic analysis of laminin A reveals diverse functions during morphogenesis in Drosophila. *Development* **118**, 325-337.

Henchcliffe, C., Garcia-Alonso, L., Tang, J. and Goodman, C. S. (1993b). Genetic analysis of laminin A reveals diverse functions during morphogenesis in Drosophila. *Development* **118**, 325-37.

Herbst, R., Carroll, P. M., Allard, J. D., Schilling, J., Raabe, T. and Simon, M. A. (1996). Daughter of sevenless is a substrate of the phosphotyrosine phosphatase Corkscrew and functions during sevenless signalling. *Cell* **85**, 899-909.

Higashijima, S., Kojima, T., Michiue, T., Ishimaru, S., Emori, Y. and Saigo, K. (1992). Dual Bar homeo box genes of Drosophila required in two photoreceptor cells, R1 and R6, and primary pigment cells for normal eye development. *Genes Dev* **6**, 50-60.

Hime, G. R., Dhungat, M. P., Ng, A. and Bowtell, D. D. (1997). D-Cbl, the Drosophila homologue of the c-Cbl proto-oncogene, interacts with the Drosophila EGF receptor in vivo, despite lacking C-terminal adaptor binding sites. *Oncogene* **14**, 2709-19.

Hiromi, Y., Mlodzik, M., West, S. R., Rubin, G. M. and Goodman, C. S. (1993). Ectopic expression of seven-up causes cell fate changes during ommatidial assembly. *Development* **118**, 1123-35.

Hopmann, R. and Miller, K. G. (2003). A balance of capping protein and profilin functions is required to regulate actin polymerization in Drosophila bristle. *Mol Biol Cell* **14**, 118-28.

Jarman, A. P., Grell, E. H., Ackerman, L., Jan, L. Y. and Jan, Y. N. (1994). Atonal is the proneural gene for Drosophila photoreceptors. *Nature* **369**, 398-400.

Joneson, T., White, M. A., Wigler, M. H. and Bar-Sagi, D. (1996). Stimulation of membrane ruffling and MAP kinase activation by distinct effectors of RAS. *Science* **271**, 810-2.

Jordan, P. and Karess, R. (1997). Myosin light chain-activating phosphorylation sites are required for oogenesis in Drosophila. *J Cell Biol* **139**, 1805-19.

Jürgens, G., Wieschaus, E., Nüsslein-Volhard,C. and Kluding, H. (1984). Mutations affecting the pattern of the larval cuticle in *Drosophila melanogaster*. *Wilhelm Roux's Arch. Dev. Biol.* **193**, 283-295.

Karess, R. E., Chang, X. J., Edwards, K. A., Kulkarni, S., Aguilera, I. and Kiehart, D. P. (1991). The regulatory light chain of nonmuscle myosin is encoded by spaghetti-squash, a gene required for cytokinesis in Drosophila. *Cell* **65**, 1177-89.

Karim, F. D., Chang, H. C., Therrien, M., Wassarman, D. A., Laverty, T. and Rubin, G. M. (1996). A screen for genes that function downstream of Ras1 during Drosophila eye development. *Genetics* **143**, 315-29.

Karim, F. D. and Rubin, G. M. (1998). Ectopic expression of activated Ras1 induces hyperplastic growth and increased cell death in Drosophila imaginal tissues. *Development* **125**, 1-9.

Kauffmann, R. C., Li, S., Gallagher, P. A., Zhang, J. and Carthew, R. W. (1996). Ras1 signalling and transcriptional competence in the R7 cell of Drosophila. *Genes Dev* **10**, 2167-78.

Kazlauskas, A. (1994). Receptor tyrosine kinases and their targets. *Curr Opin Genet Dev* **4**, 5-14.

Kimmel, B. E., Heberlein, U. and Rubin, G. M. (1990). The homeo domain protein rough is expressed in a subset of cells in the developing Drosophila eye where it can specify photoreceptor cell subtype. *Genes Dev* **4**, 712-27.

Kinashi, T., Katagiri, K., Watanabe, S., Vanhaesebroeck, B., Downward, J. and Takatsu, K. (2000). Distinct mechanisms of alpha 5beta 1 integrin activation by Ha-Ras and R-Ras. *J Biol Chem* **275**, 22590-6.

Klambt, C. (1993). The Drosophila gene pointed encodes two ETS-like proteins which are involved in the development of the midline glial cells. *Development* **117**, 163-76.

Klambt, C. (2002). EGF receptor signalling: roles of star and rhomboid revealed. *Curr Biol* **12**, R21-3.

Klein, D. E., Nappi, V. M., Reeves, G. T., Shvartsman, S. Y. and Lemmon, M. A. (2004). Argos inhibits epidermal growth factor receptor signalling by ligand sequestration. *Nature* **430**, 1040-4.

Klingensmith, J., Nusse, R. and Perrimon, N. (1994). The *Drosophila* segment polarity gene *dishevelled* encodes a novel protein required for response to the *wingless* signal. *Genes Dev.* **8**, 118-130.

Kockel, L., Vorbruggen, G., Jackle, H., Mlodzik, M. and Bohmann, D. (1997). Requirement for Drosophila 14-3-3 zeta in Raf-dependent photoreceptor development. *Genes Dev* **11**, 1140-7.

Kolodkin, A. L., Pickup, A. T., Lin, D. M., Goodman, C. S. and Banerjee, U. (1994). Characterisation of Star and its interactions with sevenless and EGF receptor during photoreceptor cell development in Drosophila. *Development* **120**, 1731-45.

Kramer, H., Cagan, R. L. and Zipursky, S. L. (1991). Interaction of bride of sevenless membrane-bound ligand and the sevenless tyrosine-kinase receptor. *Nature* **352**, 207-12.

Krasnow, R. E., Wong, L. L. and Adler, P. N. (1995). *dishevelled* is a component of the *frizzled* signalling pathway in *Drosophila*. *Development* **121**, 4095-4102.

Kumar, J. P. (2002). The Epidermal Growth Factor Receptor in *Drosophila* Eye Development. In *Drosophila* eye development, Results and Problems in Cell Differentiation vol. 37 (ed. K. Moses), pp. 59-71. Berlin Heidelberg: Springer Verlag.

Kumar, J. P., Tio, M., Hsiung, F., Akopyan, S., Gabay, L., Seger, R., Shilo, B. Z. and Moses, K. (1998). Dissecting the roles of the Drosophila EGF receptor in eye development and MAP kinase activation. *Development* **125**, 3875-3885.

Kuriyama, M., Harada, N., Kuroda, S., Yamamoto, T., Nakafuku, M., Iwamatsu, A., Yamamoto, D., Prasad, R., Croce, C., Canaani, E. et al. (1996). Identification of AF-6 and canoe as putative targets for Ras. *J Biol Chem* **271**, 607-10.

Lai, K. M., Olivier, J. P., Gish, G. D., Henkemeyer, M., McGlade, J. and Pawson, T. (1995). A Drosophila shc gene product is implicated in signalling by the DER receptor tyrosine kinase. *Mol Cell Biol* **15**, 4810-8.

Lai, Z. C. and Rubin, G. M. (1992). Negative control of photoreceptor development in Drosophila by the product of the yan gene, an ETS domain protein. *Cell* **70**, 609-20.

Le, N. and Simon, M. A. (1998). Disabled is a putative adaptor protein that functions during signalling by the sevenless receptor tyrosine kinase. *Mol Cell Biol* **18**, 4844-54.

Lee, J. D. a. T., J. E. (2002). Regulators of the Morphogenetic Furrow. In *Drosophila* eye development, Results and Problems in Cell Differentiation vol. 37 (ed. K. Moses), pp. 21-29. Berlin Heidelberg: Springer Verlag.

Lee, J. R., Urban, S., Garvey, C. F. and Freeman, M. (2001). Regulated intracellular ligand transport and proteolysis control EGF signal activation in Drosophila. *Cell* **107**, 161-71.

Leevers, S. J., Weinkove, D., MacDougall, L. K., Hafen, E. and Waterfield, M. D. (1996). The Drosophila phosphoinositide 3-kinase Dp110 promotes cell growth. *Embo J* **15**, 6584-94.

Li, S. C., Lai, K. M., Gish, G. D., Parris, W. E., van der Geer, P., Forman-Kay, J. and Pawson, T. (1996). Characterisation of the phosphotyrosine-binding domain of the Drosophila Shc protein. *J Biol Chem* **271**, 31855-62.

Li, W., Skoulakis, E. M., Davis, R. L. and Perrimon, N. (1997). The Drosophila 14-3-3 protein Leonardo enhances Torso signalling through D-Raf in a Ras 1-dependent manner. *Development* **124**, 4163-71.

Linnemann, T., Geyer, M., Jaitner, B. K., Block, C., Kalbitzer, H. R., Wittinghofer, A. and Herrmann, C. (1999). Thermodynamic and kinetic characterisation of the interaction between the Ras binding domain of AF6 and members of the Ras subfamily. *J Biol Chem* **274**, 13556-62.

Ma, C. and Moses, K. (1995). Wingless and patched are negative regulators of the morphogenetic furrow and can affect tissue polarity in the developing Drosophila compound eye. *Development* **121**, 2279-89.

Mandai, K., Nakanishi, H., Satoh, A., Obaishi, H., Wada, M., Nishioka, H., Itoh, M., Mizoguchi, A., Aoki, T., Fujimoto, T. et al. (1997). Afadin: A novel actin filament-binding protein with one PDZ domain localized at cadherin-based cell-to-cell adherens junction. *J Cell Biol* **139**, 517-28.

Martin-Blanco, E. (2000). p38 MAPK signalling cascades: ancient roles and new functions. *BioEssays* **22**, 637-45.

Matsuo, T., Takahashi, K., Kondo, S., Kaibuchi, K. and Yamamoto, D. (1997). Regulation of cone cell formation by Canoe and Ras in the developing Drosophila eye. *Development* **124**, 2671-80.

Matsuo, T., Takahashi, K., Suzuki, E. and Yamamoto, D. (1999). The Canoe protein is necessary in adherens junctions for development of ommatidial architecture in the Drosophila compound eye. *Cell Tissue Res* **298**, 397-404.

Maurel-Zaffran, C. and Treisman, J. E. (2000). pannier acts upstream of wingless to direct dorsal eye disc development in Drosophila. *Development* **127**, 1007-16.

McNeill, H. (2002). Planar polarity: location, location, location. *Curr Biol* **12**, R449-51.

McNeill, H., Yang, C. H., Brodsky, M., Ungos, J. and Simon, M. A. (1997). mirror encodes a novel PBX-class homeoprotein that functions in the definition of the dorsal-ventral border in the Drosophila eye. *Genes Dev* **11**, 1073-82.

Meisner, H., Daga, A., Buxton, J., Fernandez, B., Chawla, A., Banerjee, U. and Czech, M. P. (1997). Interactions of Drosophila Cbl with epidermal growth factor receptors and role of Cbl in R7 photoreceptor cell development. *Mol Cell Biol* **17**, 2217-25.

Miller, D. T. and Cagan, R. L. (1998). Local induction of patterning and programmed cell death in the developing Drosophila retina. *Development* **125**, 2327-35.

Mirey, G., Balakireva, M., L'Hoste, S., Rosse, C., Voegeling, S. and Camonis, J. (2003). A Ral guanine exchange factor-Ral pathway is conserved in Drosophila melanogaster and sheds new light on the connectivity of the Ral, Ras, and Rap pathways. *Mol Cell Biol* **23**, 1112-24.

Mirkovic, I., Charish, K., Gorski, S. M., McKnight, K. and Verheyen, E. M. (2002). Drosophila nemo is an essential gene involved in the regulation of programmed cell death. *Mech Dev* **119**, 9-20.

Miyamoto, H., Nihonmatsu, I., Kondo, S., Ueda, R., Togashi, S., Hirata, K., Ikegami, Y. and Yamamoto, D. (1995). canoe encodes a novel protein containing a GLGF/DHR motif

and functions with Notch and scabrous in common developmental pathways in Drosophila. *Genes Dev* **9**, 612-25.

Mlodzik, M. (2002a). Planar cell polarization: do the same mechanisms regulate Drosophila tissue polarity and vertebrate gastrulation? *Trends Genet* **18**, 564-71.

Mlodzik, M. (2002b). Tissue Polarity in the Retina. In *Drosophila* eye development, Results and Problems in Cell Differentiation vol. 37 (ed. K. Moses), pp. 89-103. Berlin, Heidelberg: Springer Verlag.

Mlodzik, M., Hiromi, Y., Weber, U., Goodman, C. S. and Rubin, G. M. (1990). The Drosophila seven-up gene, a member of the steroid receptor gene superfamily, controls photoreceptor cell fates. *Cell* **60**, 211-24.

Moloney, D. J., Panin, V. M., Johnston, S. H., Chen, J., Shao, L., Wilson, R., Wang, Y., Stanley, P., Irvine, K. D., Haltiwanger, R. S. et al. (2000). Fringe is a glycosyltransferase that modifies Notch. *Nature* **406**, 369-75.

Mouneimne, G., Soon, L., DesMarais, V., Sidani, M., Song, X., Yip, S. C., Ghosh, M., Eddy, R., Backer, J. M. and Condeelis, J. (2004). Phospholipase C and cofilin are required for carcinoma cell directionality in response to EGF stimulation. *J Cell Biol* **166**, 697-708.

Musacchio, M. and Perrimon, N. (1996). The Drosophila kekkon genes: novel members of both the leucine-rich repeat and immunoglobulin superfamilies expressed in the CNS. *Dev Biol* **178**, 63-76.

Nagaraj, R., Canon, J. and Banerjee, U. (2002). Cell Fate Specification in the *Drosophila* Eye. In *Drosophila* eye development, Results and Problems in Cell Differentiation vol. 37 (ed. K. Moses), pp. 73-88. Berlin Heidelberg: Springer Verlag.

Neuman-Silberberg, F. S. and Schupbach, T. (1993). The Drosophila dorsoventral patterning gene gurken produces a dorsally localized RNA and encodes a TGF alpha-like protein. *Cell* **75**, 165-74.

Niwa, R., Nagata-Ohashi, K., Takeichi, M., Mizuno, K. and Uemura, T. (2002). Control of actin reorganization by Slingshot, a family of phosphatases that dephosphorylate ADF/cofilin. *Cell* **108**, 233-46.

O'Neill, E. M., Rebay, I., Tjian, R. and Rubin, G. M. (1994). The activities of two Ets-related transcription factors required for Drosophila eye development are modulated by the Ras/MAPK pathway. *Cell* **78**, 137-47.

Oda, H., Uemura, T., Harada, Y., Iwai, Y. and Takeichi, M. (1994). A Drosophila homolog of cadherin associated with armadillo and essential for embryonic cell-cell adhesion. *Dev Biol* **165**, 716-26.

Olivier, J. P., Raabe, T., Henkemeyer, M., Dickson, B., Mbamalu, G., Margolis, B., Schlessinger, J., Hafen, E. and Pawson, T. (1993). A Drosophila SH2-SH3 adaptor protein implicated in coupling the sevenless tyrosine kinase to an activator of Ras guanine nucleotide exchange, Sos. *Cell* **73**, 179-91.

Paavilainen, V. O., Bertling, E., Falck, S. and Lappalainen, P. (2004). Regulation of cytoskeletal dynamics by actin-monomer-binding proteins. *Trends Cell Biol* **14**, 386-94.

Pacold, M. E., Suire, S., Perisic, O., Lara-Gonzalez, S., Davis, C. T., Walker, E. H., Hawkins, P. T., Stephens, L., Eccleston, J. F. and Williams, R. L. (2000). Crystal structure and functional analysis of Ras binding to its effector phosphoinositide 3-kinase gamma. *Cell* **103**, 931-43.

Papayannopoulos, V., Tomlinson, A., Panin, V. M., Rauskolb, C. and Irvine, K. D. (1998). Dorsal-ventral signalling in the Drosophila eye. *Science* **281**, 2031-4.

Paricio, N., Feiguin, F., Boutros, M., Eaton, S. and Mlodzik, M. (1999). The Drosophila STE20-like kinase misshapen is required downstream of the Frizzled receptor in planar polarity signalling. *Embo J* **18**, 4669-78.

Parnas, D., Haghighi, A. P., Fetter, R. D., Kim, S. W. and Goodman, C. S. (2001). Regulation of postsynaptic structure and protein localisation by the Rho-type guanine nucleotide exchange factor dPix. *Neuron* **32**, 415-24.

Pawson, T. and Scott, J. D. (1997). Signalling through scaffold, anchoring, and adaptor proteins. *Science* **278**, 2075-80.

Perkins, L. A., Johnson, M. R., Melnick, M. B. and Perrimon, N. (1996). The nonreceptor protein tyrosine phosphatase corkscrew functions in multiple receptor tyrosine kinase pathways in Drosophila. *Dev Biol* **180**, 63-81.

Pichaud, F. and Desplan, C. (2001). A new visualisation approach for identifying mutations that affect differentiation and organization of the Drosophila ommatidia. *Development* **128**, 815-26.

Pollard, T. D. and Borisy, G. G. (2003). Cellular motility driven by assembly and disassembly of actin filaments. *Cell* **112**, 453-65.

Ponting, C. P. (1995). AF-6/cno: neither a kinesin nor a myosin, but a bit of both. *Trends Biochem Sci* **20**, 265-6.

Powell, P. A., Wesley, C., Spencer, S. and Cagan, R. L. (2001). Scabrous complexes with Notch to mediate boundary formation. *Nature* **409**, 626-30.

Prasad, R., Gu, Y., Alder, H., Nakamura, T., Canaani, O., Saito, H., Huebner, K., Gale, R. P., Nowell, P. C., Kuriyama, K. et al. (1993). Cloning of the ALL-1 fusion partner, the AF-6 gene, involved in acute myeloid leukemias with the t(6;11) chromosome translocation. *Cancer Res* **53**, 5624-8.

Prober, D. A. and Edgar, B. A. (2002). Interactions between Ras1, dMyc, and dPI3K signalling in the developing Drosophila wing. *Genes Dev* **16**, 2286-99.

Queenan, A. M., Ghabrial, A. and Schupbach, T. (1997). Ectopic activation of torpedo/Egfr, a Drosophila receptor tyrosine kinase, dorsalizes both the eggshell and the embryo. *Development* **124**, 3871-80.

Raabe, T., Olivier, J. P., Dickson, B., Liu, X., Gish, G. D., Pawson, T. and Hafen, E. (1995). Biochemical and genetic analysis of the Drk SH2/SH3 adaptor protein of Drosophila. *Embo J* **14**, 2509-18.

Raabe, T., Riesgo-Escovar, J., Liu, X., Bausenwein, B. S., Deak, P., Maroy, P. and Hafen, E. (1996). DOS, a novel pleckstrin homology domain-containing protein required for signal transduction between sevenless and Ras1 in Drosophila. *Cell* **85**, 911-20.

Ramain, P., Heitzler, P., Haenlin, M. and Simpson, P. (1993). pannier, a negative regulator of achaete and scute in Drosophila, encodes a zinc finger protein with homology to the vertebrate transcription factor GATA-1. *Development* **119**, 1277-91.

Rawls, A. S., Guinto, J. B. and Wolff, T. (2002). The cadherins fat and dachsous regulate dorsal/ventral signalling in the Drosophila eye. *Curr Biol* **12**, 1021-6.

Rebay, I. and Rubin, G. M. (1995). Yan functions as a general inhibitor of differentiation and is negatively regulated by activation of the Ras1/MAPK pathway. *Cell* **81**, 857-66.

Reich, A. and Shilo, B. Z. (2002). Keren, a new ligand of the Drosophila epidermal growth factor receptor, undergoes two modes of cleavage. *Embo J* **21**, 4287-96.

Reifegerste, R. and Moses, K. (1999). The genetics of epithelial polarity and pattern in the Drosophila retina. *BioEssays* **21**, 275-285.

Reinke, R. and Zipursky, S. L. (1988). Cell-cell interaction in the Drosophila retina: the bride of sevenless gene is required in photoreceptor cell R8 for R7 cell development. *Cell* **55**, 321-30.

Robinow, S. and White, K. (1991). Characterisation and spatial distribution of the ELAV protein during Drosophila melanogaster development. *J Neurobiol* **22**, 443-61.

Rodriguez-Viciana, P., Warne, P. H., Khwaja, A., Marte, B. M., Pappin, D., Das, P., Waterfield, M. D., Ridley, A. and Downward, J. (1997). Role of phosphoinositide 3-OH kinase in cell transformation and control of the actin cytoskeleton by Ras. *Cell* **89**, 457-67.

Rodriguez-Viciana, P., Warne, P. H., Vanhaesebroeck, B., Waterfield, M. D. and Downward, J. (1996). Activation of phosphoinositide 3-kinase by interaction with Ras and by point mutation. *Embo J* **15**, 2442-51.

Rogge, R. D., Karlovich, C. A. and Banerjee, U. (1991). Genetic dissection of a neurodevelopmental pathway: Son of sevenless functions downstream of the sevenless and EGF receptor tyrosine kinases. *Cell* **64**, 39-48.

Rommel, C. and Hafen, E. (1998). Ras--a versatile cellular switch. *Curr Opin Genet Dev* **8**, 412-8.

Royet, J. and Finkelstein, R. (1997). Establishing primordia in the Drosophila eye-antennal imaginal disc: the roles of decapentaplegic, wingless and hedgehog. *Development* **124**, 4793-800.

Rutledge, B. J., Zhang, K., Bier, E., Jan, Y. N. and Perrimon, N. (1992). The Drosophila spitz gene encodes a putative EGF-like growth factor involved in dorsal-ventral axis formation and neurogenesis. *Genes Dev* **6**, 1503-17.

Saint, R., Kalionis, B., Lockett, T. J. and Elizur, A. (1988). Pattern formation in the developing eye of Drosophila melanogaster is regulated by the homoeo-box gene, rough. *Nature* **334**, 151-4.

Sambrook, J., Fritsch, E. F. and Maniatis, T. (1989). Molecular Cloning - A Laboratory Manual. Cold Spring Harbor, New York: Cold Spring Harbor Laboratory Press.

Sapir, A., Schweitzer, R. and Shilo, B. Z. (1998). Sequential activation of the EGF receptor pathway during Drosophila oogenesis establishes the dorsoventral axis. *Development* **125**, 191-200.

Sawamoto, K., Okabe, M., Tanimura, T., Mikoshiba, K., Nishida, Y. and Okano, H. (1996). The Drosophila secreted protein Argos regulates signal transduction in the Ras/MAPK pathway. *Dev Biol* **178**, 13-22.

Sawamoto, K., Winge, P., Koyama, S., Hirota, Y., Yamada, C., Miyao, S., Yoshikawa, S., Jin, M. H., Kikuchi, A. and Okano, H. (1999a). The Drosophila Ral GTPase regulates developmental cell shape changes through the Jun NH(2)-terminal kinase pathway. *J Cell Biol* **146**, 361-72.

Sawamoto, K., Yamada, C., Kishida, S., Hirota, Y., Taguchi, A., Kikuchi, A. and Okano, H. (1999b). Ectopic expression of constitutively activated Ral GTPase inhibits cell shape changes during Drosophila eye development. *Oncogene* **18**, 1967-74.

Schejter, E. D., Segal, D., Glazer, L. and Shilo, B. Z. (1986). Alternative 5' exons and tissue-specific expression of the Drosophila EGF receptor homolog transcripts. *Cell* **46**, 1091-101.

Schnepp, B., Grumbling, G., Donaldson, T. and Simcox, A. (1996). Vein is a novel component in the Drosophila epidermal growth factor receptor pathway with similarity to the neuregulins. *Genes Dev* **10**, 2302-13.

Schnorr, J. D., Holdcraft, R., Chevalier, B. and Berg, C. A. (2001). Ras1 interacts with multiple new signalling and cytoskeletal loci in Drosophila eggshell patterning and morphogenesis. *Genetics* **159**, 609-22.

Schweitzer, R., Howes, R., Smith, R., Shilo, B. Z. and Freeman, M. (1995a). Inhibition of Drosophila EGF receptor activation by the secreted protein Argos. *Nature* **376**, 699-702.

Schweitzer, R., Shaharabany, M., Seger, R. and Shilo, B. Z. (1995b). Secreted Spitz triggers the DER signalling pathway and is a limiting component in embryonic ventral ectoderm determination. *Genes Dev* **9**, 1518-29.

Sementchenko, V. I. and Watson, D. K. (2000). Ets target genes: past, present and future. *Oncogene* **19**, 6533-48.

Shilo, B. Z. (2003). Signalling by the Drosophila epidermal growth factor receptor pathway during development. *Exp Cell Res* **284**, 140-9.

Shilo, B. Z., Schejter, E. D., Segal, D., Ginsberg, D. S. and Glazer, L. (1986). The Drosophila epidermal growth factor receptor homolog: structure, evolution, and possible functions. *Symp Fundam Cancer Res* **39**, 87-97.

Shiomi, K., Takeichi, M., Nishida, Y., Nishi, Y. and Uemura, T. (1994). Alternative cell fate choice induced by low-level expression of a regulator of protein phosphatase 2A in the Drosophila peripheral nervous system. *Development* **120**, 1591-9.

Simon, M. A. (1994). Signal transduction during the development of the Drosophila R7 photoreceptor. *Dev Biol* **166**, 431-42.

Simon, M. A., Bowtell, D. D., Dodson, G. S., Laverty, T. R. and Rubin, G. M. (1991). Ras1 and a putative guanine nucleotide exchange factor perform crucial steps in signalling by the sevenless protein tyrosine kinase. *Cell* **67**, 701-16.

Simon, M. A., Dodson, G. S. and Rubin, G. M. (1993). An SH3-SH2-SH3 protein is required for p21Ras1 activation and binds to sevenless and Sos proteins in vitro. *Cell* **73**, 169-77.

Strutt, D. (2003). Frizzled signalling and cell polarisation in Drosophila and vertebrates. *Development* **130**, 4501-13.

Strutt, D., Johnson, R., Cooper, K. and Bray, S. (2002). Asymmetric localisation of frizzled and the determination of notch-dependent cell fate in the Drosophila eye. *Curr Biol* **12**, 813-24.

Strutt, D. I., Weber, U. and Mlodzik, M. (1997). The role of RhoA in tissue polarity and Frizzled signalling. *Nature* **387**, 292-5.

Strutt, H. and Strutt, D. (2002). Nonautonomous planar polarity patterning in Drosophila: dishevelled-independent functions of frizzled. *Dev Cell* **3**, 851-63.

Strutt, H. and Strutt, D. (2003). EGF signalling and ommatidial rotation in the Drosophila eye. *Curr Biol* **13**, 1451-7.

Su, L., Hattori, M., Moriyama, M., Murata, N., Harazaki, M., Kaibuchi, K. and Minato, N. (2003). AF-6 controls integrin-mediated cell adhesion by regulating Rap1 activation through the specific recruitment of Rap1GTP and SPA-1. *J Biol Chem* **278**, 15232-8.

Sullivan, W. A., M.; Hawley, R.S. (2000). *Drosophila* Protocols. Cold Spring Harbor, New York: Cold Spring Harbor Laboratory Press.

Takahashi, K., Matsuo, T., Katsube, T., Ueda, R. and Yamamoto, D. (1998). Direct binding between two PDZ domain proteins Canoe and ZO-1 and their roles in regulation of the jun N-terminal kinase pathway in Drosophila morphogenesis. *Mech Dev* **78**, 97-111.

Tepass, U., Gruszynski-DeFeo, E., Haag, T. A., Omatyar, L., Torok, T. and Hartenstein, V. (1996). shotgun encodes Drosophila E-cadherin and is preferentially required during cell rearrangement in the neurectoderm and other morphogenetically active epithelia. *Genes Dev* **10**, 672-85.

Thackeray, J. R., Gaines, P. C., Ebert, P. and Carlson, J. R. (1998). small wing encodes a phospholipase C-(gamma) that acts as a negative regulator of R7 development in Drosophila. *Development* **125**, 5033-42.

Thaker, H. M. and Kankel, D. R. (1992). Mosaic analysis gives an estimate of the extent of genomic involvement in the development of the visual system in Drosophila melanogaster. *Genetics* **131**, 883-94.

Theisen, H., Purcell, J., Bennett, M., Kansagara, D., Syed, A. and Marsh, J. L. (1994). *dishevelled* is required during *wingless* signalling to establish both cell polarity and cell identity. *Development* **120**, 347-360.

Theodosiou, N. A. and Xu, T. (1998). Use of FLP/FRT system to study Drosophila development. *Methods* **14**, 355-65.

Therrien, M., Chang, H. C., Solomon, N. M., Karim, F. D., Wassarman, D. A. and Rubin, G. M. (1995). KSR, a novel protein kinase required for RAS signal transduction. *Cell* **83**, 879-88.

Therrien, M., Wong, A. M. and Rubin, G. M. (1998). CNK, a RAF-binding multidomain protein required for RAS signalling. *Cell* **95**, 343-53.

Thomas, B. J. and Wassarman, D. A. (1999). A fly's eye view of biology. *Trends Genet* **15**, 184-90.

Tomlinson, A., Bowtell, D. D., Hafen, E. and Rubin, G. M. (1987). Localisation of the sevenless protein, a putative receptor for positional information, in the eye imaginal disc of Drosophila. *Cell* **51**, 143-50.

Tomlinson, A., Kimmel, B. E. and Rubin, G. M. (1988). rough, a Drosophila homeobox gene required in photoreceptors R2 and R5 for inductive interactions in the developing eye. *Cell* **55**, 771-84.

Tomlinson, A. and Ready, D. F. (1987). Cell fate in the *Drosophila* ommatidium. *Dev. Biol.*, 264-275.

Tomlinson, A. and Struhl, G. (1999). Decoding vectorial information from a gradient: sequential roles of the receptors Frizzled and Notch in establishing planar polarity in the Drosophila eye. *Development* **126**, 5725-5738.

Tomlinson, A. and Struhl, G. (2001). Delta/Notch and Boss/Sevenless signals act combinatorially to specify the Drosophila R7 photoreceptor. *Mol Cell* **7**, 487-95.

Treisman, J. E. and Heberlein, U. (1998). Eye development in Drosophila: formation of the eye field and control of differentiation. *Curr Top Dev Biol* **39**, 119-58.

Treisman, J. E. and Rubin, G. M. (1995). wingless inhibits morphogenetic furrow movement in the Drosophila eye disc. *Development* **121**, 3519-27.

Tsruya, R., Schlesinger, A., Reich, A., Gabay, L., Sapir, A. and Shilo, B. Z. (2002). Intracellular trafficking by Star regulates cleavage of the Drosophila EGF receptor ligand Spitz. *Genes Dev* **16**, 222-34.

Tsuda, L., Inoue, Y. H., Yoo, M. A., Mizuno, M., Hata, M., Lim, Y. M., Adachi-Yamada, T., Ryo, H., Masamune, Y. and Nishida, Y. (1993). A protein kinase similar to MAP kinase activator acts downstream of the raf kinase in Drosophila. *Cell* **72**, 407-14.

Uemura, T., Shiomi, K., Togashi, S. and Takeichi, M. (1993). Mutation of twins encoding a regulator of protein phosphatase 2A leads to pattern duplication in Drosophila imaginal discs. *Genes Dev* **7**, 429-40.

Ullrich, A. and Schlessinger, J. (1990). Signal transduction by receptors with tyrosine kinase activity. *Cell* **61**, 203-12.

Urban, S., Lee, J. R. and Freeman, M. (2001). Drosophila rhomboid-1 defines a family of putative intramembrane serine proteases. *Cell* **107**, 173-82.

Urban, S., Lee, J. R. and Freeman, M. (2002). A family of Rhomboid intramembrane proteases activates all Drosophila membrane-tethered EGF ligands. *Embo J* **21**, 4277-86.

Usui, T., Shima, Y., Shimada, Y., Hirano, S., Burgess, R. W., Schwarz, T. L., Takeichi, M. and Uemura, T. (1999). Flamingo, a seven-pass transmembrane cadherin, regulates planar cell polarity under the control of Frizzled. *Cell* **98**, 585-595.

Van Aelst, L., White, M. A. and Wigler, M. H. (1994). Ras partners. *Cold Spring Harb Symp Quant Biol* **59**, 181-6.

Van Vactor, D. L., Jr., Cagan, R. L., Kramer, H. and Zipursky, S. L. (1991). Induction in the developing compound eye of Drosophila: multiple mechanisms restrict R7 induction to a single retinal precursor cell. *Cell* **67**, 1145-55.

Verheyen, E. M. and Cooley, L. (1994). Profilin mutations disrupt multiple actin-dependent processes during Drosophila development. *Development* **120**, 717-28.

Verheyen, E. M., Mirkovic, I., MacLean, S. J., Langmann, C., Andrews, B. C. and MacKinnon, C. (2001). The tissue polarity gene nemo carries out multiple roles in patterning during Drosophila development. *Mech Dev* **101**, 119-32.

Vinson, C. R. and Adler, P. N. (1987). Directional non-cell autonomy and the transmission of polarity information by the frizzled gene of Drosophila. *Nature* **329**, 549-51.

Vinson, C. R., Conover, S. and Adler, P. N. (1989). A *Drosophila* tissue polarity locus encodes a protein containing seven potential transmembrane domains. *Nature* **338**, 263-264.

Wadsworth, S. C., Vincent, W. S., 3rd and Bilodeau-Wentworth, D. (1985). A Drosophila genomic sequence with homology to human epidermal growth factor receptor. *Nature* **314**, 178-80.

Wahlstrom, G., Vartiainen, M., Yamamoto, L., Mattila, P. K., Lappalainen, P. and Heino, T. I. (2001). Twinfilin is required for actin-dependent developmental processes in Drosophila. *J Cell Biol* **155**, 787-96.

Wassarman, D. A., Solomon, N. M., Chang, H. C., Karim, F. D., Therrien, M. and Rubin, G. M. (1996). Protein phosphatase 2A positively and negatively regulates Ras1-mediated photoreceptor development in Drosophila. *Genes Dev* **10**, 272-8.

Wasserman, J. D. and Freeman, M. (1998). An autoregulatory cascade of EGF receptor signalling patterns the Drosophila egg. *Cell* **95**, 355-64.

Wasserman, J. D., Urban, S. and Freeman, M. (2000). A family of rhomboid-like genes: Drosophila rhomboid-1 and roughoid/rhomboid-3 cooperate to activate EGF receptor signalling. *Genes Dev* **14**, 1651-63.

Weber, U., Paricio, N. and Mlodzik, M. (2000). Jun mediates Frizzled-induced R3/R4 cell fate distinction and planar polarity determination in the Drosophila eye. *Development* **127**, 3619-29.

Wiersdorff, V., Lecuit, T., Cohen, S. M. and Mlodzik, M. (1996). Mad acts downstream of Dpp receptors, revealing a differential requirement for dpp signalling in initiation and propagation of morphogenesis in the Drosophila eye. *Development* **122**, 2153-62.

Wieschaus, E. and Gehring, W. (1976). Clonal analysis of primordial disc cells in the early embryo of Drosophila melanogaster. *Dev Biol* **50**, 249-63.

Winter, C. G., Wang, B., Ballew, A., Royou, A., Karess, R., Axelrod, J. D. and Luo, L. (2001). Drosophila Rho-associated kinase (Drok) links Frizzled-mediated planar cell polarity signalling to the actin cytoskeleton. *Cell* **105**, 81-91.

Wolff, T. (2003). EGF receptor signalling: putting a new spin on eye development. *Curr Biol* **13**, R813-4.

Wolff, T. and Ready, D. F. (1993). Pattern formation in the *Drosophila* retina. In The development of *Drosophila melanogaster*, (ed. M. B. A. Martinez-Arias), pp. 1277-1326. Cold Spring Harbor: Cold Spring Harbor Press.

Wolff, T. and Rubin, G. M. (1998). *strabismus*, a novel gene that regulates tissue polarity and cell fate decisions in *Drosophila*. *Development* **125**, 1149-1159.

Wolthuis, R. M. and Bos, J. L. (1999). Ras caught in another affair: the exchange factors for Ral. *Curr Opin Genet Dev* **9**, 112-7.

Wu, J., Klein, T. J. and Mlodzik, M. (2004). Subcellular localisation of frizzled receptors, mediated by their cytoplasmic tails, regulates signalling pathway specificity. *PLoS Biol* **2**, E158.

Xu, C., Kauffmann, R. C., Zhang, J., Kladny, S. and Carthew, R. W. (2000). Overlapping activators and repressors delimit transcriptional response to receptor tyrosine kinase signals in the Drosophila eye. *Cell* **103**, 87-97.

Xu, T. and Rubin, G. M. (1993). Analysis of genetic mosaics in developing and adult Drosophila tissues. *Development* **117**, 1223-37.

Yang, C. H., Axelrod, J. D. and Simon, M. A. (2002). Regulation of Frizzled by fat-like cadherins during planar polarity signalling in the Drosophila compound eye. *Cell* **108**, 675-88.

Yang, S. H., Sharrocks, A. D. and Whitmarsh, A. J. (2003). Transcriptional regulation by the MAP kinase signalling cascades. *Gene* **320**, 3-21.

Yordy, J. S. and Muise-Helmericks, R. C. (2000). Signal transduction and the Ets family of transcription factors. *Oncogene* **19**, 6503-13.

Young, P. E., Richman, A. M., Ketchum, A. S. and Kiehart, D. P. (1993). Morphogenesis in Drosophila requires nonmuscle myosin heavy chain function. *Genes Dev* **7**, 29-41.

Zeidler, M. P., Perrimon, N. and Strutt, D. I. (1999). The four-jointed gene is required in the Drosophila eye for ommatidial polarity specification. *Curr Biol* **9**, 1363-72.

Zeidler, M. P., Perrimon, N. and Strutt, D. I. (2000). Multiple roles for four-jointed in planar polarity and limb patterning. *Dev Biol* **228**, 181-96.

Zeng, Y. A. and Verheyen, E. M. (2004). Nemo is an inducible antagonist of Wingless signalling during Drosophila wing development. *Development* **131**, 2911-20.

Zhadanov, A. B., Provance, D. W., Jr., Speer, C. A., Coffin, J. D., Goss, D., Blixt, J. A., Reichert, C. M. and Mercer, J. A. (1999). Absence of the tight junctional protein AF-6 disrupts epithelial cell-cell junctions and cell polarity during mouse development. *Curr Biol* **9**, 880-8.

Zheng, L., Zhang, J. and Carthew, R. W. (1995). *frizzled* regulates mirror-symmetric pattern formation in the *Drosophila* eye. *Development* **121**, 3045-3055.

Zipursky, S. L. and Rubin, G. M. (1994). Determination of neuronal cell fate: lessons from the R7 neuron of Drosophila. *Annu Rev Neurosci* **17**, 373-97.

VI
Appendix

List of Figures

List of tables

Abbreviations

μl	microliter
aos	argos
arm	armadillo
ato	atonal
boss	bried of sevenless
bp	base pair
cDNA	complementary DNA
chic	chicadee
cno	canoe
DER	Drosophila Egf Receptor
dgo	diego
Dl	Delta
DN	Dominant-Negative
DNA	deoxyribonucleic acid
dNTP's	Deoxynucleotide Triphosphates
dpp	decapentaplegic
Drok	Drosophila Rho-Kinase
ds	dachsous
dsh	dishevelled
DSHB	Developmental Studies Hybridoma Bank
EGF	Epidermal Growth Factor
Egfr	Epidermal growth factor receptor
Elav	embryonic lethal abnormal vison
eq	equator
ey	eyless
fj	four jointed
FLP	Flipase
fmi	flamingo
fng	fringe
FRT	FLP recombination target
ft	fat
fz	frizzled
GFP	Green Fluorescent Protein
GTP	Guanosine-triphosphate
hh	Hedgehog
JNK	Jun N-terminal Kinase
kb	kilo base
kek	kekkon
lamA	laminin A
M	Molar
MAPK	Mitogen Activated Protein Kinase
MF	morphogenetic furrow
N	Notch
nmo	nemo
PCP	planar cell polarity
PCR	Polymerase Chain Reaction
PDGF	Platelet Derived Growth Factor
PI3K	Phospho-inositol-3-Kinase
pk-sple	prickle spiny-legs
pnr	pannier
pnt	pointed

PTEN	Phosphatase and Tensin homologue
PVR	Platelet Derived/ Vascular Endothelial Growth Factor
R1-8	photoreceptor 1-8
rh1	rhodopsin1
rho	rhomboid
rl	rolled
rlt	roulette
RTK	Receptor Tyrosine Kinase
S	Star
sca	scabrous
ser	serrate
sev	sevenless
shg	shotgun
spi	spitz
ssh	slingshot
stbm	strabismus
sty	sprouty
svp	sevenup
top	torpedo
tsr	twinstar
tub	tubulin
twf	twinfillin
UAS	Upstream activating sequence
VEGF	Vascular Endothelial Growth Factor
w	white
wg	wingless
wt	wild type
zip	zipper

Publication derived from this work:

Gaengel, K. and Mlodzik, M. (2003). Egfr signalling regulates ommatidial rotation and cell motility in the Drosophila eye via MAPK/Pnt signalling and the Ras effector Canoe/AF6. *Development* **130**, 5413-23.